Wound Healing, Distortion and Generation of Cartilage

Paul G.J. ten Koppel

Contents

Chapter 1

Introduction and outline of the thesis

Introduction

Clinical perspective

Cartilage is present in joints, intervertebral disks, ribs, nasal and laryngeal skeleton, and trachea. Some histologic features are common to all sites. Others are clearly different, like the content of collagen or elastic fibers. A marked difference concerns the presence of perichondrium. Contrary to articular cartilage, which bears no perichondrium, cartilage elsewhere is covered by perichondrium on all sides.

Cartilage may demonstrate a scala of developmental and injury-induced pathology. Cartilage surgery is part of several surgical disciplines like orthopedics, otorhinolaryngology, plastic and reconstructive surgery, and traumatology.

Otorhinolaryngology includes the surgical treatment of acquired or congenital pathology of the cartilaginous skeleton of auricle, nose, larynx and trachea. With regard to airway problems, endoscopic and functional evaluation is a prerequisite for correct assessment of the pathology of supporting cartilages, and for the planning of treatment.

Facial trauma often leads to injuries of the nasal cartilage. Trauma of the nose seems extremely common in children [1–3]. Only a minority of the children are presented for diagnosis or treatment to a general physician or specialist. In particular the cartilage of the nasal septum is vulnerable. The cartilaginous septum shows regional differences in thickness and strength. The thinnest parts are the most vulnerable zones and appear to be preferred sites for fracturing [4–7]. The fracture lines correspond with the most common types of septal deviation in children aged between 4 and 12 years [8,9]. Probably, the majority of septal deviations are developing after a septal fracture, although in most cases neither the patients nor their parents have any remembrance of a specific trauma in the past.

An internal trauma of the laryngeal wall may not occur as frequently as facial injuries but the clinical consequences are often serious. Lesions of the soft tissues and cartilaginous skeleton of the airway due to intubation or prolonged presence of an endotracheal tube can lead to narrowing of the airway lumen, severely interfering with respiration. Treatment of such injury-induced stenoses, most frequently observed at the subglottic level, is difficult and not without risk of failure [10,11].

Another special feature of injuries to nose, larynx and trachea in children is –next to early symptoms– the late manifestation of complaints and anomalies [7,12–15]. The question was raised whether traumatic lesions or surgery might influence further growth and be the cause of later and/or progressive airway obstruction?

Structure and biology of cartilage

Cartilage is composed of chondrocytes and matrix substance. Three different types of cartilage can be distinguished: fibrous, hyaline and elastic. These cartilage characteristics are expressed in the specific matrix content. Fibro-cartilage contains collagen type I fibres, hyaline cartilage contains mainly type II fibres; the ground substance of elastic cartilage is the same as in hyaline cartilage but for the presence of more elastic fibres. All cartilage types are a-vascular and a-lymphatic. These biological properties are reflected by the high elasticity but poor regenerative potential of injured cartilage –without 'restitutio ad integrum'– as observed in clinical practice [6,16,17].

The well-vascularized perichondrium, which covers cartilage, is the main source for nutrients and oxygen to chondrocytes. The transition between cartilage and perichondrium is gradual, and is referred to as cambium or transitional layer. This layer contains cartilage progenitor cells [18]. Injury of the perichondrium (elevation or transaction) triggers cells in the cambium layer to generate new cartilage during the process of wound healing [19–24].

The cartilage matrix is hydrophilic and has the capacity to attract large amounts of water. Where as, on the other hand the collagen network in the cartilage matrix limits the total water content to 80 percent [25]. This balanced system of forces determines the elasticity of cartilage. The cartilage becomes floppy when the water content of the matrix is lowered [26], the cartilage matrix will swell when the collagen fibres are damaged. Thus changing the balanced forces in the cartilage matrix will change the elasticity and could bring about distortional changes [25–33].

Injury-induced distortion of cartilage: an experimental analysis of intrinsic and extrinsic factors

In clinical practice the otolaryngologist is either confronted with a cartilage defect that needs to be grafted or with a distortion that needs to be corrected. For a successful cartilage reconstruction, integration of the cartilage graft with the surrounding cartilage is an essential (imperative) condition.

In Chapter 2A the present concept of wound healing of cartilage structures was summarized with emphasis on the role of perichondrium and the age of cartilage. Next to wound healing processes, distortional changes can interfere with a renewed optimal connection between graft and surrounding tissues within a cartilage structure. Therefore, the distortional effects of trauma upon a flat (Chapter 2B) and circular (Chapter 2C) structure were studied. In Chapter 2B the direct distortional changes in septal cartilage in response to trauma were evaluated. It was hypothesized that the degree of distortion is correlated to the depth of trauma. In Chapter 2C the immediate

effects of various types of trauma on the cricoid ring were studied. In this experimental study the cricoid was excised from the experimental animal. Then, it was possible to analyse the response of the cartilage cricoid ring, without the influence of inserting ligaments, membranes and muscles. In patients a distortion of the split cricoid ring is not only determined by the intrinsic forces present in the cricoid ring but also by extrinsic forces exerted by ligaments and membranes, which are attached to the outer and inner circumference of the cricoid ring. In Chapter 2D the role of these extrinsic factors were studied upon the direct and long-term distortion of the split cricoid.

Improving wound healing to prevent distortion of cartilage structures: exploration of a few new methods

Effective cartilage reconstruction should ideally fill the defect and correct or at least prevent further distortion of a cartilage structure. We hypothesized that progressive distortion in the split cricoid ring could be prevented through a cartilage implant that is fully integrated with the surrounding cartilage. Because an autologous cartilage implant is not readily available, many studies are being conducted to generate new autologous cartilage tissue by techniques called 'Tissue Engineering'. Tissue Engineering is the application of the principles of life sciences and engineering to develop biological substitutes for the restoration or replacement of tissue or organ function. A biomaterial can be used as a scaffold for the replacement tissue. The new tissue has to be formed in this scaffold by cells that have somehow invaded the scaffold. In earlier studies in our department it was demonstrated that new cartilage can be engineered from a composite graft of demineralised bone matrix (DBM) with perichondrium as cell source. The newly engineered cartilage might be completely incorporated in the surrounding cricoid cartilage [34,35].

In Chapter 3A the engineering of cartilage from perichondrium wrapped around DBM was studied in more detail. We questioned the role of perichondrium upon the generation of cartilage with respect to the degree of vascularisation of the perichondrium. Perichondrium is a reliable source for tissue engineering of cartilage in-vivo. Whether cartilage can be generated from perichondrium ex-vivo was studied in Chapter 3B. In Chapter 3C different potential cartilage grafts were tested with special focus on the connection of a cartilage graft to its neighbouring cartilage.

References

[1] Pirsig, W., [The injured nose of the newborn. A review (author's transl)]. Monatsschr Kinderheilkd, 1979. 127(1): p. 14-9.

[2] East, C.A. and G. O'Donaghue, Acute nasal trauma in children. J Pediatr Surg, 1987. 22(4): p. 308-10.

[3] Alvarez, H., et al., Sequelae after nasal septum injuries in children. Auris Nasus Larynx, 2000. 27(4): p. 339-42.

[4] Murray, J.A., The behaviour of nasal septal cartilage in response to trauma. Rhinology, 1987. 25(1): p. 23-7.

[5] Murray, J.A., The distribution of stress in the nasal septum in trauma: an experimental model. Rhinology, 1987. 25(2): p. 101-7.

[6] Verwoerd, C.D., et al., Wound healing of the nasal septal perichondrium in young rabbits. ORL J Otorhinolaryngol Relat Spec, 1990. 52(3): p. 180-6.

[7] Meeuwis, J., H.L. Verwoerd-Verhoef, and C.D. Verwoerd, Normal and abnormal nasal growth after partial submucous resection of the cartilaginous septum. Acta Otolaryngol, 1993. 113(3): p. 379-82.

[8] van Loosen, J., H.L. Verwoerd-Verhoef, and C.D. Verwoerd, The nasal septal cartilage in the newborn. Rhinology, 1988. 26(3): p. 161-5.

[9] van Velzen, D., et al., Persistent pattern of variations in thickness of the human nasal septum: implications for stress and trauma as illustrated by a complex fracture in a 4-year-old boy. Adv Otorhinolaryngol, 1997. 51: p. 46-50.

[10] Ludemann, J.P., et al., Complications of pediatric laryngotracheal reconstruction: prevention strategies. Ann Otol Rhinol Laryngol, 1999. 108(11 Pt 1): p. 1019-26.

[11] Younis, R.T., R.H. Lazar, and A. Bustillo, Revision single-stage laryngotracheal reconstruction in children. Ann Otol Rhinol Laryngol, 2004. 113(5): p. 367-72.

[12] Verwoerd, C.D., et al., The influence of partial resection of the nasal septum on the outgrowth of nose and upper jaw [proceedings]. ORL J Otorhinolaryngol Relat Spec, 1977. 39(3): p. 174.

[13] Adriaansen, F.C., et al., A morphometric study of the growth of the subglottis after endolaryngeal trauma. Int J Pediatr Otorhinolaryngol, 1986. 12(2): p. 217-26.

[14] Adriaansen, F.C., et al., Morphometric study of the growth of the subglottis after interruption of the circular structure of the cricoid. Orl J Otorhinolaryngol Relat Spec, 1988. 50(1): p. 54-66.

[15] Verwoerd, C.D.A., et al., Trauma of the cricoid and interlocked stress. Acta Otolaryngol, 1991. 111(2): p. 403-9.

[16] Meeuwis, C.A., woundhealing of the cartilage septum, in dissertation. 1988. p. chapter 7.

[17] Verwoerd, C.D., et al., Wound healing of autologous implants in the nasal septal cartilage. Orl J Otorhinolaryngol Relat Spec, 1991. 53(5): p. 310-4.

[18] Duynstee, M.L., et al., The dual role of perichondrium in cartilage wound healing. Plast Reconstr Surg, 2002. 110(4): p. 1073-9.

[19] Skoog, T., L. Ohlsen, and S.A. Sohn, Perichondrial potential for cartilagenous regeneration. Scand J Plast Reconstr Surg, 1972. 6(2): p. 123-5.

[20] Ohlsen, L., Cartilage regeneration from perichondrium. Experimental studies and clinical applications. Plast Reconstr Surg, 1978. 62(4): p. 507-13.

[21] Engkvist, O., et al., The cartilaginous potential of the perichondrium in rabbit ear and rib. A comparative study in vivo and in vitro. Scand J Plast Reconstr Surg, 1979. 13(2): p. 275-80.
[22] Bean, J.K., H.L. Verwoerd-Verhoef, and C.D.A. Verwoerd, Chondroneogenesis in a Collagen Matrix. Fundamentals of bone growth, 1991. chapter 8: p. 113-120.
[23] Hartig, G.K., R.M. Esclamado, and S.A. Telian, Comparison of the chondrogenic potential of free and vascularized perichondrium in the airway. [Review]. Ann Otol Rhinol Laryngol, 1994. 103(1): p. 9-15.
[24] Hartig, G.K., R.M. Esclamado, and S.A. Telian, Chondrogenesis by free and vascularized rabbit auricular perichondrium. Ann Otol Rhinol Laryngol, 1994. 103(11): p. 901-4.
[25] Maroudas, A.I., Balance between swelling pressure and collagen tension in normal and degenerate cartilage. Nature, 1976. 260(5554): p. 808-9.
[26] Fry, H.J.H., Cartilage and cartilage grafts: the basic properties of the tissue and the components responsible for them. Plast Reconstr Surg, 1967. 40(5): p. 426-39.
[27] Gibson, T., R.C. Curran, and W.B. Davis, The survival of living homograft cartilage in man. Transplant Bull, 1957. 4(3): p. 105-6.
[28] Gibson, T. and B.W. Davis, The distortion of the autogenous cartilage grafts: its cause and prevention. Br. J. Plast. Surg., 1958. 10: p. 257-274.
[29] Stenstrom, S.J., A 'natrural' technique for correction of congenitally prominent ears. Plastic Reconstructive Surgery, 1963. 32: p. 509-518.
[30] Fry, H.J.H., Interlocked stresses in human nasal septal cartilage. Br J Plast Surg, 1966. 19(3): p. 276-8.
[31] Fry, H.J.H., The interlocked stresses of articular cartilage. Br J Plast Surg, 1974. 27(4): p. 363-4.
[32] Helidonis, E., et al., Laser shaping of composite cartilage grafts. Am J Otolaryngol, 1993. 14(6): p. 410-2.
[33] Wong, B.J., et al., Feedback-controlled laser-mediated cartilage reshaping [In Process Citation]. Arch Facial Plast Surg, 1999. 1(4): p. 282-7.
[34] Bean, J.K., et al., Reconstruction of the growing cricoid with a composite graft of demineralized bovine bone and autogenous perichondrium; a comparative study in rabbits. Int J Pediatr Otorhinolaryngol, 1993. 25(1-3): p. 163-72.
[35] Bean, J.K., H.L. Verwoerd-Verhoef, and C.D. Verwoerd, Reconstruction of the anterior laryngeal wall with a composite graft of demineralized bovine bone matrix and autogenous perichondrium. An experimental study in adult rabbits. Orl J Otorhinolaryngol Relat Spec, 1994. 56(4): p. 224-9.

Chapter 2

Wound healing and distortion of cartilage

2A

Wound healing of cartilage structures in the head and neck region

International Journal of Pediatric Otorhinolaryngology 1998;43:241–251

Wound healing of cartilage structures in the head and neck region

Henriette L. Verwoerd-Verhoef, Paul G.J. ten Koppel,
Gerjo J.V.M. van Osch, Cees A. Meeuwis, Carel D.A. Verwoerd

Abstract

This study was performed to determine the various processes involved in the behaviour of hyaline cartilage during the wound healing period after trauma or surgery of vulnerable structures like the nasal septal cartilage and the cricoid. The results of different procedures (perpendicular and parallel to the cartilage surface) in young and young-adult animals were analyzed: septal incision at different locations (young-old), cricoid split (young-old), suturing cartilage, closing defects with autologous cartilage (young), biomaterials (young) and newly engineered cartilage in 4- and 24-week-old rabbits (series of ten animals). Cartilage of the young rabbit and child have similar hyaline cartilage with a varying distribution in thickness. Thinner areas are more susceptible to malformations. Incisions through younger cartilage give rise to some new cartilage formation covered by a new layer of perichondrium; through older, differentiated cartilage the incision causes superficial but permanent necrosis. Edges of cut cartilage mostly do heal by formation of fibrous junctions. This forms a weak spot, sensitive to deviations. The same fate goes for the healing between the autologous graft and the surrounding pre-existent cartilage. Trauma parallel to the surface, leads to inconsistent quantity of neocartilage. With ageing the wound healing and regenerative capacities decrease. In general, biomaterials are less accepted by the surrounding tissues and would impede further growth. Only newly engineered, and thus less differentiated (younger) cartilage of hyaline nature, appeared to be well accepted at the interface with the edges of a cartilage defect. There are indications that the release of growth factors might play a role in cartilage wound healing. In the child as well as the adult, wound healing of hyaline cartilage structures is incomplete, and surgery remains 'experimental' surgery. The clinical implications of gradual loss of the regenerative capacity of hyaline cartilage should be further investigated.

Introduction

Hyaline cartilage in structures of head and neck as well as in joints is very sensitive to trauma. Cartilage wound healing is not only a dominant process in the period immediately after trauma but also has serious consequences for the later development of malformations, in particular in growing children. Cartilage healing underlies the success of many interventions in head and neck surgery. Common procedures like septoplasty and more elaborate reconstruction of congenitally or traumatically deformed cartilage structures in the larynx and outer ear may require implantation of autologous grafts harvested from other sites in the body. Then, cartilage wound healing has to occur not only in the recipient bed but also at the donor site.

In all the above-mentioned situations the most important problem is the reparative reaction of cartilage. In the case of surgical transection or grafting, the reconnection between the separate cartilaginous parts is crucial. Moreover, attention should be directed not only to the immediate postoperative appearance but also to the maintenance of a lasting result [1], especially when surgery is performed in children.

In many clinical and experimental studies the assessment of cartilage viability has been described, specially of cartilage grafts. The overall conclusion is that autologous cartilage grafts can survive well and adequately at various locations [2–4]. The importance of the presence of perichondrium has been stressed or denied [5]. However, despite the widely spread use of those grafts in cartilage defects, insufficient union and loss of grafting material through absorption in the long run, has regularly been reported [6–8]. Since more and more attention in this decade has been paid to grafting for augmentation and implants in cartilage defects, the 'engineering' in vivo or in vitro has received much interest and consequently, induced more research. In former studies we have described the heterotopic induction of hyaline cartilage by embedding a composite 'graft' of demineralized bone enveloped in a pedicled ear perichondrium flap. Three to 6 weeks after embedding, this composite implant has for the greater part been cartilaginized and can be applied for cartilage reconstruction and grafting [9,10].

Hyaline cartilage of the nasal septum or cricoid and elastic cartilage of the outer ear which has many characteristics of hyaline cartilage, might be injured in two directions: (i) parallel to the surface due to a lesion of the surface, with or without loss of perichondrium; and (ii) perpendicular to the surface due to fracturing or surgical incision.

In this study it was identified whether the direction of the 'cutting line' or lesion, and the age of the cartilage have influence on the wound healing processes of this tissue. Therefore, short- and longer-term effects of different

injuries have been investigated in young growing and adult rabbits. Reaction to injuries parallel and perpendicular to the cartilage surface are compared.

Secondly, the interface and junction between host cartilage and autologous grafts are assessed. Additionally, the acceptance of the above-mentioned demineralized bone matrix–perichondrium grafts is discussed.

The question was raised whether the behavior of the very young cartilage tissue, which is newly produced as the potential graft, is different from other grafts, as far as its wound healing capacity is concerned. Especially, it is compared with autologous grafts, derived from other locations in the body and of the same age as their host cartilage.

It was suggested by Silver and Glasgold that growth factors such as IGF-I might play a role in cartilage wound healing and repair during trauma to articular cartilage [11]. They also described that TGF-βs increase the production of fibroblasts, fibronectin and collagen. Izumi et al. reported that in particular TGF-β1 is important in initiating and promoting the expression of collagen type II [12].

In this study some preliminary observations on the presence of TGF-β in injured cartilage are included.

Materials and methods

Cartilage wound healing is compared in eight series of experiments (n=5–10 per series). The investigations involve transsections or incisions perpendicular to the cartilage, and surface injuries parallel to the surface like abrasion of the septum after tunneling or endolaryngeal trauma to the cricoid. In all series of young (4 weeks of age) and young adult (24 weeks), perpendicular and parallel lesions have been carried out surgically. Using light microscopy, the effects were histologically studied 3 and 7 days, and 2, 8 and 20 weeks later. The paraffin sections were stained with Hematoxylin-Eosin (cricoid) or Pas/Alcian blue (septum). Histochemical staining with Sirius red was carried out on sections of normal septal and cricoid cartilage (8 weeks old) to demonstrate the collagen network in the matrix.

The following items have been investigated:

1. Processes of wound healing at the interface;
2. Regeneration of perichondrium;
3. The fate of autologous grafts (reimplantation of resected parts) and, of newly formed grafts, induced by demineralized bone matrix enveloped in ear perichondrium and implanted 3 weeks later in a septum or cricoid defect;

4. In a pilot study: the presence of TGF-β by utilizing immunohisto-histochemical staining with an antibody against TGF-β1, -β2 and -β3 (Genzyme).

Some of the above-mentioned series were described earlier in other studies, with another question presented [8,10,13–17].

Results

In normal hyaline cartilage of nasal septum and cricoid, a collagen network could be observed in the matrix. Stained with Sirius red and visualized by double-refracting light, the sections showed that the collagen fibers are aligned perpendicular to the surface in the wide, intermediate zone but run parallel to the surface in the superficial layer of the cartilaginous structure (Fig. 1). This layer is the transitional zone between perichondrium and cartilage.

Wound healing perpendicular to the surface

In the young rabbit, traumatization of cartilage perpendicular to its surface, resulted within 3 days in regression and necrosis of the tissue, lining the cut end (Fig. 2). Then, the pericellular capsules which are aligned parallel

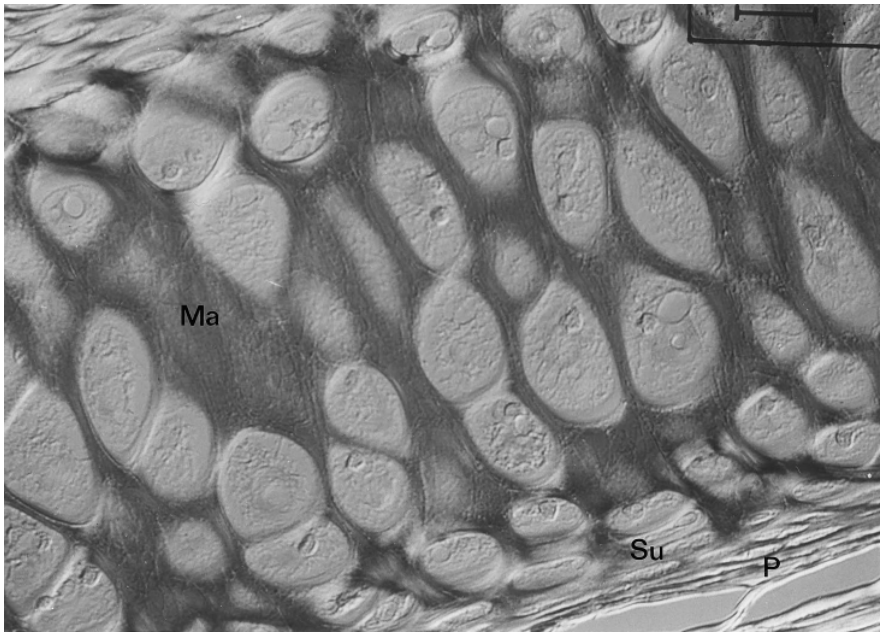

Fig. 1. Histochemical staining (Sirius red) of the collagen network in the matrix is visualized by double refracting light. In the superficial layer (Su) the cells and collagen fibers run parallel to the surface and to the perichondrium (P); in the intermediate part the fibers of the cartilage matrix (Ma) are aligned perpendicular to the surface. Magnification x40.

to the section line, are empty and the matrix is less stained. The adjacent zone showed higher activity with large, round and centrally situated nuclei indicating abundant proliferation (mitoses). One week—7 days—after trauma, filaments present in the matrix, have closed ranks and are arranged in bundles which demarcate the border between the viable cartilage and the regressive zone (Fig. 3). They are continuous with the perichondrial fibers. The necrotic material is invaded by macrophages and polymorphonuclear cells from the contiguous exsudate (Fig. 3). When new cartilage is formed in the defect, it is separated from the viable cartilage by a necrotic zone (Fig. 4). In later stages this zone has developed into a firm layer of fibrous tissue. After 4–6 weeks the demarcating fibers will cover the rounded stump, protecting the cartilage fragment (Fig. 5).

In the adult rabbit (24 weeks), splitting of cartilage was identified by the absence of wound healing potential. The process of repair in the cartilage did not occur: no reaction of chondrocytes, no mitotic activity but erosion of the wound area (Fig. 6). Fibrous strings have been formed from the cut end which will incidentally connect with another.

Wound healing parallel to the surface

Injury to the surface of the cartilage in young rabbits, caused similar processes of necrosis, macrophage activity and repair with fibrous demarca-

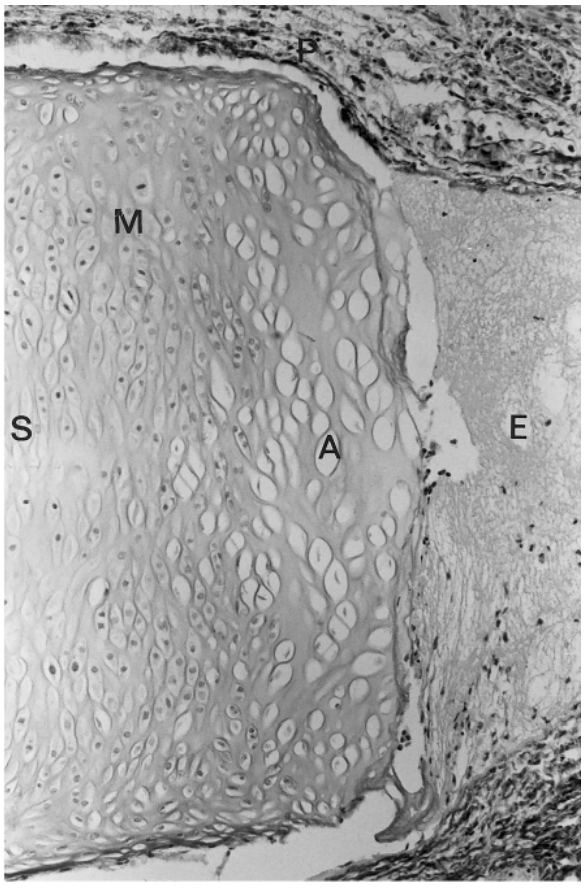

Fig. 2. Cartilage wound healing, 3 days after cartilage resection in nasal septum of a young, 4-week-old rabbit. S, proliferative zone of nasal septum; A, adjacent superficial zone withregressive changes; P, perichondrium; M, mitosis; E, exsudate with neutrophils. Pas/Alcian blue staining. Magnification x10.

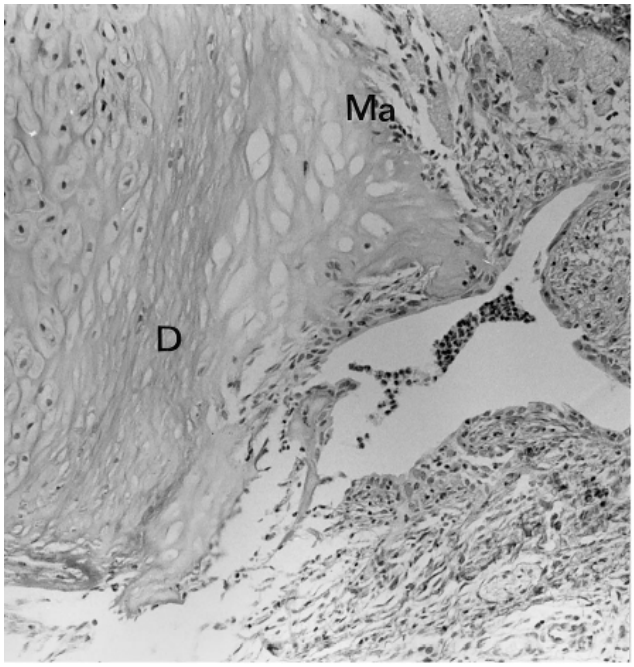

Fig. 3. Demarcation (D) between active zone of viable cartilage and necrotic area (septum, 7 days after trauma). Concentration of collagen fibers. Necrotic tissue, resorbed by macrophages (Ma). Pas/Alcian blue staining. Magnification x10.

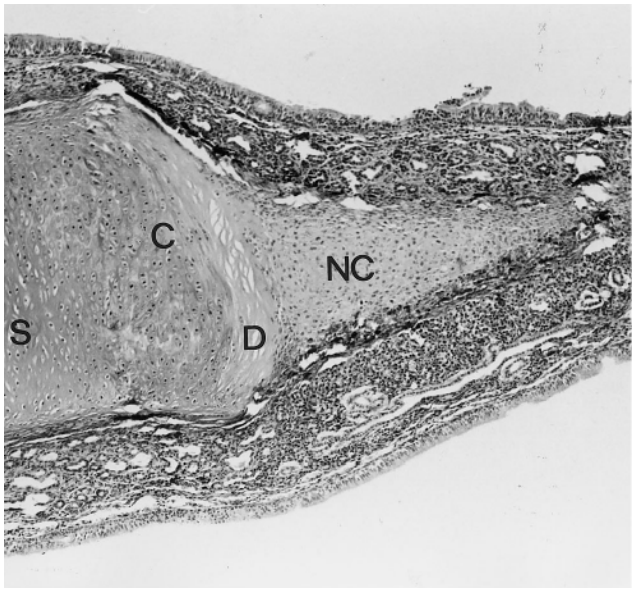

Fig. 4. New cartilage (NC) formed by the perichondrium, and separated from the viable area by demarcation zone (D) of necrotic tissue (septum (S), 2 weeks after resection). Increase in volume through proliferation of the septum cartilage (C). Pas/Alcian blue staining. Magnification x4.

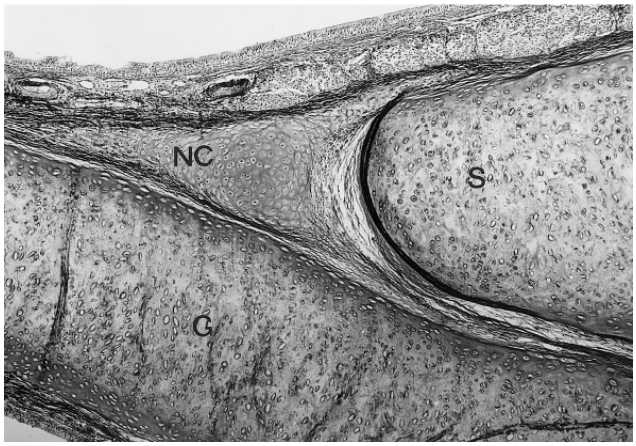

Fig. 5. Restoration of nasal septum, 8 weeks after implantation of autologous graft. S, septum; G, graft; NC, new cartilage. Stumps with complete perichondrial cover. Overlap with side-to-side connection and deviation. Pas/Alcian blue staining. Magnification x4.

tion of cartilage. When the perichondrium of septum or cricoid is also traumatized, the majority of the perichondrial layer will not be repaired.

In the series of endolaryngeal trauma, a variable quantity of new young cartilage might be formed, in continuity with (Fig. 7a) or unrelated (ectopic) to the original cartilage structure (Fig. 7b).

Intact cartilage could be stained with antibody against TGF-β1, -β2 and β3 (Fig. 8a). Injury to the cartilage surface resulted in loss of the immunohistochemical staining of the chondrocytes after 3 days (Fig. 8b).

When in the adult rabbit the surface of the cartilage is damaged, the tendency to demarcate the area of scarring has decreased considerably. There is no restoration of injured perichondrium. After endolaryngeal injury to the cricoid surface, remnants of matrix probably fixed to the fibrils of the transitional zone are found within the swollen submucosal layer (Fig. 9). Some weeks later these 'spurs' have been absorbed.

Wound healing at the interface, after grafting or transplantation

Wound healing of the incision surface (perpendicular) of the graft was similar to the reaction in the pre-existent cartilage, described above. Thus, the scarring occurred on both sides of the junction and therefore, the junction was in most cases fibrous and not cartilaginous in nature (Fig. 5). Even suturing of the two parts could not prevent scarring nor enhance a cartilaginous union. Regularly, the connection was not only fibrous but through overlap of the two segments, also side-to-side in stead of end-to-end (Fig. 5). Space between the elevated perichondrium and underlying cartilage, e.g. near the ends of the overlapping parts of septal cartilage, was frequently filled with newly generated cartilage (Fig. 5).

In the majority of animals provided with a composite graft of demineralized bone matrix and perichondrium, which was embedded and cartilaginized in the auricle for 3 weeks, and then implanted and sutured in a cricoid defect, the connection between the graft and the host cartilage was completely or for the major part cartilaginous in 18 out of 20 animals (Fig. 10). Then, a remarkable difference in the aspect of the two cartilage segments (young immature versus differentiated cartilage) is associated with a complete union of tissues.

Discussion

The collagen fibers of articular hyaline cartilage have a multidirectional orientation [11]. In nasal septum and laryngeal cartilage structures, the orientation is in principle in two directions, with fibers running parallel in the superficial zones, and perpendicular to the surface in the intermediate zone.

Injury to the superficial layer (parallel to the surface) of young cartilage of septum or larynx as well as to the intermediate zone (perpendicular to the surface) is characterized by regressive changes of the outer zone with loss of chondrocytes (necrosis) and loss of matrix proteoglycans possibly due to resorption by macrophages, and polymorphonuclear cells eliminating enzymes and cytokines. The necrosis is an instant process. Also in the infant, cartilage ulceration has been described to occur within 96 h of intubation [18].

The effect of surgery itself was restricted to the most superficial layer of cartilage bordering the cutting edge; in the young rabbit the zone of necrosis measured not more than ±0.3 mm. Tan et al. suggested that when inflammation is involved, the cartilage might undergo more progressive necrosis causing distortion and fragmentation of the cartilage structure [18].

Mucoperichondrial elevation for septal surgery will regularly cause intraperichondrial lesions [14]. These might lead to some new cartilage formation within the space which has come available through surgery.

When the normal demarcation by perichondrium is not completely restored or fails to occur, regeneration of a mixture of hyaline and fibrocartilage might even induce ectopic cartilage formation. This is a special problem when ectopic cartilage is found in the submucosal lining, also leading to obstruction and stenosis of the airway [17,18].

Perpendicular lesions of young cartilage result in maximal activation of the adjacent zone [14–16]. Activation and proliferation of the chondrocytes might probably also lead to the production of more extracellular matrix. In the split cartilage, separation between the necrotic and active zones is demarcated by a concentration of fibers seen as scar tissue deposition which is continuous with the perichondrium. After the phase of macrophage activity,

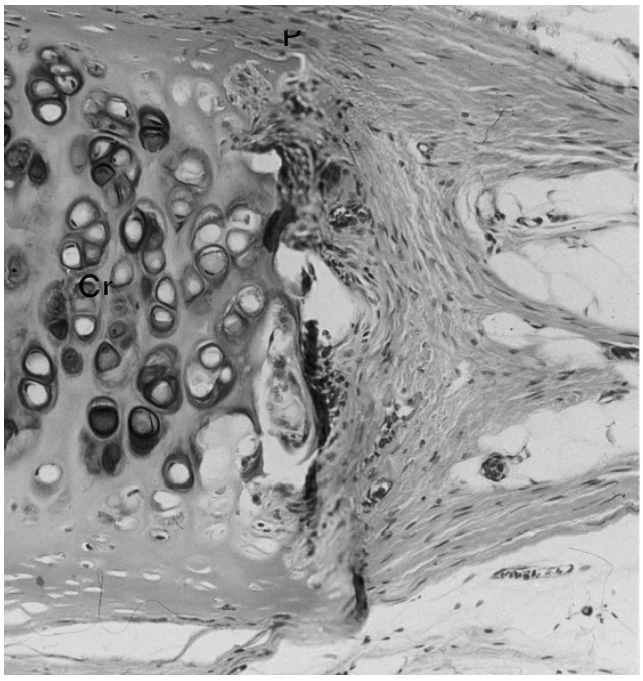

Fig. 6. Cartilage injury (split) in cricoid (Cr) of adult animals (24 weeks). Firm fibrous cover, continuous with the perichondrium (P), 8 weeks after trauma; erosion of cartilage along section line, without regeneration of cartilage. Hematoxylin-eosin staining. Magnification x25.

the next stage is characterized by two viable stumps covered by one fibrous layer, the perichondrium. This process of 'encapsulation' is in fact a collagen fiber packing which permanently prevents the complete union of two vital cartilage segments.

When splitting is followed by an immediate overlap of the cut ends due to the release of interlocked stresses [14], the scar repair is similar. Then, the fibrous connection is parallel to the surface. In the nasal septum the common perichondrial fibers would provide a more or less stable connection.

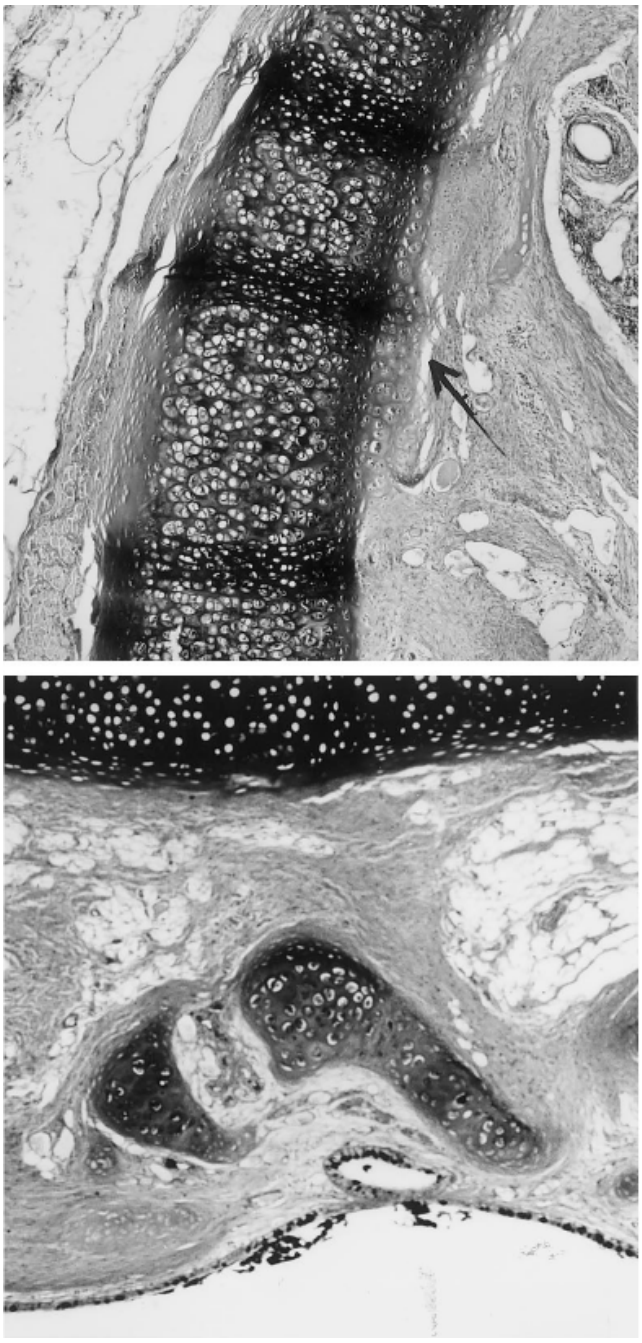

(a)

(b)

Fig. 7. Chondroneogenesis in the rabbit, 8 weeks after endolaryngeal lesion at the age of 4 weeks: (a) in continuation with the injured surface (see arrow), and (b) ectopic cartilage formation. Locally, no repair of perichondrium. Hematoxylin-eosin staining. Magnification x4.

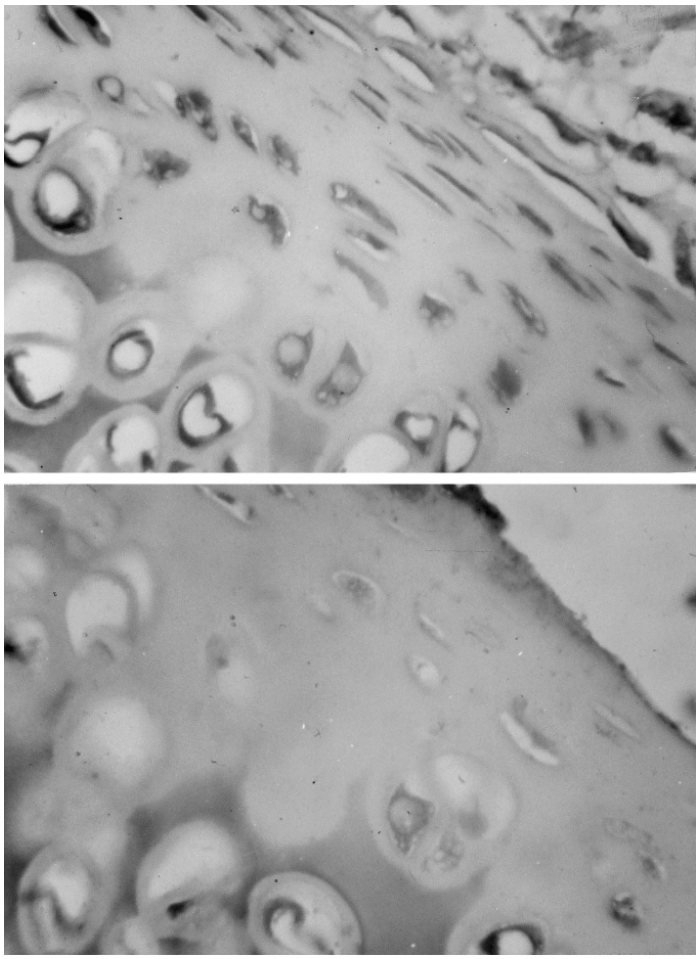

Fig. 8. Immunohistochemical staining with antibody against TGF- (1, 2 and 3). (a) Intact cricoid cartilage with dark red staining of the cells; (b) injured cartilage surface of cricoid (see arrow) with absence of staining after 3 days.

By outgrowth of the ends, however, the overlap will increase, leading to a septal spine or deviation during further development. The new, mostly hyaline cartilage which might regenerate in spaces between elevated perichondrium and cartilage would cause a local increase in thickness of the septum inducing passage problems for the nasal airflow.

Likewise, new hyaline—collagen type II—cartilage or collagen type I fibrocartilage is incidentally produced in a fresh defect. It was demonstrated that the thicker the cartilage fragments are the more chondrogenesis would occur locally [14]. In the septum the thickest cartilage appeared to be found in the basal part between the vomer lamina. Also then, however, the process of regression, necrosis and phagocytosis in the outer zone will raise a barrier for re-union of the cartilage parts.

Next to the depth of the defect, maturity of the cartilage is an important factor determining whether cartilage repair occurs in joints [11]. Also in the specimens of our study, the potential to provide demarcation of the injured cartilage through collagen fibers, appeared to decrease with ageing. The

cartilage structures of young animals demonstrated repair with scarring, however, without complete restoration. In the adult rabbits, the perpendicular as well as the parallel traumatized surface demonstrated regressive changes with loss of cells and matrix without any real repair. Evidently, the repair period for hyaline cartilage of head and neck structures is also age-linked.

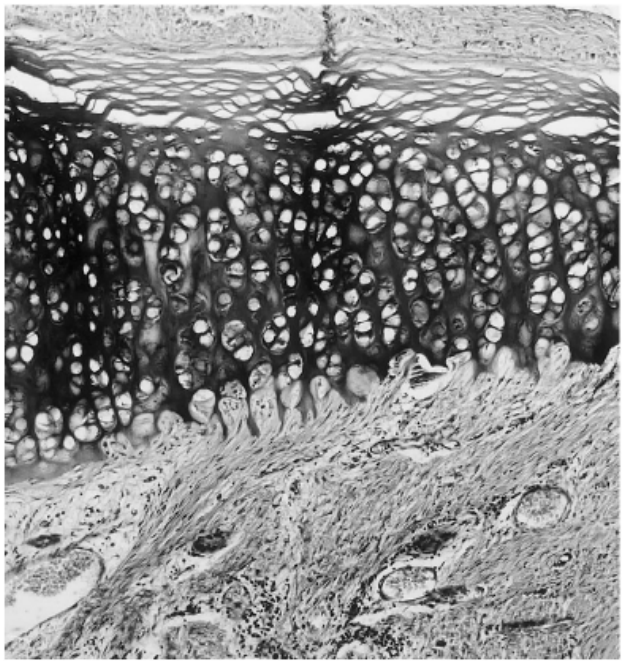

Fig. 9. Laryngeal lesion with erosion of cartilage surface and loss of perichondrium in the adult rabbit, 8 weeks after trauma. Hematoxylin-eosin staining. Magnification x10.

In summary the processes of wound healing in cartilage are characteristic for age and direction of surgery, i.e. perpendicular or parallel to the surface.

According to Silver and Glasgold any wound healing response which does not lead to replacement of type II collagen and proteoglycan synthesis will result in tissue with abnormal morphologic and mechanical properties [11]. They indicate that cartilage cannot repair itself because of the rapid scar tissue formation.

An indication that growth factors might be involved in the pathogenesis of scarring, was implicated in a recent study on growth factors in subglottic stenosis [19]. The presence of growth factors like TGF-β1 and -β2 was demonstrated in the subglottic mucosal tissue of patients with various degrees of acquired subglottic stenosis. Our pilot study could suggest that during the period of resorption of necrotic material and the following abundant proliferation of fibroblasts and collagen synthesis, TGF-β which is apparently also present in healthy hyaline cartilage, is released into the submucosal region. In concurrence with the suggestion of Scioscia et al., it might be hypothesized that these TGF-βs released into the submucosa could act as catalysts in the process of airway stenosis [19]. Further study concerning the release of TGF-βs and the reaction of antibodies specific to any one of the

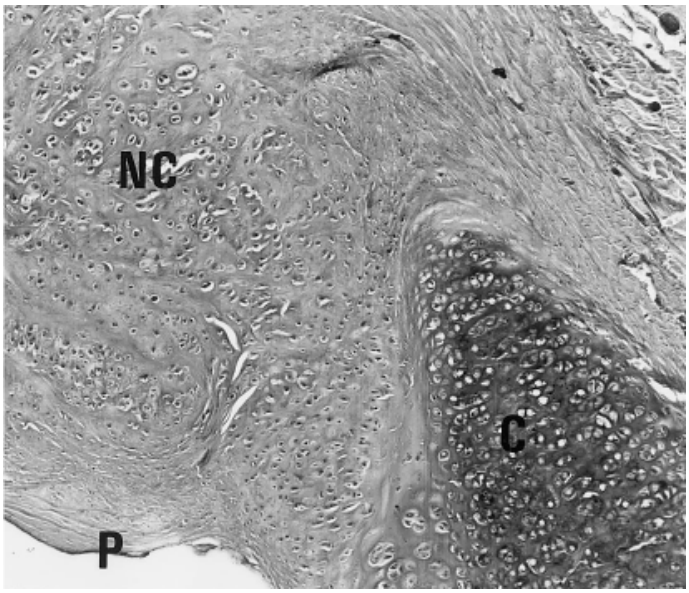

Fig. 10. Union of composite demineralized bone matrix-perichondrium graft and host cartilage of rabbit cricoid. Detail of interface, 20 weeks after implantation; NC, new cartilage graft; C, cricoid cartilage; P, perichondrium. Hematoxylin-eosin staining. Magnification x4.

TGF-β isoforms is now carried out to evaluate the significance of this above-mentioned observation. In particular, it is important to assess whether TGF-βs might play a role at the sites of repair.

Even in the case of the formation or transplantation of normal young hyaline cartilage an incomplete juncture between the ends of the segments can affect the normal physical properties of the cartilage structure, especially during further growth. Angulation located at the junction, and other deformations will be the final result [15]. On the other hand, implantation of newly engineered autologous cartilage containing less differentiated chondrocytes and demonstrating collagen type II, appeared to be capable of complete reunion with the original cartilage fragments, when neatly fixed to the host cartilage [8,9]. Probably the release of growth factors like IGF-I, also present in this young cartilage tissue, might have a growth-promoting effect on cartilage and play a role in this optimal wound healing process. Factors which could contribute to such a 'restitutio ad integrum' are under examination.

References

[1] B.S. Bauer, Discussion to: Free cartilage grafts: the role of perichondrium, Plast. Rec. Surg. 73 (1984) 922–923.

[2] L.A. Peer, Fate of autogenous septal cartilage after transplantation in human tissues, Arch. Otolaryngol. 34 (1941) 696–709.

[3] P.J. Donald, A. Col, Cartilage implantation in head and neck surgery, Otolaryngol. Head and Neck Surg. 90 (1982) 85–89.

[4] D.G. Heatly, R.A. Clary, F.T. Garner, R.P. Lusk, Auricular cartilage versus costal cartlage as a grafting material in experimental laryngotracheal reconstruction, Laryngoscope 105 (1995) 983–987.

[5] G.H. Zalzal, R.T. Cotton, A.J. McAdams, Cartilage grafts—present status, Head Neck Surg. 8 (1986) 363– 374.

[6] M.J. Duncan, H.G. Thomson, J.F.K. Mancer, Free cartilage grafts: the role of perichondrium, Plast. Rec. Surg. 73 (1984) 916–921.

[7] C.A.J. Prescott, D. Laing, Medium term fate of cartilage grafts from children after laryngo-tracheoplasty, Int. J. Ped. Otorhinolaryngol. 27 (1987) 163–171.

[8] J.K. Bean, H.L. Verwoerd-Verhoef, J. Meeuwis, C.D.A. Verwoerd, Reconstruction of the growing cricoid with a composite graft of demineralized bovine bone and autogenous perichondrium, Int. J. Ped. Otorhinolaryngol. 25 (1993) 163–172.

[9] H.L. Verwoerd-Verhoef, P.G.J. ten Koppel, G.J.V.M. van Osch, C.D.A. Verwoerd, Induction in vivo of cartilage grafts for craniofacial reconstruction, Am. J. Rhinol. 12 (1998) 27–31.

[10] W. Pirsig, J.K. Bean, H. Lenders, C.D.A. Verwoerd, H.L. Verwoerd-Verhoef, Cartilage transformation in a composite graft of demineralized bovine bone matrix and ear perichondrium used in a child for the reconstruction of the nasal septum, Int. J. Ped. Otorhinolaryngol. 32 (1995) 171–181.

[11] F.H. Silver, A.I. Glasgold, Cartilage wound healing; an overview, Otolaryngol. Clin. North Am. 28 (5) (1995) 847–864.

[12] T. Izumi, S.P. Scully, A. Heydemann, et al., Transforming growth factor β1 stimulates type II collagen expression in cultured periosteum-derived cells, J. Bone. Miner. Res. 7 (1992) 115.

[13] F.C.P.M. Adriaansen, H.L. Verwoerd-Verhoef, R.O. vd Heul, C.D.A. Verwoerd, A histologic study of the growth of the subglottis after endolaryngeal trauma, Int. J. Ped. Otorhinolaryngol. 12 (1986) 205–215.

[14] C.D.A. Verwoerd, H.L. Verwoerd-Verhoef, C.A. Meeuwis, Stress and wound healing of the cartilaginous nasal septum, Acta Otolaryngol. (Stockh.) 107 (1989) 441–445.

[15] C.D.A. Verwoerd, H.L. Verwoerd-Verhoef, C.A. Meeuwis, R.O. vd Heul, Wound healing of autologous implants in the nasal septal cartilage, ORL. 53 (1991) 310–314.

[16] J.K. Bean, H.L. Verwoerd-Verhoef, C.D.A. Verwoerd, Injury- and age-linked differences in wound healing and stenosis formation in the subglottis, Acta Otolaryngol. (Stockh.) 115 (1995) 317–321.

[17] F.C.P.M. Adriaansen, L.J. Hoeve, H.L. Verwoerd-Verhoef, R.O. vd Heul, C.D.A. Verwoerd, Ectopic cartilage in subglottic stenosis: hamartoma or reaction to trauma?, Int. J. Ped. Otorhinolaryngol. 23 (1992) 221–227.

[18] H.K.K. Tan, L.D. Holinger, J.C. Chen, F. Gonzalez-Crussi, Fragmented, distorted cricoid cartilage: an acquired abnormality, Ann. Otol. Rhinol. Laryngol. 105 (1996) 348–355.
[19] K.A. Scioscia, M.M. April, F. Miller, B.L. Gruber, Growth factors in subglottic stenosis, Ann. Otol. Rhinol. Laryngol. 105 (1996) 936–943.

2B

The immediate effects of local trauma on the shape of the cricoid cartilage

International Journal of Pediatric Otorhinolaryngology 1998;43:1–10

The immediate effects of local trauma on the shape of the cricoid cartilage

Paul G.J. ten Koppel, Gerjo J.V.M. van Osch,
Carel D.A. Verwoerd, Henriette L. Verwoerd-Verhoef

Abstract

Injury-induced abnormal development of the cricoid ring has been demonstrated in previous growth studies. In this study we focused on the immediate effects of various types of lesions to the cricoid, eliminating the influence of inserting muscles. In isolated, vital cricoids (cricoid explants) the anterior arch was split, creating a small gap between the cut ends. Previous injury to the internal surface of the cricoid ring resulted in a three to four fold increase of the diameter of the gap, actually widening the interrupted cricoid. On the contrary, injuring the external surface of the cricoid cartilage prior to anterior cricoid split, leads to an overlap of the cut edges, and a narrowing of the ring. These injury-specific changes in shape of the cricoid ring are ascribed to the release of interlocked stresses, present in the cartilage. It is suggested that the demonstrated methods to change the shape of the cricoid ring in a predictable way, are relevant for the treatment of patients with cricoid malformation.

Introduction

An external laryngeal trauma is regularly the cause of a cricoid fracture [16]. Surgical splitting of the cricoid (anterior or anterior-posterior) is frequently part of the treatment of patients with subglottic stenosis [5–7,12,14,15]. Does trauma to the cricoid cartilage affect the shape of the cricoid ring?

In young experimental animals it was observed that the interruption of the circular continuity on the anterior side (anterior cricoid split (ACS)) will exert a short- and long-term effect on the morphology of the cartilaginous cricoid ring [2]. The most important effect was an immediate opening between the ends of the transected cartilage. During further growth a specific abnormal form was induced through stretching of the outgrowing ends. In general, an ACS in young rabbits resulted in a slight enlargement of the airway lumen, 20 weeks later.

The long-term effects of several types of injury to the growing cricoid ring were demonstrated previously [1,18]. Standardized trauma to the inner surface of the cricoid cartilage at a young age resulted in later malformations of the ring with inward collapse of the thinner parts of the cartilage [1]. When this injury was combined with an ACS, reverse bending of the split parts convex became concave was observed [18].

For these injury-induced and injury-specific patterns of malformation, various causal factors have been reported such as poor wound healing of cartilage, muscle action around the cricoid and the release of tension, the so-called interlocked stresses, at the traumatized edges of the cartilage [3]. Earlier, this last-mentioned phenomenon of interlocked stresses was extensively studied and described for human costal cartilage by Gibson and Davis [11] and for human nasal septal cartilage by Fry [8–10]. Fry demonstrated that traumatization on one side of ex-vivo denuded nasal septum resulted in bending of the cartilaginous septal plate to the other side. In vivo, the nasal septum also appeared to release its interlocked stresses after incision of the cartilage [19].

Like nasal septal cartilage, cricoid cartilage is hyaline in nature and covered with perichondrium. This study was designed:

1. To assess whether the immediate deformation of the cricoid ring observed in vivo after an anterior cricoid split, is also present in fresh extirpated cricoid (cricoid explants), thus eliminating the influence of the inserting muscles;
2. To determine the effects of cricoid splitting following injury to the cartilage surface;

3. To reconsider the role of interlocked stresses in relation to cricoid deformation.

Materials and methods

Surgical procedure

A total of 21 New Zealand white rabbits, weighing 1300–3200 g, were included in this study. The animal protocol was approved by the Animal Ethics Committee, Erasmus University Medical Center Rotterdam (protocol no. 1269501). The animals were divided in three groups; in each group the same age distribution was represented (between 8 and 52 weeks). Anaesthesia was effectuated with 2% xylazine-hydrochloride (Rompun) 0.5 ml/kg and 10% ketamine-hydrochloride (Ketalin) 0.5 ml/kg via intramuscular injection. After extirpation of the larynx the animals were euthanized with intravenous pentobarbital (Euthesate). To reach and harvest the larynx including the proximal part of the trachea, a midventral incision through skin and subcutis was made. The cricoids with adherent perichondrium were carefully dissected (Fig. 1). To prevent dehydration, the specimens were moistened with 0.9% saline solution. Directly after extirpation, the following procedures were performed:

- Group A: anterior median cricoid split (ACS).
- Group B: circumferential injury (by burr) over the height of the cricoid arch (2–3mm), on the internal (luminal) side of the cricoid cartilage, followed by ACS.
- Group C: circumferential injury (by burr) over a height of 2–3 mm, on the external (peripheral) side of the cricoid ring, followed by ACS.

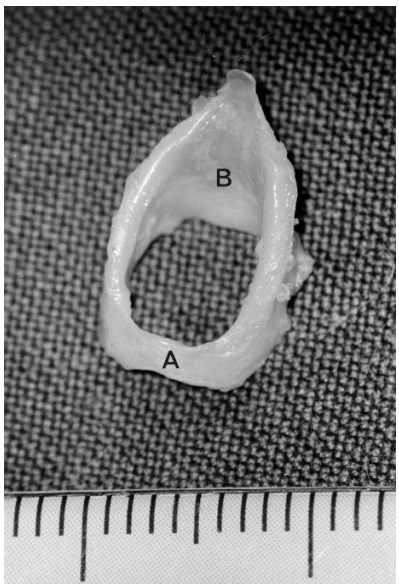

Fig. 1. Freshly dissected rabbit cricoid; scale in mm. A. anterior arch, B. lamina (magnification 4x).

Measurements

Immediately after splitting, the gap between the cut ends was measured with sliding calipers, precision 0.05 mm (Helios, Germany). The specimens were photographically documented.

Histological evaluation

To evaluate the injury to the cartilage, the cricoid specimens were processed for histology. The specimens were fixed in 4% phosphate formaline (pH 7.4), decalcified with 10% EDTA and embedded in paraffin wax. The sections (7 µm) were stained with Alcian-blue.

Statistical analysis

All specimens were measured twice within 2 min, by one observer. The mean value of the difference between two measurements was 0.17 ±0.14 mm. For all groups A, B and C the averages of two measurements were used to calculate the mean and standard deviation of the diameter of the 'gap' between the cut ends. Furthermore, one-way analysis of variance (ANOVA) was performed to calculate significances between all groups.

Results

Morphometrical observations

In all animals of group A, splitting of the anterior arch resulted in an immediate opening between the cut edges, measuring 1.49 ±0.50 mm (Figs. 2 and 3A). In group B and C it was noticed that prior to cricoid splitting, an internal or external circumferential injury, had no effect on the shape of the cartilage ring.

When the cricoid was transected (ACS) following injury to the internal side (group B), the cut ends stretched out even more than in group A; consequently the gap increased and measured 5.66 ±1.12 mm (Figs. 2 and 3B). On the other hand, trauma to the peripheral (external) surface of the cricoid followed by an anterior cricoid split (group C) caused a decrease of the circumference of the split ring through inward bending of the cut ends. Then, a gap was mostly absent, and in the majority of the cases even an overlap (-0.78 ±1.12 mm) of the tips of the cut edges could be identified (Figs. 2 and 3C).

The differences in gap size that were observed between group A, B and C were significant ($P < 0.001$). No age effects could be detected.

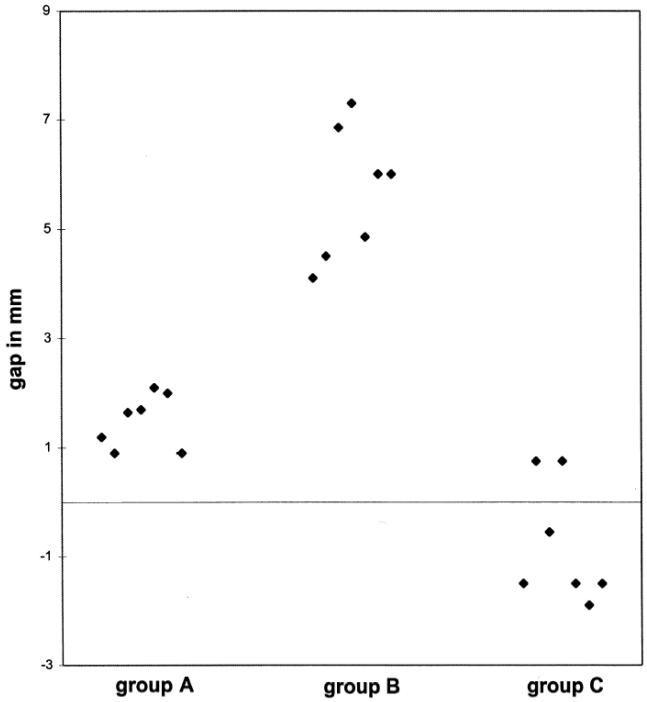

Fig. 2. Gap between the cut ends in mm. Group A: intact surface, Group B: injury to the internal side, Group C: injury to the external side.

Histological observations

In all specimens of group B and C, the perichondrium was removed by the burr, on the internal or external side of the ring, respectively. Also the most superficial layer of the cartilage was generally injured. This was clearly demonstrated by the irregular contour of the surface, where the matrix substances seemed to be 'leaking' from the cartilage (Fig. 4). Since it was impossible to standardize the trauma up to 100%, the depth of the lesion incidentally reached deeper but never exceeded 50% of the total thickness of the cricoid ring.

Discussion

In hyaline cartilage of nose and rib, interlocked stresses are considered to be an important biomechanical factor for ensuring cartilage tissue of its resilient and elastic properties [9,10]. Due to the water-binding capacity of protein polysaccharides in the cartilage matrix, a turgor is present which induces tensile forces (interlocked stresses) in the collagen network, in particular of the subperichondrial, transitional region [11]. Fry demonstrated that the water-binding capacity is diminished by immersion of the (nasal septal) cartilage in hyaluronidase [9]. This procedure would lower the turgor of the cartilage resulting in a decrease or even disappearance of the interlocked stresses. Likewise submerging the cricoid specimens in 70% alcohol for 24 h,

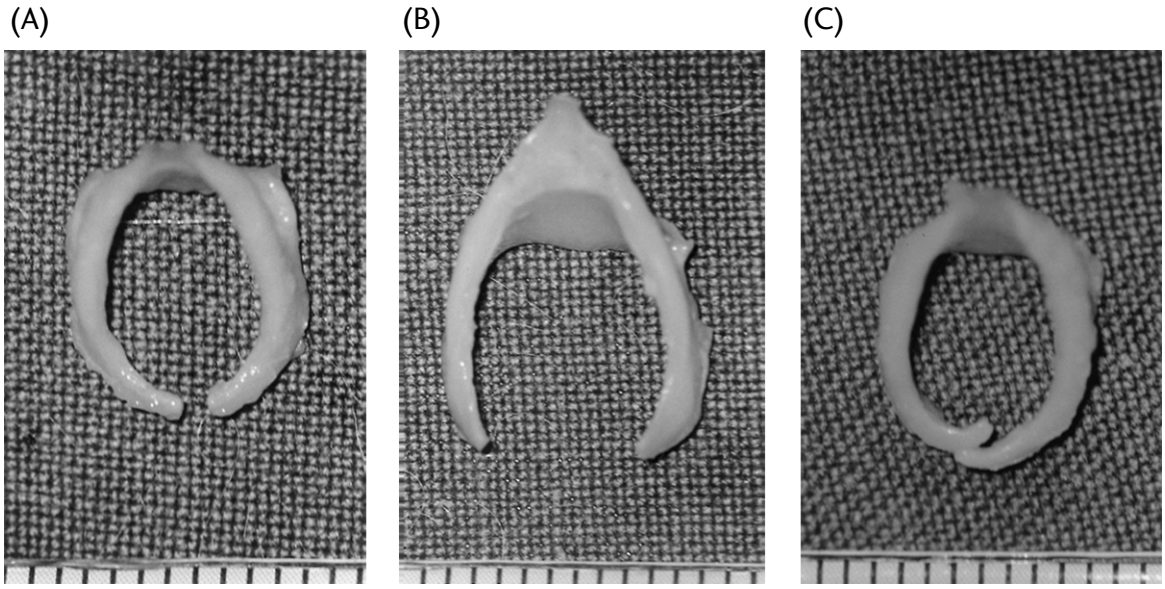

Fig. 3. ACS in cricoid explants. (A) intact surface; (B) after injury to the internal side; (C) after injury to the external side.

and thus dehydrating the matrix, lowered the turgor. This reduced the characteristic deforming effect of trauma (own observations).

The release of the interlocked stresses is incited by trauma to the collagen network, and will result in an immediate adaptive change in form of septal or costal cartilage [8–11]. Lesion of the superficial layer of the cartilage appeared to result in a bending of the cartilage with its convexity to the injured side. Also in hyaline cartilage of the cricoid ring, trauma causes instant effects probably based on the release of interlocked stresses. The effects were earlier demonstrated in-vivo [18], and are now confirmed by this ex-vivo study. In-vivo as well as ex-vivo a cricoid split will disrupt the continuity of the cartilaginous ring and the consequence is an immediate gap. It is therefore concluded that the gap is not caused by contraction of the inserting muscles.

Moreover, this study showed that luminal or peripheral injury to the surface of the cricoid cartilage also has a cumulative effect on the shape of the cricoid ring when split. The gap increased by three to four when the internal surface (group B) was injured previously. The variability of the gap diameter per group might depend on the extent of the injury to the cartilage. The existence of the stresses on both luminal and peripheral side of the cartilaginous ring is underlined by the fact that a reverse effect could be realized by traumatizing the external surface (group C). The reaction of the split cricoid ring to injury of the internal or external surface widening or narrowing, is essentially similar to the bending of septal or costal cartilage, as described above [8,11].

In young growing animals, other malformations of the injured ring became even more distinct with increase in age, indicating that anomalies like collapse of a non-interrupted ring are developmental effects, related to growth [18]. In adult animals such injuries induced similar defects, however without any remodelling of the ring [4]. Earlier, it was therefore hypothesized that in adult animals hyaline cartilage has lost the majority of its interlocked stresses [4]. However, in matured cricoid explants, splitting still caused an opening of the ring, which was larger in diameter when the internal surface was traumatized as well. Therefore, we now conclude that some turgor remains present in mature cartilage. Separate from the absence of growth, stiffness of the ring through increased calcium deposit might prevent larger malformations.

In clinical practice, trauma to the external surface of the cricoid ring in combination with a fractured cricoid often leads to an acute compromised airway with overlap of the fractured ends [16]. This could be determined like in our ex-vivo model by adaptive changes in form of (parts of) the ring, next to dislocation or infraction. The surgeon should be aware of the fact thatdissection or injury of the external contour of the cricoid might unfavourably affect the form.

In most patients with subglottic stenosis, splitting of the cricoid ring combined with cartilage interposition is the treatment of choice [5–7,12,14,15]. Our investigations suggest that the interrupted cricoid ring could be widened by a 'controlled' injury to the luminal surface of the cricoid. It is to be examined whether it is technically possible to selectively

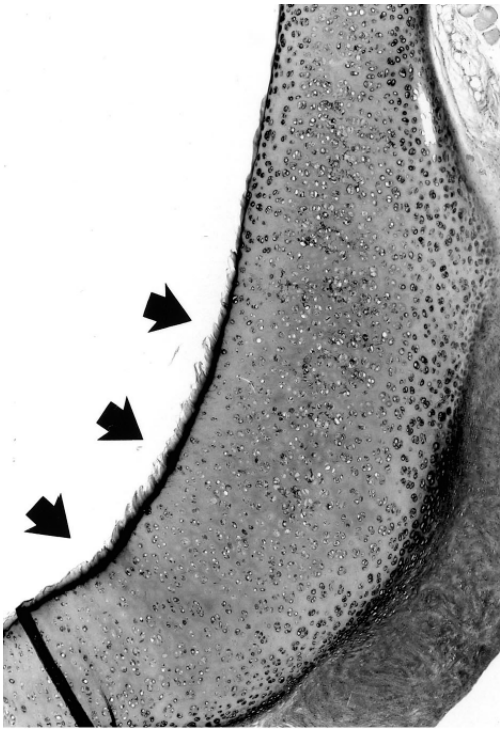

Fig. 4. Detail of transverse, histological section of the cricoid. Injury to internal surface extending to the subperichondrial cartilage. Note the irregular contour of the surface, caused by leakage of the matrix substances (see arrows). Magnification 40x.

traumatize the luminal cartilage surface while leaving the mucosa intact. In this way an ACS followed by a submucosa dissection of the cricoid in combination with selective scoring of the cartilaginous internal surface might further enlarge the airway lumen, especially in patients with an elliptical cricoid ring [13,17].

Conclusion

(1) The combination of an ACS and superficial injury to the cartilage on the external or internal side of the isolated cricoid ring invariably leads to immediate and predictable changes in the shape of the (injured) ring.
(2) ACS and external injury to the extirpated cricoid results in an immediate stenosis; ACS and internal injury results in a widening of the interrupted cricoid ring.
(3) Knowledge of these changes contributes to the interpretation of cricoid malformation in patients with acquired subglottic stenosis.
(4) The predictable and immediate effects of local trauma upon the shape of the cricoid ring, observed in these experiments for the first time, is a highly important phenomenon for larynx surgery, because of the potential influence (positive or negative) on the airway lumen.
(5) Injury-induced release of interlocked stresses in hyaline cartilage could explain the occurrence of deformations after injury of the cartilaginous cricoid ring.

Acknowledgements

The authors like to thank the Department of Pathology (Marcel Vermey, Erasmus University Rotterdam) for the kind hospitality at their laboratory and the Animal Experimental Center, Erasmus University Rotterdam, for care of the rabbits.

References

[1] F.C. Adriaansen, H. L. Verwoerd-Verhoef, R.O. Van der Heul, C.D. Verwoerd, A histologic study of the growth of the subglottis after endolaryngeal trauma, Int. J. Pediatr. Otorhinolaryngol. 12 (1986) 205–215.

[2] F.C. Adriaansen, H.L. Verwoerd-Verhoef, R.O. van der Heul, C.D. Verwoerd, Morphometric study of the growth of the subglottis after interruption of the circular structure of the cricoid, Orl. J. Otorhinolaryngol. Relat. Spec. 50 (1988) 54–66.

[3] J.K. Bean, H.L. Verwoerd-Verhoef, C.D. Verwoerd, Intrinsic and extrinsic factors relevant to the morphology of the growing cricoid ring after a combined anterior and posterior cricoid split: an experimental study in rabbits, Int. J. Pediatr. Otorhinolaryngol. 29 (1994) 129–137.

[4] J.K. Bean, H.L. Verwoerd-Verhoef, C.D. Verwoerd, Injury and age-linked differences in wound healing and stenosis formation in the subglottis, Acta Otolaryngol. 115 (1995) 317–321.

[5] R.T. Cotton, S.D. Gray, R.P. Miller, Update of the Cincinnati experience in pediatric laryngotracheal reconstruction, Laryngoscope 99 (11) (1989) 1111–1116.

[6] N. Evans, G.B. Todd, Laryngo-tracheoplasty, J. Laryngol. Otol. 88 (7) (1974) 589–597.

[7] B. Fearon, R. Cotton, Surgical correction of subglottic stenosis of the larynx in infants and children. Progress report, Ann. Otol. Rhinol. Laryngol. 83 (4) (1974) 428–431.

[8] H.J.H. Fry, Interlocked stresses in human nasal septal cartilage, Br. J. Plast. Surg. 19 (3) (1966) 276–278.

[9] H.J.H. Fry, Cartilage and cartilage grafts: the basic properties of the tissue and the components responsible for them, Plast. Reconstr. Surg. 40 (5) (1967a) 426–439.

[10] H.J.H. Fry, Nasal skeletal trauma and the interlocked stresses of the nasal septal cartilage, Br. J. Plast. Surg. 20 (2) (1967b) 146–158.

[11] T. Gibson, B.W. Davis, The distortion of the autogenous cartilage grafts: its cause and prevention, Br. J. Plast. Surg. 10 (1958) 257–274.

[12] B. Grahne, Surgical treatment of severe traumatic and functional stenosis of the larynx, Hno 21 (8) (1973) 234–236.[German]

[13] L.D. Holinger, R.W. Oppenheimer, Congenital subglottic stenosis: the elliptical cricoid cartilage, Ann. Otol. Rhinol. Laryngol. 98 (9) (1989) 702–706.

[14] M.M. Lesperance, G.H. Zalzal, Assessment and management of laryngotracheal stenosis, Pediatr. Clin. North Am. 43 (6) (1996) 1413.

[15] J.W. Ochi, C.M. Bailey, J.N. Evans, Pediatric airway reconstruction at Great Ormond Street: a 10 year review. III. Decannulation and suprastomal collapse, Ann. Otol. Rhinol. Laryngol. 101 (8) (1992) 656–658.

[16] J.A. Schild, E.C. Denneny, Evaluation and treatment of acute laryngeal fractures, Head Neck 11 (6) (1989) 491–496.

[17] A.E. Schlesinger, G. Jr. Tucker, Elliptical cricoid cartilage: a unique type of congenital subglottic stenosis, Am. J. Roentgenol. 146 (6) (1986) 1133–1136.

[18] C.D.A. Verwoerd, J.K. Bean, F.C. Adriaasen, H.L. Verwoerd-Verhoef, Trauma of the cricoid and interlocked stress, Acta Otolaryngol. 111 (2) (1991) 403–409.

[19] C.D.A. Verwoerd, H.L. Verwoerd-Verhoef, C.A. Meeuwis, Stress and woundhealing of the cartilaginous nasal septum, Acta Otolaryngol. (Stockh) 107 (1989) 441–445.

2C

Controlling incision-induced distortion of nasal septal cartilage: a model to predict the effect of scoring of rabbit septa

Plastic and Reconstructive Surgery 2003;111(6):1948–57

Controlling incision-induced distortion of nasal septal cartilage: a model to predict the effect of scoring of rabbit septa

Paul G. J. ten Koppel, Jan-Max van der Veen, David Hein, Fred van Keulen, Gerjo J. V. M. van Osch, Henriette L. Verwoerd-Verhoef, Carel D. A. Verwoerd

Abstract

Cartilage can be shaped by scoring. In an exploratory study in living adult animals, this phenomenon was demonstrated in cartilage of the nasal septum. Bending was observed immediately after superficial scoring of the cartilage surface, and the cartilage always warped in the direction away from the scored side. The scored piece of cartilage still showed its initially distorted shape 10 weeks after primary surgery. In ex vivo experiments, a clear relation between incision depth and bending of septal cartilage was observed. Under these controlled conditions, the variation between different septa was small. Deformation of the septal specimens was increased by introducing single superficial incisions deepening to half the thickness of the cartilage. A positive correlation between incision depth and bending was demonstrated. A model was used to accurately predict the degree of bending of the cartilage after making an incision of a particular depth. Hence, the effect of cartilage scoring can be predicted. Because the results of this controlled study showed excellent reproducibility for different septa, it is expected that this model can be extrapolated to human nasal septum cartilage. This would enable the surgeon to better predict the result of cartilage scoring, either preoperatively or perioperatively.

Introduction

In septorhinoplasty and otoplasty, the surgical correction of cartilage deformities is challenging. Cartilage can be reshaped by using a scoring technique in which multiple incisions are made on one side of the cartilage surface while anticipating the degree of bending [1]. These incisions should be superficial, with each made parallel to the previous incision. Additional cuts can be made as needed to increase the degree of cartilage bending. Next to the number of incisions, the depth of each incision might relate to the degree of bending. Murakami et al. [2] questioned the usefulness of this technique. In their study, no relation was found between depth of incision and degree of distortion. Furthermore, in the living specimen the definitive result can also be affected by the wound healing process and scar formation [3,4]. Therefore, the long-term results of cartilage scoring are expected to be variable.

The purpose of the current study was to develop a quantitative model to predict the effect of scoring of a cartilaginous structure. We started with a small, exploratory in vivo study to evaluate long-term effects. Scoring of nasal septal cartilage was performed in a poorly controlled way in living rabbits. The scored piece of cartilage was left pedicled to the septum with no attachments to other nasal structures except for the septal mucoperichondrial cover. This served to exclude factors other than wound healing of the scored cartilage. The long-term effects of the superficial unilateral scoring showed that the deformation was permanent, and little change in degree of bending was observed during the follow-up period in different rabbits. Next, we used a strictly controlled ex vivo procedure to test whether a quantitative correlation between depth of an incision and degree of bending could be found. An excised piece of cartilage was cut at an increasing depth, and after each incision the degree of bending was monitored. This study provides evidence that the initial effect of scoring of cartilage can be predicted when the performance is carefully controlled; to our knowledge this is the first study in which incision depth is correlated to cartilage bending.

Materials and methods

All animal experimental procedures in this study were approved by the Animal Ethics Committee (protocol no. 1269501) and were performed in accordance with the guidelines of the Erasmus University Rotterdam.

In vivo experiments

Surgical procedure. Five adult New Zealand White rabbits (>30 weeks old, 3500 to 4500 g) were used. Anesthesia was intramuscularly injected

using 2% xylazine-hydrochloride (Rompun; Bayer, Leverkusen, Germany), 0.5 ml/kg body weight, and 10% ketamine-hydrochloride (Ketalin; Apharma, Arnhem, Netherlands), 0.5 ml/kg body weight.

The nostril aperture in the rabbit is very small; therefore, it is technically impossible to reach the septum by this approach. Consequently, it was reached through the nasal dorsum, as earlier described by Verwoerd et al. [5] After shaving the nasal dorsum, a median longitudinal incision was made to the nasal bone. The internasal and nasofrontal suture line was divided. Then, both nasal bones were out-fractured and the periosteum was spared over the nasomaxillary suture line. Next, the upper lateral cartilages were reached and

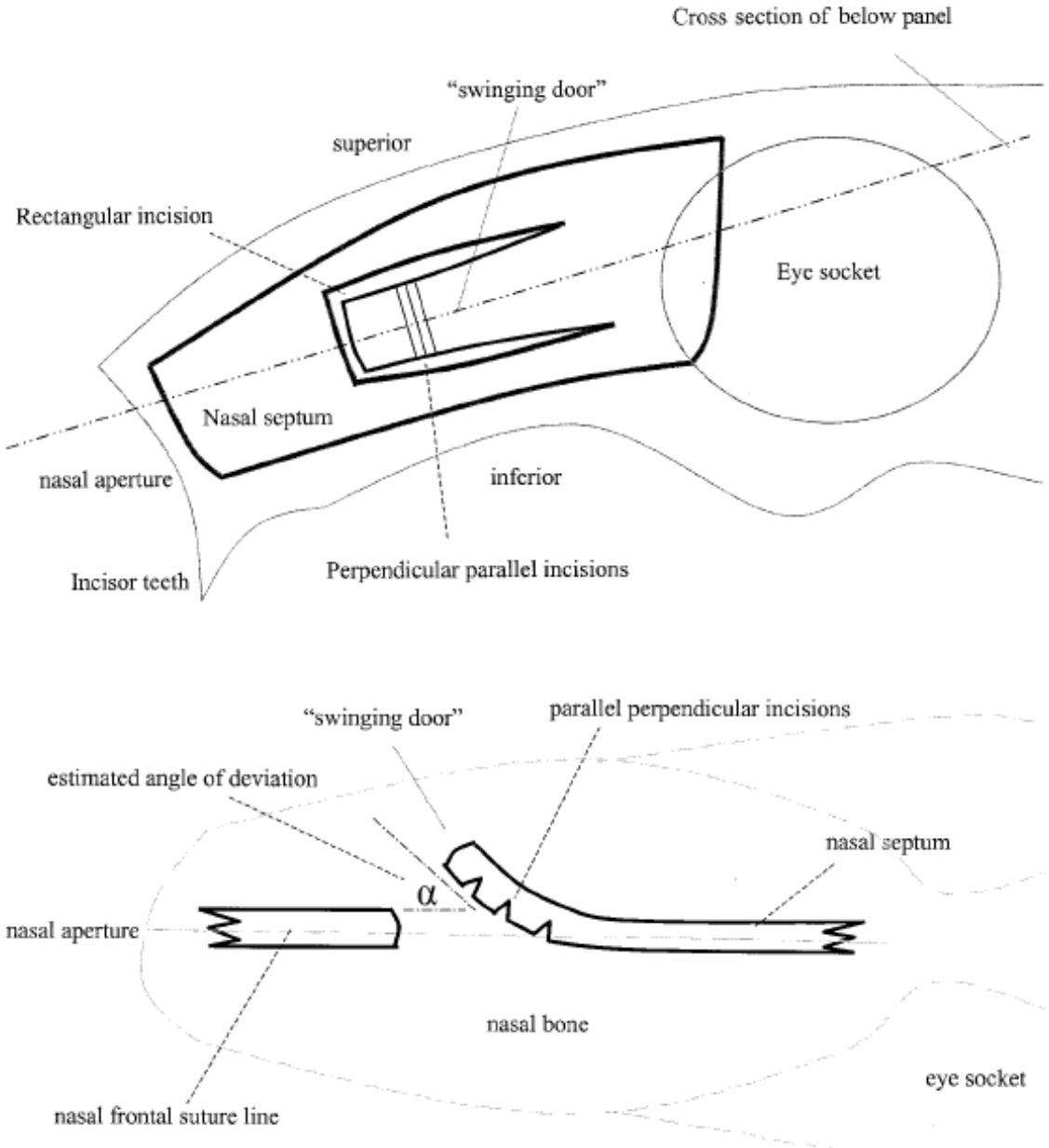

Fig. 1. Schematic outline of the surgical anatomy of the rabbit nose and head. (Above) Side view of a created swinging door. (Below) Top view of the swinging door; the septum is scored on one side.

separated from the nasal septum. The overlying mucoperichondrial cover was incised at the cranial end of the septum just underneath the nasal dorsum. Starting from this incision, the nasal mucosa could be easily elevated on both sides from the septal cartilage downward to the caudal end of the septum. A rectangular incision was made in the denuded cartilage septum, leaving the posterior aspect of the rectangle pedicled to the septum; this is called the swinging door principle (Fig. 1, above and Fig. 2, above, left). Immediately after this procedure, the septal cartilage lengthens because of the release of the so-called interlocked stresses, and an overlap occurs between the swinging door and the nasal septum. Verwoerd et al. [6] described this phenomenon earlier in our laboratory. Therefore, the swinging door was reduced such that it was freely moveable in the excised rectangle of the cartilage septum. The swinging door was scored on one side (randomly, either on the left or right side of the nose). Repeated parallel superficial incisions were made, leaving the swinging door to curl at 30 to 45 degrees (moderately bent) to the opposite site (Fig. 1, below and Fig. 2, above, right). In general, three to four incisions were sufficient. Under these conditions, it was technically

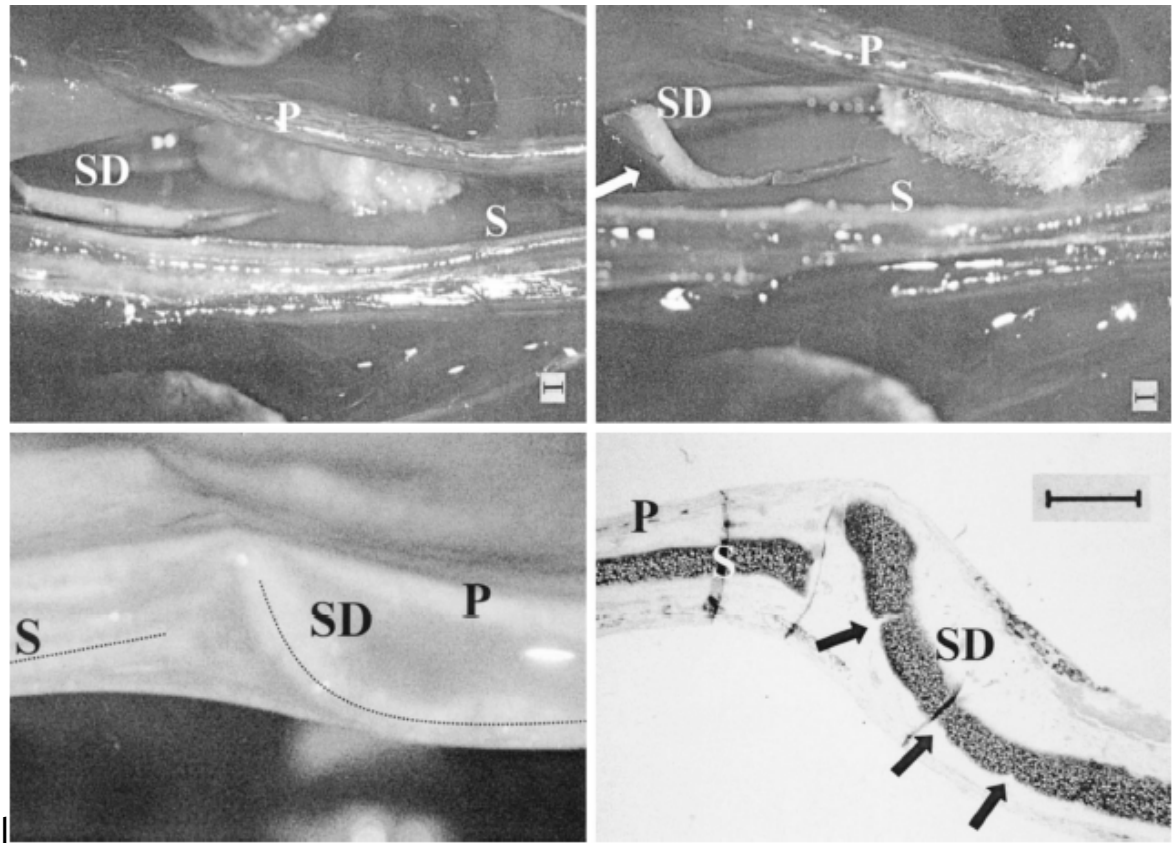

Fig. 2. For all panels (P, perichondrium; S, nasal septum; SD, swinging door; scale indicates 1 mm). (Above, left) Preparation of the swinging door during primary surgery. (Above, right) Intraoperative view; the cartilage is scored and bent (arrow, site of scoring). (Below, left) Macroscopic view 10 weeks after primary surgery; the dashed line represents the sectioned cartilage septum. (Below, right) Microscopic view; note the variable incision depth. Arrows, site of scoring.

impossible to adjust the desired incision depth. However, at the end of the follow-up period, histologic examination of the surgically treated septum showed that incisions never reached deeper than half the cartilage thickness. Thereafter, the mucoperichondrium was draped over the septum to completely cover the swinging door without tension, and the incisions were closed. At least 10 weeks after initial surgery, the animal was killed and the septum was excised.

Measurements. Because the operation site was tunnel-shaped and the upper-lateral cartilage obstructed a direct view from above, the angle of deviation (α) of the pedicled cartilage could be only roughly estimated during surgery (Fig. 2, above, right). Therefore, the following ordinate scale was used: straight (0 to 15 degrees), slightly bent (16 to 30 degrees), moderately bent (31 to 45 degrees), severely bent (46 to 60 degrees), and angulated (61 to 90 degrees). Ten weeks after the initial surgery, the septum was excised, the cartilage was cut along the deviated part, and the angle was estimated (Fig. 2, below, left). Then, the excised septum was processed for histologic study by embedding in paraffin; the sections were stained with Thionine (Fig. 2, below, right).

Ex vivo experiments

Surgical procedure. Eight New Zealand White rabbits weighing 1500 to 4000 g were included. Immediately after each rabbit was killed by intravenous pentobarbital (Euthasate), the complete cartilage septum was excised, stored at −20 °C, and packed in airtight plastic until further preparation.

Sample preparation. For each series of ex vivo experiments, a nasal septum was allowed to defrost at room temperature while still packed in plastic. The septum was cut rectangularly to uniform dimensions, 25x8 mm, and was glued to a holder using cyanoacrylate-based glue (CC-33a strain gauge cement, Kyowa Hakko Kogyo Co., Kyowa, Japan). To prevent dehydration and to minimize gravitational effects, the septum was placed in a bath of physiological saline.

Instruments. Using a thickness gauge, great effort was made to precisely measure the septum thickness along the line of incision. A pin was placed against the underside of the septum, and a freely movable linear variable differential transducer gauge was placed on top (Fig. 3, above). The precision of the displacement gauge was greater than 0.005 mm. Cutting was performed at a distance of 13mmfrom the holder. At this site, before the incision, the thickness was measured at eight consecutive points over the entire width of the specimen. Then, eight thickness samples were collected and the mean was calculated. Next, the variation of the thickness along the cutting line was calculated. This parameter is important, because variation in cartilage thickness or surface irregularities could bias the incision depth. Hence,

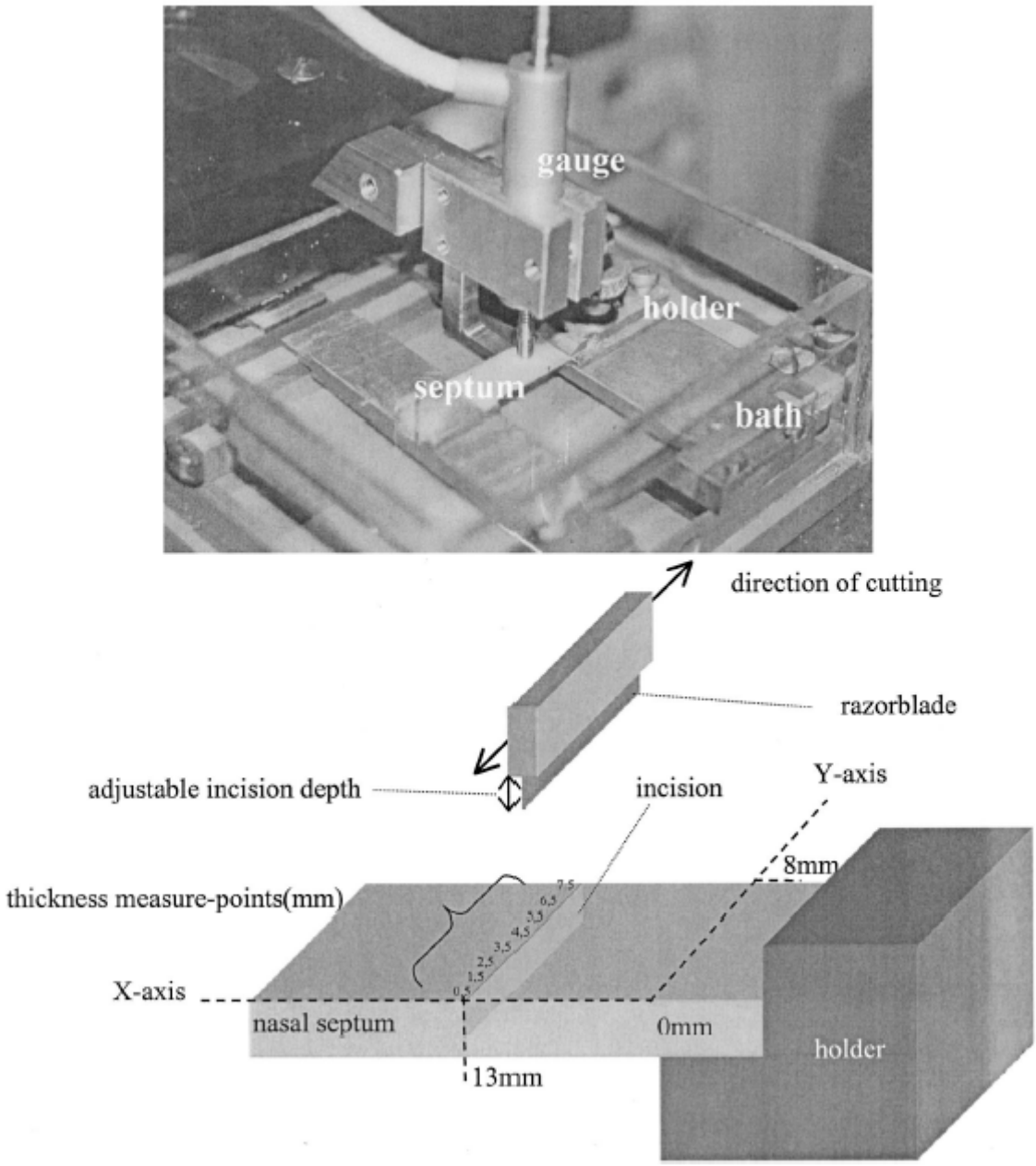

Fig. 3. Sequence of the ex vivo experiment. (Above) The Perspex bath with 0.9% saline; the nasal septal cartilage is fixed to a holder and the thickness gauge is indicated. (Below) Schematic outline of the experiment. The thickness is measured 0.5 to 7.5 mm from the free cartilage edge so that the complete width of 8 mm is adequately covered. Along this line, the cartilage is repeatedly cut with increasing depth.

the depth of incision is not equally distributed over the entire width of the septum. Figure 4 shows the variation of thickness in each specimen along the cutting line. To visualize thickness variations, we assumed the surface irregularities to be symmetric on both sides, and we graphically presented half the thickness of the septum. The schematic outline of the cutting experiment is illustrated in Figure 3, below. The incisions were made using a razor blade (GEM, Scientific Single Edge Blade, American Safety Razor, Industrial Product

Division, Verona, Va.). This blade was fixed in a brass holder to adjust the depth of the incision and attached to a one-dimensional movable carriage to diminish the effect of knife tilting during the incision. Calibration of the knife was performed using a microscope, magnification 50X (Olympus, BH2-HLSH), equipped with a camera (Sanyo, CCD video camera model no. VC 1960). In this way, the cutting depth could be adjusted to a precision level of less than 0.02 mm.

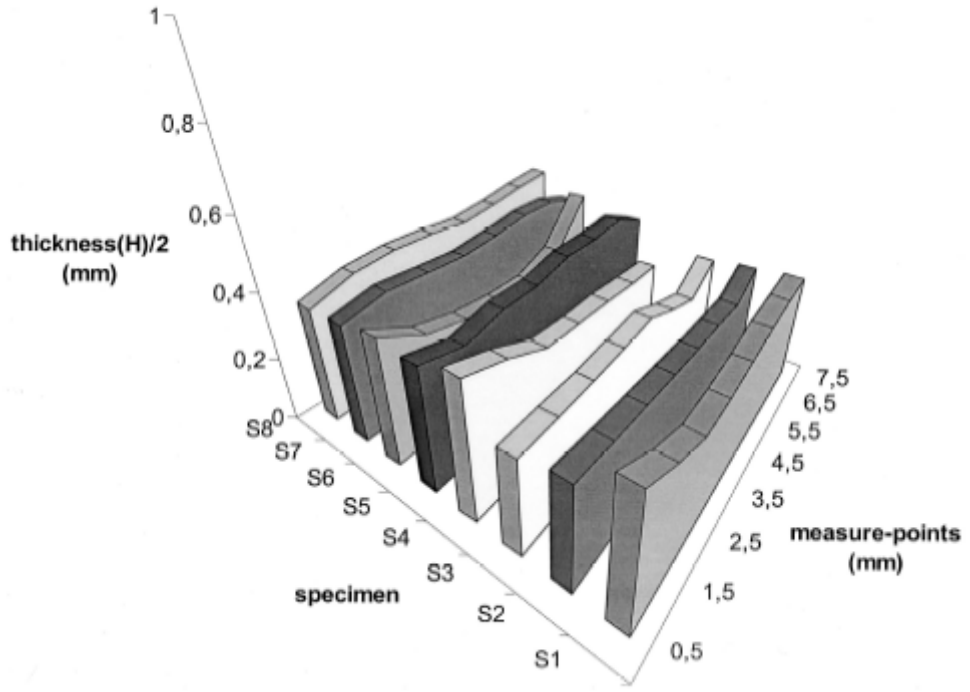

Fig. 4. Thickness (H) measured in eight specimens. To show the surface irregularities on one side of the septal cartilage, the true total thickness values are halved.

Signals and image acquisition. The nasal septum was placed on an X-Y table. The position of the septum fixed to the holder, the incision site, and the free tip of the septum was recorded by a HCS MX5 video camera for online examination capability.

Cutting experiments. Repeated incisions were made on top of the cartilage strip, located at 13 mm from the septum holder toward the free movable end (Fig. 3, below). The depth of each incision was increased step-by-step from 0.05 mm to 0.50 mm. The whole experiment was performed in a basin of physiological saline to prevent the cartilage from dehydration and to minimize gravitational effects.

We emphasize here that in contrast to the in vivo experiments, only one incision was made of increasing depth.

Statistical analysis. At the incision site, the mean thickness of the septum (H) was calculated. The depth of the incision (D) was calculated as a ratio (D_r) to the septum thickness, where $D_r = D/H$.

Because we found a linear relation between the depth of incision and degree of bending, we formulated a word model to describe this relationship. Bending was defined as the displacement of the free tip from the horizontal. Hence, the angle of deviation (α) was easily calculated. For each septum, bending (B) was expressed as a function of the relative incision depth (D_r). A line was fit through this set of observations by using the least squares method. The linear regression coefficient (*a*) was calculated for each septum. Furthermore, the standard error of the estimate (∈) was calculated. A model could be used to estimate the bending (in degrees) based on incision depth (D_r), where $B\alpha = a.D_r \pm \in$.

Results

Exploration of the long-term result of scoring: In vivo experiments

Immediately after creating the swinging door in the nasal septum, an overlap of the excised cartilage parts was observed. This phenomenon is one aspect of the internal strains present in the nasal septum and was previously described by Verwoerd et al. [6] During further surgery, curling of the straight rectangular piece of septal cartilage was observed directly after a few superficial parallel incisions were made. Scoring was continued until bending could be evaluated as moderate (30 to 45 degrees); three to four superficial incisions were sufficient to achieve this result. Ten weeks after surgery, the cartilage remained bent in all specimens toward the nonscored side. Although some variation in the degree of bending was observed, reverse bending was found in none of the specimens. The bending remained moderate (30 to 45 degrees) in three specimens. In one specimen the cartilage was slightly bent (15 to 30 degrees); in another the scored piece demonstrated angulation (60 to 90 degrees). Histologic examination showed vital cartilage; the incisions were still present 10 weeks after initial surgery. A variable amount of newly generated cartilage was observed at the site of subperichondrial dissection (Fig. 2, below, right).

Controlled experimental procedure to evaluate predictability of distortion: Ex vivo experiments

The average thickness along the line of incision of each individual specimen was calculated. The mean thickness of all of the different specimens was 0.68 mm (range, 0.56 to 0.81 mm). Therefore, incision depth was calculated as a ratio to the septum thickness. The cartilage thickness of the entire septum varies significantly. All of our specimens were thicker along the long sides of the rectangular incisions, which represent the part of the septum close to the upper lateral cartilages and the base close to the vomer in the

nose (Fig. 4). Therefore, the 'relative' incision depth of the septal cartilage will vary along the cutting line. The mean depth of incision as a ratio to the thickness of each cartilage septum ranged from 0.06 to 0.09 at an incision depth of 0.05 mm, and 0.62 to 0.89 at an incision depth of 0.50 mm.

Superficial scoring of the septum at a depth of 0.05 mm showed variable results; not all specimens became bent. Bending toward the nonscored side was observed in all specimens at a minimal incision depth of 0.10 mm. The angle between the fixed proximal part and free distal end of the nasal septum could be increased step-by-step with increasing incision depth (Fig. 5). No differences in bending were found between the septa taken from young and adult rabbits; therefore, all septa were considered as one group. The linear regression coefficient was calculated at 32.8 (p value = 0.06). Variation between specimens increased markedly above an incision ratio of 0.6 (Fig. 6). When the incision depth was restricted to maximal half-thickness, the linear regression coefficient was calculated at 30.9 (p value = 0.05). In conclusion, bending (B) is related to incision depth (D_r) when incisions are made up to half the cartilage thickness: $B\alpha = 30.9 \cdot D_r \pm 0.05$.

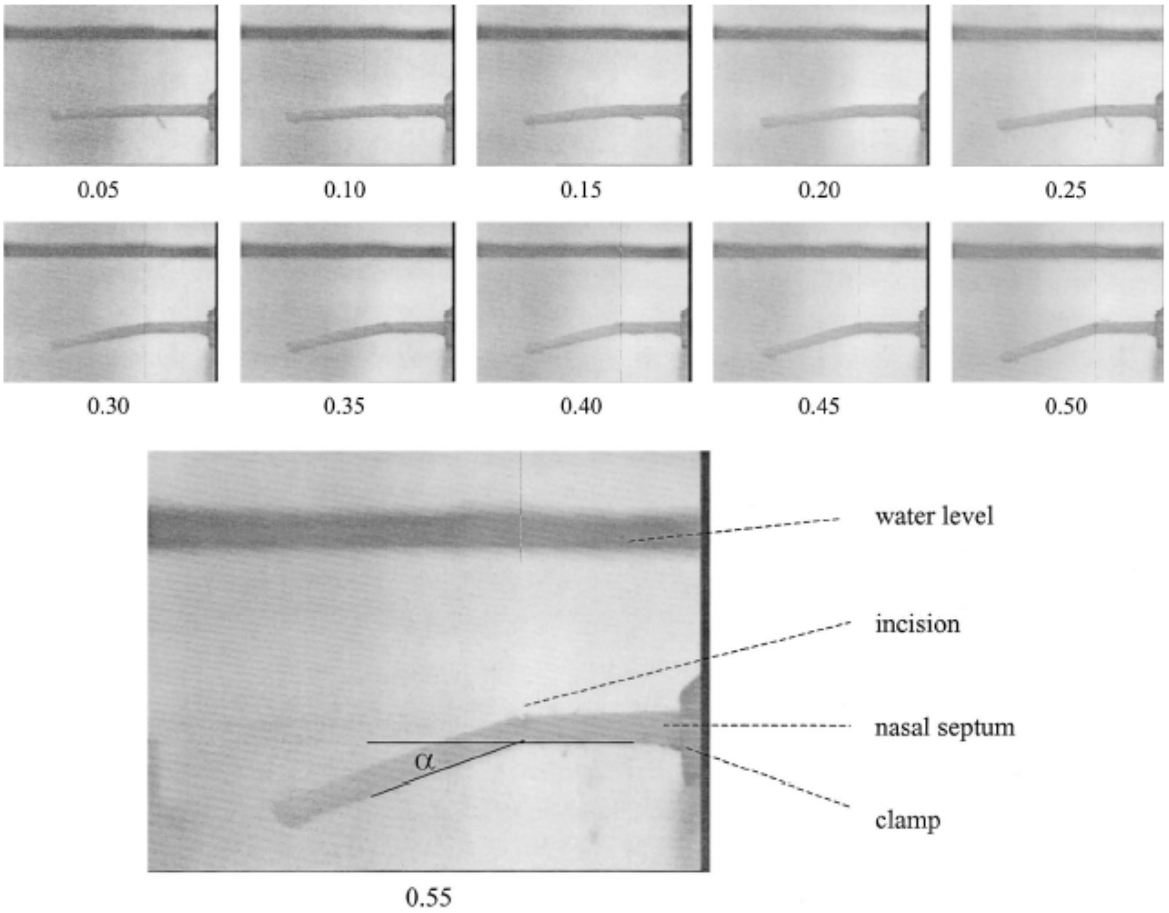

Fig. 5. On-line video monitor during ex vivo cutting experiments. Numbers indicate increasing incision depth in millimeters. The angle (α) is calculated.

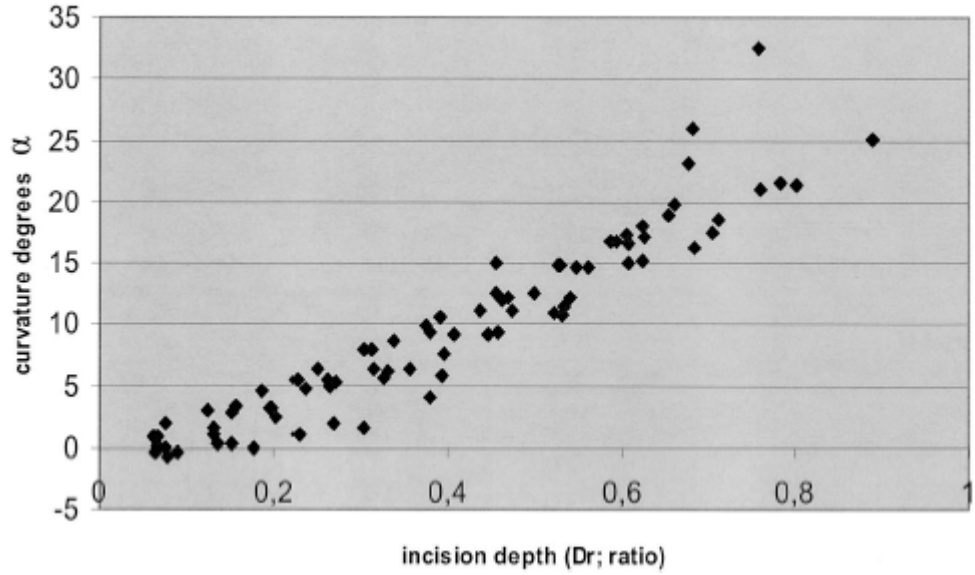

Fig. 6. Septal deviation in eight specimens. Incision depth is calculated as a ratio to the septum thickness (D_r); the angle (α) is measured between the proximal fixed part and distal freely movable tip.

Discussion

In septorhinoplasty and otoplasty, knowledge of the biomechanical behaviour of cartilage is of paramount importance. Scoring techniques are used to shape cartilage and are especially useful when delicate, small changes in cartilage curvature are desired or when a warped nasal septum must be straightened. Therefore, scoring is particularly relevant in rhinoplasty [2,7]; in otoplasty [8] suturing techniques are more practical for creating a true fold in the human pinna [9]. Scoring techniques are also known as directional tools. Bending or straightening of a piece of cartilage can be achieved by making superficial cuts; directly after cuts are made on one side of the cartilage, bending can be observed toward the untouched side. Fry and Robertson [10] and Gibson and Davis [11] demonstrated this pattern of bending in cartilage through a series of cutting experiments. Fry hypothesized the presence of internal stresses within the cartilage matrix and suggested that swelling effects are the potential mechanism for the existence of residual stresses and strains in cartilaginous tissue. The negatively charged cartilage matrix induces an osmotic pressure. Fry [12] demonstrated complete disappearance of residual stresses after intravenous injection of papain. Injection of this proteolytic enzyme attacks the negatively charged polysaccharide complex of the cartilage matrix, thus lowering the swelling pressure; the cartilage becomes limp. The swelling pressure is balanced by strains generated in the collagen network of the cartilage matrix [13]. In cutting experiments, the collagen network of the cartilage matrix is unilaterally damaged, inducing curling or

bending. As demonstrated in several cutting experiments, the interaction between swelling pressure and disruption of collagen fibrils leads to a new equilibrium and, consequently, to wrapping or straightening of the cartilage [8,10,14]. In earlier ex vivo experiments, bending of the scored cartilage remained present or increased slightly when the specimen was incubated for a few days [11,12].

In an exploratory study, we questioned whether the shape of a vital piece of scored nasal septal cartilage will change with time in vivo. Factors such as wound healing are involved in the final structure of the scored cartilage. Therefore, the nasal septal cartilage was scored in the live rabbit. Although some variation was observed, the initial created curvature had not changed greatly months after the primary surgery. To adequately measure the cartilage bending, the scored piece of cartilage was left pedicled to the remaining septum; therefore it was technically not possible to incise the cartilage at a specific depth. The inevitable variation in the superficial cuts made in the incision depth might also have contributed to the variable outcome. However, reverse bending of the septal cartilage was observed in none of the specimens. These results indicate the usefulness of controlled scoring techniques to reshape cartilaginous structures. With a more standardized procedure, the effect might be more reproducible and the outcome predictable. To be predictable, a correlation between incision depth and bending of the cartilage specimen must exist. To test this, a controlled series of experiments was performed using fresh rabbit septal cartilage. Incisions of only 0.05 mm (6.2 to 8.9 percent of the cartilage thickness) demonstrated variable results. Increasing the incision depth up to 0.10 mm (12.8 to 17.8 percent of the cartilage thickness) resulted in bending toward the intact side of the septal cartilage in all specimens. The surface irregularities along the incision line result from the variation of the total cartilage thickness, which has been measured up to 0.07 mm. Therefore at an incision depth of 0.05 mm, the cartilage might not be completely cut over the entire width of the specimen. Another explanation for the variable results when the septum is superficially incised could be the micro-architecture of the septum. As with other cartilage structures, such as the knee joint, collagen fibers of the cartilage matrix run parallel to the cartilage surface, whereas in the deeper portions a perpendicular direction is frequently found. A single superficial incision might not adequately cut through this layer; the remaining parallel fibers might prevent the septum from bending. Experiments in our laboratory suggest that this superficial layer must be completely incised to provide a threshold before bending will occur (data not shown). The thickness of this superficial layer of rabbit septal cartilage is close to 0.10 mm (approximately 15 percent of the total thickness). At an incision depth of at least 0.10 mm, bending was observed in all specimens.

In the experiments, each subsequent incision was gradually deepened by 0.05 mm so that the angle was increased step-by-step until an incision depth of 0.50 mm was reached. The variation between the different specimens increased markedly above an incision depth of more than 50 percent of the cartilage thickness (Fig. 6). Firmness of the cartilage septum is likely to decrease disproportionately at such incision depths; consequently, gravitation and variation of cartilage thickness within one specimen might become important confounding factors. A clear linear correlation was found between the depth of the incision and the measured angle of the specimen when the cartilage was incised up to a maximal depth of 50 percent of the cartilage thickness. The correlation coefficient (a) was calculated for each individual septum. Because the variation between the specimens was minimal, all septa were considered as one group. With this information, a model to predict distortion on incision was developed. For each individual incision depth (D_i), bending ($B\alpha$) of the specimen can be calculated using the formula $B\alpha = a.Di \pm \epsilon$, where a = 30.9 and ϵ = 0.05. For example, for the effect of a single incision of 25 percent of the total thickness, bending of the cartilage specimen is expected as such: 30.9 x 0.25 ±0.05 = 7.7 degrees ±0.05 degrees. This amount of bending might seem marginal; however, it must be noted that only one incision is made. Although the effect of one single incision is not of clinical relevance, it clearly shows that scoring gives consistent results and that cartilage is not an unpredictable material. In the clinical situation, multiple incisions will be made. Preliminary results have shown that each single incision added to the following incision linearly increases the degree of bending. This linearity holds true until the distance between the incisions becomes smaller than the incision depth (data not shown).

Although our results were consistent, in other experiments the scoring outcome was much more variable and the results less reproducible. For example, Murakami et al. [2] and Murray [15] were unable to reproduce earlier work performed by Fry [1] demonstrating interlocked stresses in cartilage. Murakami et al. found inconsistencies probably because of the heterogeneity of the specimens in which some of the perichondrium was left attached to the cartilage. Furthermore, their specimens could have disintegrated, because their experiments were performed up to 48 hours after donor death with no attempt to preserve the cartilage during this period. Because the effects of partial cartilage incisions have been disappointing to many investigators, full-thickness incisions are also being used to straighten bent cartilage, [2,7,16] or cartilage grafts are even crushed, as reported by Rubin [17]. Both of these techniques, however, weaken the cartilage graft dramatically and could have an adverse effect on the structural support of the nose, leading to saddle nose deformity. Besides scoring, other techniques are used to reshape cartilage. When a mechanically deformed cartilage is irradiated with laser energy,

internal stresses within the cartilage matrix will diminish. Consequently, cartilage may be moulded into the desired preset shape [18]. When the therapeutic interval is narrow, generating temperatures of up to 70 °C, chondrocyte degeneration and necrosis easily occur. Therefore, the viability of lasershaped cartilage has been questioned. After scoring or thermal ablation techniques, internal stabilization using Kirschner wires has been advocated [19]. Disadvantages of the latter technique, however, include extrusions and postoperative pain.

Conclusions

In vivo no significant morphological changes of the scored nasal septum were observed in the septa of adult rabbits 10 weeks after surgery. The septa generally retained their imposed shape, and reverse bending has not been observed. Under the controlled conditions of this study, incision depth was clearly correlated to cartilage bending. For clinical application, it is important that incisions are not too superficial; at least the superficial layer must be incised, which is about 15 percent of the total thickness of the cartilage. Hence, the degree of bending as the result of an incision (or a series of incisions) of a certain depth can be predicted. This allows preoperative or perioperative planning of the scoring procedure to reshape cartilaginous structures while accounting for maximal retention of the mechanical properties of the structures. Furthermore, it should be possible to design equipment that enables the surgeon to make incisions of a specific preset depth to avoid making incisions that are either too superficial and ineffective or too deep and destructive.

Acknowledgements

The authors thank Jan Sterk from the technical university in Delft, the Netherlands, for his assistance in setting up the ex vivo experiments, and the Animal Experimental Center of the Erasmus University Rotterdam for taking good care of the rabbits.

References

[1] Fry, H. J. Interlocked stresses in human nasal septal cartilage. Br. J. Plast. Surg. 19: 276, 1966.

[2] Murakami, W. T., Wong, L. W., and Davidson, T. M. Applications of the biomechanical behavior of cartilage to nasal septoplastic surgery. Laryngoscope 92: 300, 1982.

[3] Murray, J. A. The behaviour of nasal septal cartilage in response to trauma. Rhinology 25: 23, 1987.

[4] Oneal, R. M., Dodenhoff, R. J., and McClatchey, K. D. The role of perichondrium in modifying curved cartilage: An experimental study. Ann. Plast. Surg. 19: 343, 1987.

[5] Verwoerd, C. D., Urbanus, N. A., Mastenbroek, G. J., and Verwoerd-Verhoef, H. L. The role of the septal cartilage and the premaxillo-maxillary sutures in the outgrowth of the upper jaw. Acta Morphol. Neerl. Scand. 15: 227, 1977.

[6] Verwoerd, C. D. A., Verwoerd-Verhoef, H. L., and Meeuwis, C. A. Stress and wound healing of the cartilaginous nasal septum. Acta Otolaryngol. (Stockh.) 107: 441, 1989.

[7] Min, Y-G., and Chung, J. W. Cartilaginous incisions in septoplasty. J. Otorhinolaryngol. Relat. Spec. 58: 51, 1996.

[8] Stenstrom, S. J. A. "Natural" technique for correction of congenitally prominent ears. Plast. Reconstr. Surg. 32: 509, 1963.

[9] Mustarde´, J. C. The treatment of prominent ears by buried mattress sutures: A ten-year survey. Plast. Reconstr. Surg. 39: 382, 1967.

[10] Fry, H., and Robertson, W. V. Interlocked stresses in cartilage. Nature 215(96): 53, 1967.

[11] Gibson, T., and Davis, W. B. The distortion of the autogenous cartilage grafts: Its cause and prevention. Br. J. Plast. Surg. 10: 257, 1958.

[12] Fry, H. Cartilage and cartilage grafts: The basic properties of the tissue and the components responsible for them. Plast. Reconstr. Surg. 40: 526, 1967.

[13] Maroudas, A. I. Balance between swelling pressure and collagen tension in normal and degenerate cartilage. Nature 260(5554): 808, 1976.

[14] ten Koppel, P. G., van Osch, G. J., Verwoerd, C. D., and Verwoerd-Verhoef, H. L. The immediate effects of local trauma on the shape of the cricoid cartilage. Int. J. Pediatr. Otorhinolaryngol. 43: 1, 1998.

[15] Murray, J. A. The distribution of stress in the nasal septum in trauma: An experimental model. Rhinology 25: 101, 1987.

[16] Beeson, W. H. The nasal septum. Otolaryngol. Clin. North Am. 20: 743, 1987.

[17] Rubin, F. F. Permanent change in shape of cartilage by morselization. Arch. Otolaryngol. 89: 602, 1969.

[18] Wong, B. J., Milner, T. E., Harrington, A., et al. Feedback- controlled laser-mediated cartilage reshaping. Arch. Facial Plast. Surg. 1: 282, 1999.

[19] Gunter, J. P., Clark, C. P., and Friedman, R. M. Internal stabilization of autogenous rib cartilage grafts in rhinoplasty: A barrier to cartilage warping. Plast. Reconstr. Surg. 100: 161, 1997.

2D

Intrinsic and extrinsic forces determine the distortion of the split cricoid ring

International Journal of Pediatric Otorhinolaryngology 2004;68:1279–1288

Intrinsic and extrinsic forces determine the distortion of the split cricoid ring

Paul G.J. ten Koppel, Henriette L. Verwoerd-Verhoef,
Gerjo J.V.M. van Osch, Carel D.A. Verwoerd

Abstract

Objective: An anterior cricoid split (ACS) causes an immediate distortion of the cricoid cartilage resulting in an anterior gap due to retraction of the cut ends. The objective of this animal study is to investigate: (1) to what extent the distortion after ACS is influenced by non-cartilaginous structures like tunica elastica, membranes, ligaments and muscles, which are connected to the cricoid; (2) how distortion is changing with further development; (3) in what way the distortion is affected by scoring of the internal surface of the cricoid; and (4) whether an immediate or late injury-induced distortion is related to age.

Methods: Surgical interventions were performed in 20 young (8 weeks of age, 1300–1600 g) and 5 adult (28 weeks of age, 3500–4000 g) New Zealand White rabbits. The immediate effects were measured, and then the animals were followed for 20 weeks to study the long-term effects of the various procedures.

Results:

1. The gap, immediately following an ACS, increased after additional transection of the cricothyroid ligament and the cricotracheal membrane, and even more when the cricovocal membrane was elevated from the inner surface of the cricoid arch;
2. The degree of distortion after various interventions in young animals appeared to increase substantially during further growth;
3. When the abovementioned successive surgical steps were combined with scoring of the internal surface of the cricoid arch, a marked malformation of the split cricoid did develop with warping of the cut ends in lateral direction and a latero-cephalic rotation, the latter due to the action of the cricothyroid muscles;
4. The immediate distortion appeared to be similar in young and adult animals. During a follow-up of 20 weeks, a progressive distortion of the split cricoid ring was observed in the young growing rabbits. In adult animals, no significant progression of the distortion was found.

Conclusions: The immediate and long-term distortion of the split cricoid is determined by the release of intrinsic forces of the cartilage, and extrinsic forces from non-cartilaginous structures like ligaments, muscles, membranes and tunica elastica.

Introduction

Anterior and combined anterior–posterior cricoid splits are common practice in surgical treatment of subglottic stenosis in children. An anterior cricoid split (ACS) immediately leads to a gap between the cut ends due to distortion of the split cricoid ring, which in children is completely cartilaginous. Injury-induced distortion is a specific feature of cartilaginous structures. Cartilage as supporting tissue differs from bone by its elasticity and buoyancy. These properties are related to interlocked [1] or intrinsic [2] stresses, generated by the waterbinding properties of proteoglycans within a threedimensional network of collagen fibers present in the cartilage. Partial interruption of this network by an injury directly changes the pattern of intrinsic stresses resulting in a distortion of the cartilage. Hardly any clinical data are available on the later growth of a distorted cricoid. Animal experiments have demonstrated specific cricoid anomalies to develop after various types of splits and other lesions [3–5]. In vivo the cricoid is suspended in a symmetrical complex of muscles, membranes and ligaments. Consequently, it is exposed to mechanical forces related to breathing, swallowing, speech and gravity. Apparently, these external forces, exerted from different directions, are counterbalanced by the intact cartilaginous ring of the cricoid. Whether this balance is affected by a split or other injury of the cricoid ring had not yet been investigated.

Previously, two types of injury-induced distortion have been studied in isolated cricoids [6]. It was demonstrated that an ACS results in a gap between the cut ends, whereas additional scoring of the internal surface (ACS + S) of the cricoid promptly leads to further widening of this gap. This experimental study tries to answer the question whether in vivo external forces from ligaments, muscles, membranes and tunica elastica contribute to the degree of distortion of the cricoid, immediately after an ACS and ACS + S, and during long-term follow-up. The dimensions of the gap serve as a measure for the degree of distortion.

Materials and methods

Surgical interventions were primarily performed in 20 young New Zealand White rabbits (8 weeks of age, 1300–1600 g), which were followed for 20 weeks to study the long-term effects of the various procedures. In order to show the relevance of age and growth at the time of surgery, a few selected interventions were also performed in five adult New Zealand White rabbits (28 weeks of age, 3500–4000 g). The animal protocol was approved by the Animal Ethics Committee of the Erasmus University Medical Center Rotterdam (protocol no. 1269501). Anesthesia was effectuated through intramuscular injection with 2% xylazine-hydrochloride (Rompun•) 0.5 ml/kg, and 10% ketamine-hydrochloride (Ketalin•) 0.5 ml/kg. All animals survived surgery and showed no signs of respiratory distress. No animals were lost during the experimental period.

Experimental set-up

In the young animals, five experimental conditions were studied during surgery: series 1a, 1b', 1b, 2a and 2b. Four of these conditions were further evaluated after a follow-up of 20 weeks: 1A, 1B, 2A and 2B. The surgical procedures were planned in such a way that a minimal number of animals were used (Table 1). Series 3 included five adult rabbits. For reference, the cricoid was measured in five young and five adult non-operated animals.

Table 1. Experimental set-up for surgical interventions in young animals.

Surgery steps	Follow-up series				Primary surgery series	
1	X	X	X	X	1a	n=20
		|	|	|		
1,2		X	X	X	1b'	n=10*
		|	|	|		
1,2,3		X	X	X	1b	n=15
			|	|		
1,2,3,4			X	X	2a	n=5
				|		
1,2,3,4,5				X	2b	n=5
20 weeks follow-up	1A n=5	1B n=5	2A* n=5	2B n=5		

(1) Anterior cricoid split (ACS); (2) vertical incision cricothyroid ligament and horizontal transection cricotracheal ligament; (3) elevation cricovocal membrane from cricoid; (4) scoring cricoid arch; (5) transection of cricothyroid muscle.

* In series 2A, step 2 was not measured at primary surgery, therefore, not 15 but 10 animals could be included in series 1b'.

Anatomy

The cricotracheal ligament connects the inferior border of the cricoid cartilage to the first tracheal ring. The mid-ventral cricothyroid ligament is running from the upper rim of the cricoid cartilage to the lower rim of the thyroid cartilage [7]. The soft tissue lining of the subglottic lumen (conus elasticus /cricovocal membrane) includes a layer of elastic fibers (tunica elastica), which supports the mucosa and is suspended to the cricoid. This tunica elastica continues in caudal direction in the soft tissue lining of the trachea [8,9]. The cricothyroid muscle originates on the ventro-lateral surface of the cricoid arch and runs in dorso-cranial direction to its insertion on the thyroid cartilage.

Surgical procedures

In all animals, the operation site was shaved and disinfected with 70% ethanol. To reach the larynx, a mid-ventral incision through the skin was made. Overlying strap muscles were divided in the midline. In each of the experiments, one or more of the following surgical procedures were included (Table 1):

1. anterior cricoid split (ACS) leaving the soft tissue lining of the subglottic airway intact;
2. vertical incision of the cricothyroid ligament and horizontal transection of the cricotracheal membrane;
3. elevation of the soft tissue lining, including the cricovocal membrane, from the cricoid arch;
4. 'scoring' of the internal contour on both halves of the split cricoid arch by four parallel craniocaudal (vertical) incisions;
5. transection of the cricothyroid muscle close to its insertion on the cricoid.

Surgery was completed by repositioning of the strap muscles and closure of the skin in two layers. Twenty weeks after primary surgery, the neck was surgically explored for the second time to measure the dimension of the anterior gap.

In vivo measurements

In the live animals, the width of the anterior gap in the cricoid arch was measured with sliding callipers [0.05 mm, Helios, Germany] after each subsequent surgical step. In young rabbits, the anterior gap is likely to increase because of the enlargement of the cricoid ring during growth. Therefore, the dimensions of the gap are presented in millimeters, and as the ratio gap/circumference of the cricoid ring, at the age concerned.

The mean circumferences were calculated from measurements of ex vivo cricoids taken from five young and five adult non-operated animals. Since the cricoid ring is not round but oval-shaped, the maximal and minimal length (L) and width (W) of the inner (I) and outer (O) contour were measured. The circumference of the ring, used for reference, was estimated with the following formula:

$$¼ ((L_o+L_i)+(W_i+W_o))\pi$$

Statistical analysis

In young animals, growth of the cricoid ring during follow-up is expected. Therefore, the median, interquartile range and total range of the anterior gap were calculated in millimeters and in ratio to the cricoid circumference. As a consequence of the design of the study, the number of animals included after various surgical interventions, varied from 20 to 5 (Tables 1, 3 and 4). A non-parametric test for independent samples (Mann–Whitney U-test) was used to calculate significant enlargement of the anterior cricoid gap in millimeters and ratio after successive surgical interventions.

In adult animals, growth during follow-up is not expected. Therefore, the median, interquartile range and total range of the anterior gap were calculated in millimeters only.

Since for long-term follow-up the measurements (at 8 and 28 weeks of age) in all individual animals were paired, a non-parametric test for related samples (Wilcoxon signed ranks test) could be used in all series. A confidence limit of at least 95% (P-value < 0.05) was defined statistically significant.

Additional observations

At the end of the experimental period, the subglottic region was inspected in all adult animals, with a 1.7 and 3 mm 0° Hopkins endoscope (Storz•). Selected specimens of the subglottic region were processed for histology. Tissue material was fixated in 4% phosphate buffered formalin (pH 7.4), decalcified with 10% EDTA and embedded in paraffin. Transversal sections (7 μm) were stained with thionine.

Results

In the non-operated control animals, the median circumference of the cricoid ring was found to measure 20.8 mm at the age of 8 weeks and 26.2 mm at 28 weeks (Table 2).

Table 2. Circumference of the cricoid ring in control animals.

Young animals 8 weeks; n=5			Adult animals 28 weeks; n=5		
Circumference in mm			Circumference in mm		
median	interquartile range	total range	**median**	interquartile range	total range
20.8	20.0-21.9	19.5-22.4	**26.2**	25.4-27.0	24.8-27.2

Macroscopic observations–dimensions of the anterior gap

Primary surgery in young animals (8 weeks of age): series 1a, 1b', 1b, 2a and 2b (Table 3 and Fig. 1)

A split through the cricoid arch (series 1a) resulted in an immediate but small gap with a median of 0.3 mm, and a total range of 0.1–0.6 mm. Additionally, transection of the cricotracheal ligament with longitudinal division of the cricothyroid ligament (series 1b') induced a more than two-fold distraction of the cut ends. The median gap dimension measured was 0.7 mm (0.4–1.1 mm). Separating the soft tissue lining of the subglottic lumen from the inner surface of the cricoid arch (series 1b) further increased the ventral gap to 1.8 mm (1.4–2.3 mm). In Fig. 1, all measurements in series 1a, 1b' and 1b are outlined. After each of these surgical interventions, an increase of the anterior gap was calculated as significant (Table 3). By scoring of the inner surface of the cricoid ring (series 2a), the gap between the cut ends was enlarged to 2.9 mm (2.2–4.0 mm). Additional resection of the cricothyroid muscle (series 2b) did not significantly alter the median dimension of the gap (3.9 mm with a total range of 3.2–4.2 mm). Examples of the anterior gap as observed in series 1a, 1b and 2a are demonstrated in Fig. 2.

Twenty weeks after primary surgery in young animals: series 1A, 1B, 2A and 2B (Table 3 and Fig. 3)

For all the conditions studied, the gap between the cut ends increased significantly during the postsurgical period. When the cricoid was only split (series 1A), the initial gap of 0.3 (0.1–0.6 mm) augmented to 2.6 mm (1.8–2.8 mm). After ACS combined with transection of the cricotracheal and cricothyroid ligaments with elevation of the soft tissue lining (series 1B) the gap increased from 1.8 mm (1.4–2.3 mm) to 4.8 mm (2.3–6.8 mm). The normally oval-

shaped cricoid ring is transformed into a U-shaped structure (Fig. 4). Between series 1A and 1B, a significant difference in the dimensions of the gap was calculated (Table 3).

Table 3. The dimensions of the anterior gap in young animals at surgery, and 20 weeks later.

	Primary surgery gap in mm *ratio: gap/circumference*				Follow-up 20 weeks gap in mm *ratio: gap/circumference*		
surgery steps	**median**	interquartile range	total range		**median**	interquartile range	total range
1	**0.3** *0.014*	0.2-0.3 *0.010–0.014*	0.1-0.6 *0.005–0.028* *series 1a*	➡ *p=0,043*	**2.6** *0.100*	2.0-2.8 *0.077–0.107*	1.8-2.8 *0.070–0.107* *series1A*
	p=<0.001 ⇩				p=0.041 ⇩		
1,2	**0.7** *0.034*	0.7-0.9 *0.032-0.043*	0.4-1.1 *0.019-0.053* *series1b'*				
	p=<0.001 ⇩						
1.2.3	**1.8** *0.087*	1.6-2.1 *0.077-0.101*	1.4-2.3 *0.067-0.111* *series1b*	➡ p=0,043	**4.8** *0.184*	3.2-5.9 *0.123-0.226*	2.3-6.8 *0.088-0.260* *series1B*
	p=0.001 ⇩				p=0.009 ⇩		
1,2,3,4	**2.9** *0.139*	2.2-3.8 *0.106-0.183*	2.2-4.0 *0.106-0.192* *series 2a*	➡ p=0,043	**12.7** *0.487*	10.5-17.5 *0.402-0.670*	9.0-19.0 *0.345-0.728* *series 2A*
	p=0,142 ⇩				p=0,251 ⇩		
1,2,3,4,5	**3.9** *0.188*	3.2-4.2 *0.154-0.202*	3.0-4.4 *0.154-0.212* *series 2b*	➡ p=0,043	**14.9** *0.570*	13.7-20.2 *0.525-0.774*	13.1-20.5 *0.502-0.785* *series2B*

⇩ Nonparametric tests for independent samples (Mann-Whitney *U*-test). ➡ Nonparametric test for related samples (Wilcoxon signed ranks test). (1) Anterior Cricoid Split (ACS); (2) vertical incision cricothyroid ligament and horizontal transection cricotracheal ligament; (3) elevation cricovocal membrane from cricoid; (4) scoring cricoid arch; (5) transection of cricothyroid muscle.

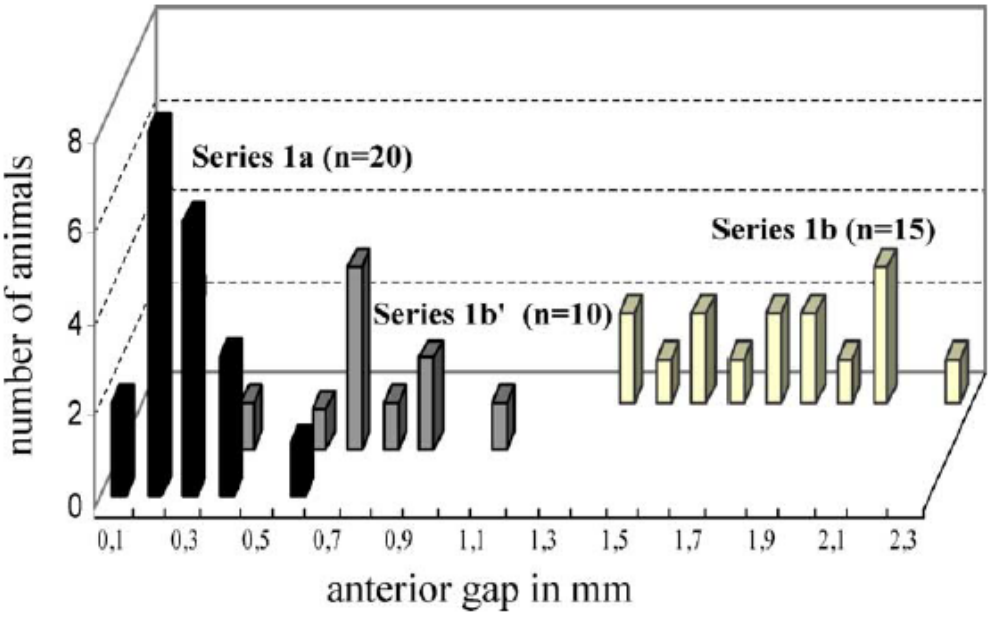

Fig. 1. The anterior gap measured at primary surgery after an anterior cricoid split (series 1a) and vertical incision of the cricothyroid ligament and horizontal transection of the cricotracheal ligament (series 1b') and elevation of the cricovocal membrane from the cricoid (series 1b).

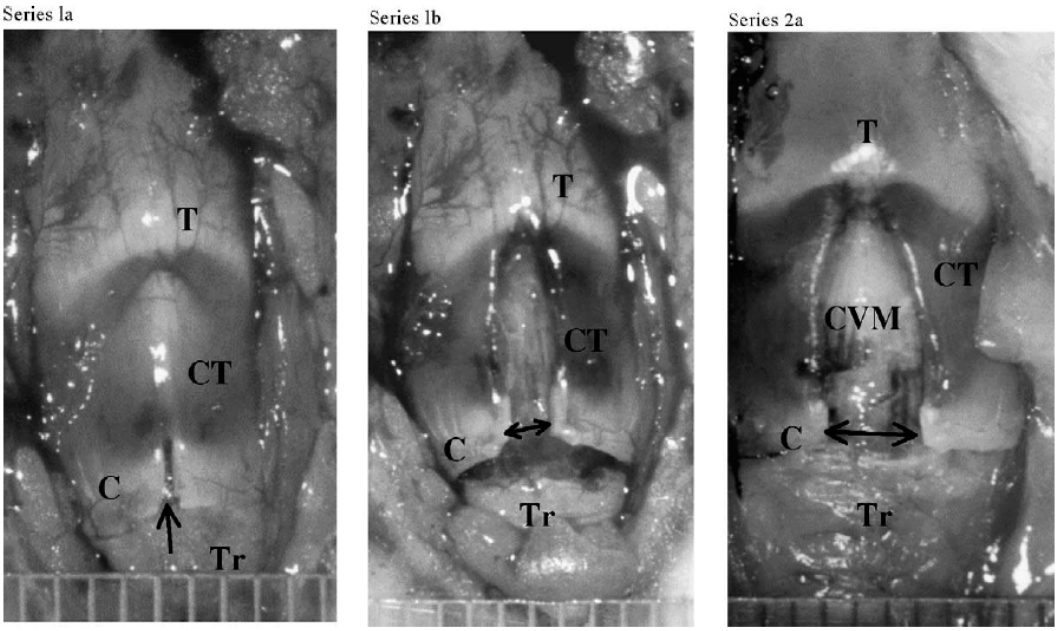

Fig. 2. Ventral view of the larynx at 8 weeks; see Table 1 for surgery steps. C = cricoid cartilage; T = thyroid cartilage; Tr = first tracheal ring; CT = cricothyroid muscle; CVM = cricovocal membrane; ↔ gap between the cut ends.

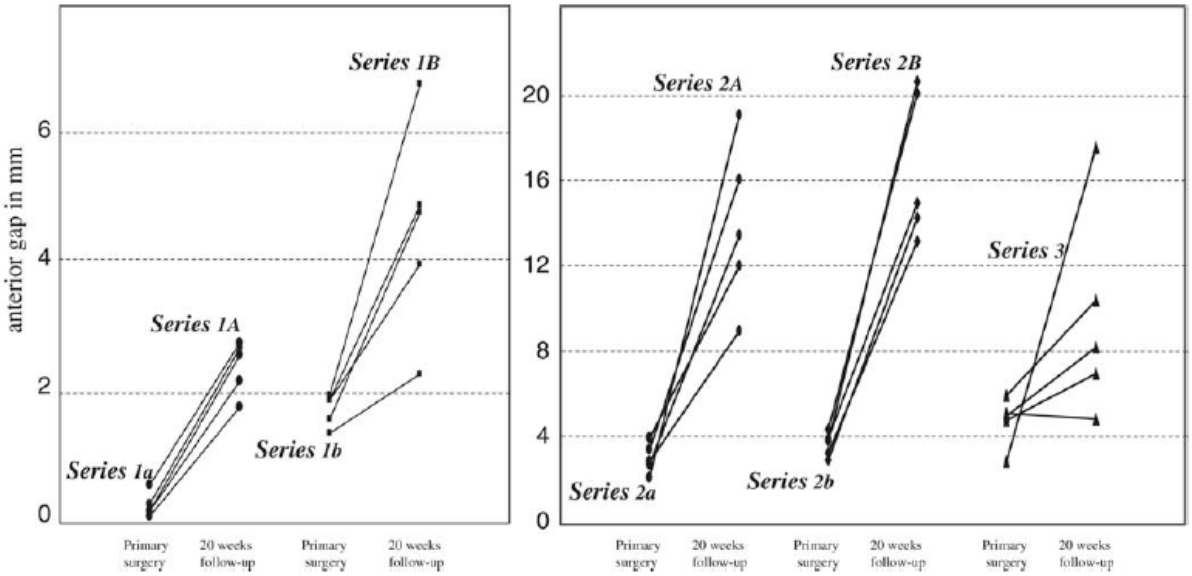

Fig. 3. Increase of the anterior gap during 20 weeks follow-up of series 1a-A, 1b-B, 2a-A, 2b-B (primary surgery at the age of 8 weeks) and series 3 (primary surgery at the age of 28 weeks); surgical steps are summarized in Table 1, the measurements in Tables 2 and 3.

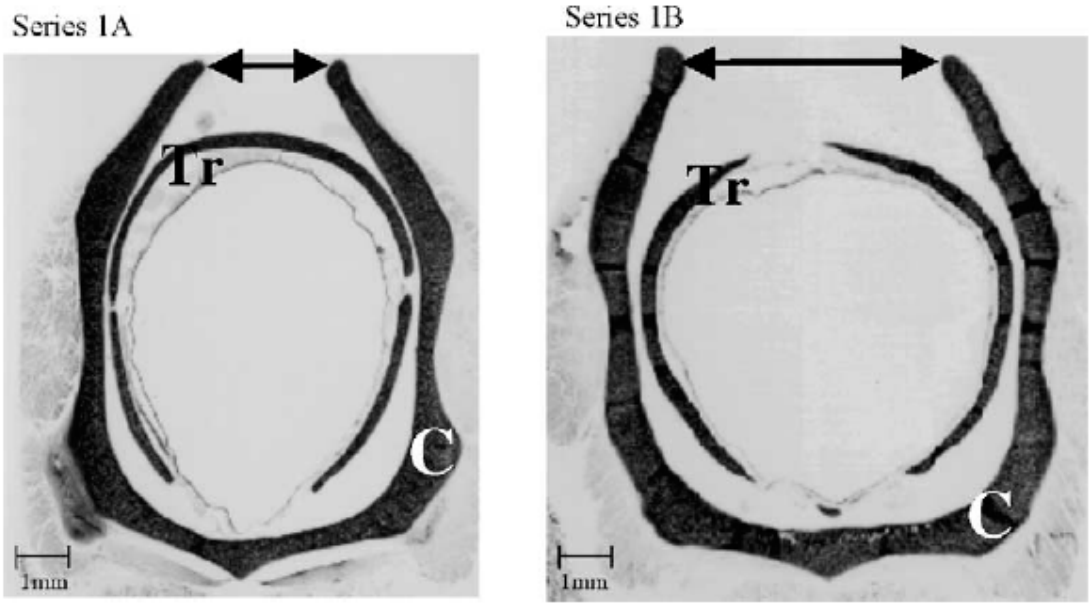

Fig. 4. Histologic sections of series 1A and 1B, 20 weeks after primary surgery at the age of 8 weeks; see Table 1 for surgery steps. C = cricoid cartilage; Tr = first tracheal ring; ↔ gap between the cut ends. The anterior gap in series 1A shows a lesser degree of distortion and, thus, a smaller anterior gap than in series 1B (see Table 2).

Additional scoring of the inner surface of the cricoid demonstrated marked developmental consequences 20 weeks later. Then, in four out of five animals (series 2A), the free ends of the transformed cricoid were warped outwards with a rotation of the lower margin in latero-cephalic direction (Figs. 5 and 6). In case the cricothyroid muscle was transected as well (series 2B), only one animal demonstrated a rotation as observed in series 2A, whereas the other four showed warping of the anterior cut ends without rotation.

The outward warping is reflected in the dimensions of the anterior gap. In series 2A, the distance between the cut ends increased from 2.9 mm (2.2–4.0 mm) at surgery to 12.7 mm (9.0–19.0 mm) 20 weeks later; in series 2B, the gap was enlarged from 3.9 mm (3.0–4.4 mm) to 14.9 mm (13.1–20.5 mm). No significant differences were demonstrated between series 2A and 2B as far as the dimensions of the gap were concerned.

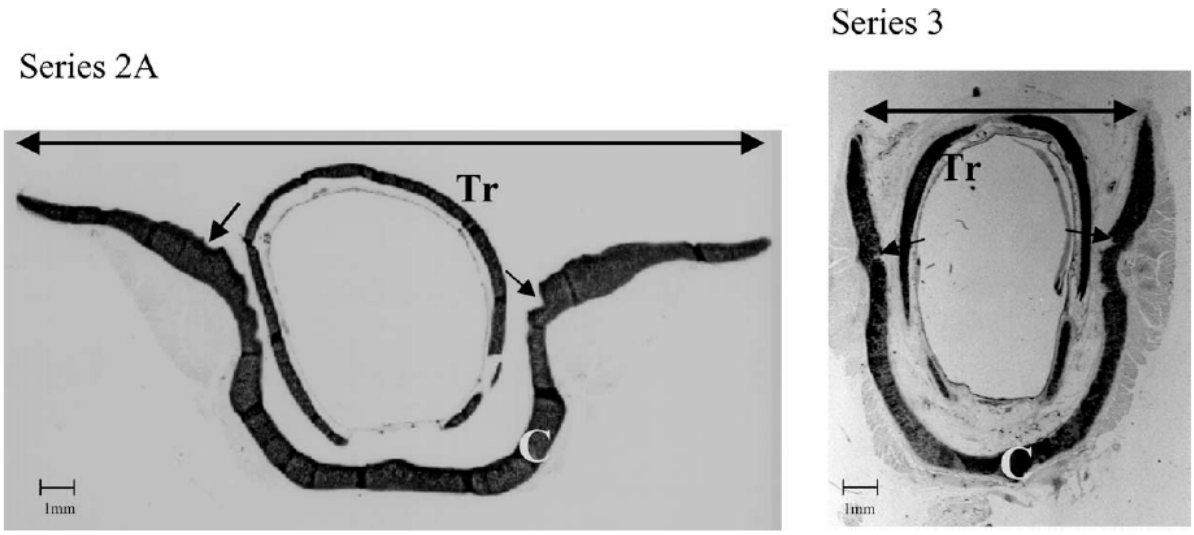

Fig. 5. Histologic sections 20 weeks after primary surgery in young (series 2A) and in adult animals (series 3); see Table 1 for surgery steps. C = cricoid cartilage; Tr = first tracheal ring; ↔ gap between the cut ends, scale indicates millimetres; → effects of scoring of the internal side. Series 2A shows a tulip-like distortion; series 3 demonstrates less distortion.

Primary surgery in adult animals (28 weeks of age): series 3 (Table 4)

The observations in adult animals are similar to those described for the young rabbits. A small gap, occurring after an ACS of 0.2 mm (0.2–0.4 mm), is widening stepwise during separation of the adhering structures and finally measuring 2.5 mm (1.4–3.0 mm). By scoring of the internal surface of the cricoid, the anterior gap was enlarged to 5.0 mm (2.9–6.0 mm).

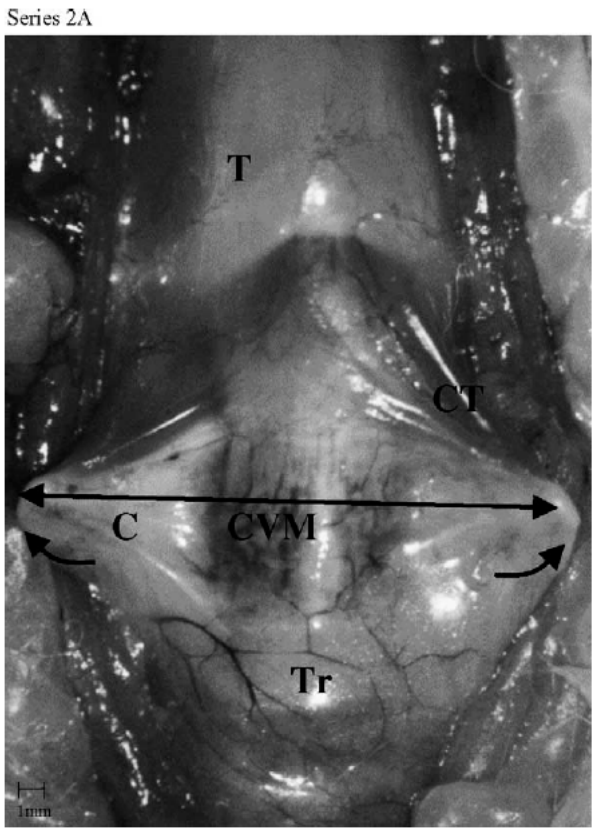

Fig. 6. Ventral view of the rabbit larynx in series 2A, observed 20 weeks after surgery at the age of 8 weeks; see Table 1 for surgery steps. C = cricoid cartilage; T = thyroid cartilage; Tr = first tracheal ring; CT = cricothyroid muscle; CVM = cricovocal membrane; ↔ gap between the cut ends of a grossly distorted cricoid (see Fig. 5). ↖↘ Rotation in latero-cephalic direction of the lower margin of the ventral ends of the split cricoid (see Fig. 5).

Twenty weeks after primary surgery in adult animals: series 3 (Table 4 and Fig. 3)

Also in these animals, warping of the split cricoid appeared to be a late effect of scoring, however, to a lesser extent than in animals operated at a young age (Fig. 5). Plotting of this series (Fig. 3) demonstrated that only in one out of five animals the gap reached the higher values previously found in series 2A and 2B. No significant difference was found in this series 3 between the measurements at the time of surgery and after the follow-up period.

Additional observations

At the end of the experimental period, the subglottic airway was found to be patent. Neither granulation tissue nor stenosis were observed at endoscopy.

Microscopic sections of specimens, 20 weeks after scoring of the internal surface of the cricoid ring, showed that most lesions were superficial and never reached deeper than half of the thickness of the cartilage (Fig. 5). Occasionally, some reactive neocartilage was observed at the scoring site. The soft tissue lining of the subglottic lumen demonstrated a normal aspect.

Table 4. The dimensions of the anterior gap in young animals at surgery, and 20 weeks later.

	Primary surgery (gap in mm)				Follow-up 20 weeks (gap in mm)		
surgery steps	**median**	inter-quartile range	total range		**median**	inter-quartile range	total range
1	**0.2**	0.2-0.4	0.2-0.4				
	p=0,041 ⬇						
1,2	**0.6**	0.6-0.7	0.6-0.7				
	p=0,043 ⬇						
1.2.3	**2.5**	1.9-2.9	1.4-3.0				
	p=0,041 ⬇						
1,2,3,4/5*	**5.0**	3.85-5.6	2.9-6.0 series3*	➡ p=0.080	**8.2**	5.95-13.95	4.9-17.5 series3*

⬇ /➡ Non-parametric test for related samples (Wilcoxon signed ranks test). (1) Anterior cricoid split (ACS); (2) vertical incision cricothyroid ligament and horizontal transection cricotracheal ligament; (3) elevation cricovocal membrane from cricoid; (4) scoring cricoid arch; (5) transection of cricothyroid muscle. * Series 3 is a heterogeneous group; in two animals, surgery steps 1–5 were performed; in three animals, steps 1–4 were performed.

Discussion

Injury-specific distortions of cartilage structures have been ascribed to intrinsic forces or interlocked stresses present within the cartilage. This study answers the question whether extrinsic forces from ligaments, muscles, membranes and tunica elastica contribute to a distortion in vivo.

The influence of adhering structures on the immediate distortion of the split cricoid

In young animals, it was shown that the anterior gap after ACS (0.3 mm) enlarges after transection of the cricothyroid and cricotracheal ligaments (0.7 mm), and to an even larger extent after additional elevation of the cricovocal

membrane from the endolaryngeal surface of the cricoid arch (1.8 mm). As the latter dimension is in the same range (1.49 ±0.5 mm) as was earlier observed in ex vivo isolated cricoids, we conclude that in vivo the adhering soft tissues actually restrict the split-induced distortion of the cartilage [6]. In particular, the tunica elastica seems to play an important role.

The influence of adhering structures on the evolution of cricoid distortion after ACS, during growth

During the 20-week-long period of growth of the rabbits into adulthood, the distortion appeared to be progressive. The anterior gap increased from 0.3 to 2.6 mm after ACS, and from 1.8 to 4.8 mm after ACS in combination with separation of the adhering structures. This observation demonstrates that also the growth-related progression of the cartilage distortion is limited by the adhering membranes and ligaments.

Immediate and long-term distortion of the split cricoid after scoring of the endolaryngeal surface of the cricoid arch

It is well known that making a series of parallel incisions (scoring) in the nasal septum on one side results in an immediate bending of the cartilage. The previously straight septum becomes concave to the non-injured side [1]. Essentially, the same phenomenon is presented by the immediate unbending of the left and right halve of a split cricoid arch, due to scoring of the internal surface (series 2a and 2b). Consequently, the distance between the two cut ends has increased and the cricoid has taken on a U-form.

As we previously demonstrated for the nasal septum, the degree of cartilage bending is depending on the depth of the scoring incisions [10]. Therefore, the variation in the dimensions of the anterior cricoid gap after scoring could be explained by the varying depth of the incisions.

After further growth (20 weeks follow-up), the scored parts of the cricoid showed an obvious warping, changing the initial U-form into a tulip-like configuration (Fig. 5) and, thus, contributing to the large distance measured between the cut edges. It is evident that scoring affects the future growth pattern of a split cricoid.

Progressive distortion of an intact cricoid ring has been previously reported to develop after an endolaryngeal injury in the young rabbit [4,11]. The injury resulted in a circular scar considered to be responsible for partial collapse of the cricoid. Observations in series 2A and 2B show that a similar progressive distortion might develop due to an altered growth pattern of the cartilage without any scarring of the soft tissue lining being present.

Effects of muscle action

A minor but interesting difference was found between series 2A and 2B. Only in series 2A with an intact cricothyroid muscle, the split cricoid demonstrated next to warping, an outward rotation of the inferior ventral margins (Fig. 6). Resection of the cricothyroid muscles (series 2B) appeared to prevent this rotation but did not diminish the progressive warping of the ventro-lateral parts of the cricoid.

Senders et al. found that denervation of the cricothyroid muscle induced an immediate increase of distraction of the cut ends [12]. It is possible that in our study the animals were too deeply sedated to show such an effect after resection of the cricothyroid muscle. In the long-term follow-up, however, unlike Senders et al. [12] we did find a marked effect of the cricothyroid muscle upon the final morphology of the split ring. It appeared to have resulted in a latero-cephalic rotation of the lower margin of the split cricoid (Fig. 6).

Previously, Bean et al. [5] concluded that after a combined anterior–posterior split, the cricopharyngeal muscle is responsible for an increased widening of the anterior gap due to outward inclination of both cricoid halves. A similar effect is not feasible in this study as the thick posterior lamina was left untouched.

Distortion of the cricoid in relation to age

Young growing and adult fully grown animals showed essentially the same degree of distortion, immediately after ACS and ACS combined with separation of adhering structures. This may not be a surprising observation as in both stages the cricoid in rabbits is completely cartilaginous. A widening of the anterior gap was found in both age groups after additional scoring of the internal surface of the split cricoid arch. However, the progression of the distortion in adult animals appeared to be less prominent than in young rabbits. This observation strongly suggests that growth enhances the long-term distortion.

Concluding remarks

There are only a few publications dealing with the histopathology of human specimens of subglottic stenosis [13–16]. The majority focuses on wound reaction and scar formation of mucosa, submucosa and cartilage. Chen and Holinger [14] reported a gross distortion of the cricoid in specimens of very young patients with subglottic stenosis. Regression and some repair of cartilage were also observed in surgical specimens obtained by partial cricoid resection

followed by end-to-end anastomosis (Prof. Dr. Ph. Monnier, ENT Department of the University of Lausanne) [16]. The few cases, in which no previous ACS was performed, the resected cricoid arch showed no obvious distortion [16]. The specimens of Chen–Holinger series tended to be of a younger age than the Monnier series. This suggests that the occurrence of distortion could be related to the age at the time of injury. This hypothesis is further supported by earlier experimental studies in which distortion of the cricoid after a similar endolaryngeal trauma was observed to develop in young animals only [11] and not in adult rabbits [17]. Moreover, Mankarious et al. [18] recently described an age-related difference in the occurrence of a distortion after an endolaryngeal trauma involving the perichondrial layer of the cricoid cartilage.

Finally, it may be concluded that our study demonstrated for the first time a mechanical balance between the intrinsic 'stability' of injured cartilage and extrinsic forces such as generated by membranes, ligaments, muscles and tunica elastica.

Actually these extrinsic factors modulate the immediate autonomous distortion of the cricoid cartilage after injury as well as the progression of such a distortion in the long run. We demonstrated that the postnatal development of the split cricoid can be thoroughly influenced, and thus, manipulated by various surgical interventions. Whether this is also possible for an abnormal (congenital or posttraumatic) cricoid remains to be evaluated.

Acknowledgements

The authors like to thank Marjan H. Wieringa, Ph.D., epidemiologist, for her critical review of the statistical analysis.

References

[1] H.J. Fry, Interlocked stresses in human nasal septal cartilage, Br. J. Plast. Surg. 19 (1966) 276–278.

[2] C.W. Senders, S.P. Tinling, The intrinsic response of the cricoid cartilage to vertical division, Int. J. Pediatr. Otorhinolaryngol. 28 (1993) 33–39.

[3] F.C. Adriaansen, H.L. Verwoerd-Verhoef, R.O. van der Heul, C.D. Verwoerd, Morphometric study of the growth of the subglottis after interruption of the circular structure of the cricoid, ORL J. Otorhinolaryngol. Relat. Spectrosc. 50 (1988) 54–66.

[4] C.D. Verwoerd, J.K. Bean, F.C. Adriaansen, H.L. Verwoerd-Verhoef, Trauma of the cricoid and interlocked stress, Acta Otolaryngol. 111 (1991) 403–409.

[5] J.K. Bean, H.L. Verwoerd-Verhoef, C.D. Verwoerd, Intrinsic and extrinsic factors relevant to the morphology of the growing cricoid ring after a combined anterior and posterior cricoid split: an experimental study in rabbits, Int. J. Pediatr. Otorhinolaryngol. 29 (1994) 129–137.

[6] P.G. ten Koppel, G.J. van Osch, C.D. Verwoerd, H.L. Verwoerd-Verhoef, The immediate effects of local trauma on the shape of the cricoid cartilage, Int. J. Pediatr. Otorhinolaryngol. 43 (1998) 1–10.

[7] M.M. Reidenbach, The cricothyroid space: topography and clinical implications, Acta Anat. 157 (1996) 330–338.

[8] M.M. Reidenbach, Normal topography of the conus elasticus. Anatomical bases for the spread of laryngeal cancer, Surg. Radiol. Anat. 17 (1995) 107–111.

[9] M.M. Reidenbach, The attachments of the conus elasticus to the laryngeal skeleton: physiologic and clinical implications, Clin. Anat. 9 (1996) 363–370.

[10] P.G. ten Koppel, J.M. van der Veen, D. Hein, F. van Keulen, G.J. van Osch, H.L. Verwoerd-Verhoef, C.D. Verwoerd, Controlling incision-induced distortion of nasal septal cartilage: a model to predict the effect of scoring of rabbit septa, Plast. Reconstr. Surg. 111 (2003) 1948–1957 (Discussion, pp. 1958–1959).

[11] F.C. Adriaansen, H.L. Verwoerd-Verhoef, R.O. Van der Heul, C.D. Verwoerd, A morphometric study of the growth of the subglottis after endolaryngeal trauma, Int. J. Pediatr. Otorhinolaryngol. 12 (1986) 217–226.

[12] C.W. Senders, P. Eisele, Independent effects of denervating the cricothyroid muscle and stenting on the anterior cricoid split: canine model, Int. J. Pediatr. Otorhinolaryngol. 17 (1989) 213–224.

[13] G.F. Tucker, L. Newton, R.J. Ruben, Histopathology of acquired subglottic stenosis. A documented case report, Ann. Otol. Rhinol. Laryngol. 90 (1981) 335–338.

[14] J.C. Chen, L.D. Holinger, Acquired laryngeal lesions, Arch. Otolaryngol. Head Neck Surg. 121 (1995) 537–543.

[15] S.J. Gould, J. Graham, Long term pathological sequelae of neonatal endotracheal intubation, J. Laryngol. Otol. 103 (1989) 622–625.

[16] M.L. Duynstee, R.R. de Krijger, Ph. Monnier, C.D. Verwoerd, H.L. Verwoerd-Verhoef, Subglottic stenosis after endolaryngeal intubation in infants and children: result of wound healing processes, Int. J. Pediatr. Otorhinolaryngol. 62 (2002) 1–9.

[17] J.K. Bean, H.L. Verwoerd-Verhoef, C.D. Verwoerd, Injuryand age-linked differences in wound healing and stenosis formation in the subglottis, Acta Otolaryngol. 115 (1995) 317–321.
[18] L.A. Mankarious, S.R. Cherukupally, A.B. Adams, Gross and histologic changes in the developing rabbit subglottis in response to a controlled depth of injury, Otolaryngol. Head Neck Surg. 127 (2002) 442–447.

Chapter 3

Engineered cartilage to enhance wound healing

3A

The efficacy of perichondrium and a trabecular demineralized bone matrix for generating cartilage

Plastic and Reconstructive Surgery1998;102(6):2012–20

The efficacy of perichondrium and a trabecular demineralized bone matrix for generating cartilage

Paul GJ ten Koppel, Gerjo JVM van Osch,
Carel DA Verwoerd, Henriette L Verwoerd-Verhoef

Abstract

A pedicled auricular perichondrial flap wrapped around trabecular demineralized bovine bone matrix can generate an autologous cartilage graft. In earlier experimental studies, it was demonstrated that this graft could be used for nasal and cricoid reconstruction. It was assumed that the vascularization of the perichondrial flap was obligatory, but it was never proven that the flap should be pedicled. Moreover, for clinical use, the dimensions of the auricle would set restrictions to the size of the graft generated. Therefore, the possibility to generate cartilage with a composite graft of a free perichondrial flap wrapped around demineralized bovine bone matrix, by using young New Zealand White rabbits, was studied. This composite graft was implanted at poorly (subcutaneously in the abdominal wall; n=12), fairly (subcutaneously in the pinna; n=12), and well-vascularized sites (quadriceps muscle; n=12). As a control, trabecular demineralized bovine bone matrix was implanted without perichondrial cover. Half of these grafts (n=6) were harvested after 3 weeks, and the remaining grafts (n=6) after 6 weeks of implantation. In histologic sections of these grafts, the incidence of cartilage formation was scored. Furthermore, the amount of newly formed cartilage was calculated by computerized histomorphometry. Trabecular demineralized bovine bone matrix without perichondrial cover demonstrated early resorption; no cartilage or bone was formed. In demineralized bovine bone matrix wrapped in perichondrium, early cartilage formed after 3 weeks at well- and fairly vascularized sites. No cartilage could be detected in grafts placed at a poorly vascularized site after 3 weeks; minimal cartilage formed after 6 weeks. In summary, the highest incidence of cartilage formed when trabecular demineralized bovine bone matrix was wrapped either in a pedicled auricular perichondrial flap or in a free perichondrial flap, which was placed at a well-vascularized site. Second, a significantly higher percentage of the total area of the graft was cartilaginized at well-vascularized sites after 3 weeks. The newly generated cartilage contained collagen type II and proteoglycans with hyaluronic acid binding regions, whereas collagen type I was absent, indicating the presence of hyaline cartilage. This study demonstrates that new cartilage suitable for a graft can be generated by free perichondrial flaps, provided that the site of

implantation is well vascularized. Consequently, the size of such a graft is no longer limited to the dimensions of the auricle.

Introduction

Reconstruction of cartilage defects with cartilage graft is a regular challenge for otorhinolaryngologists, plastic and reconstructive surgeons, and orthopedic surgeons. To fill a cartilage defect, autologous cartilage is preferable to avoid the risk of transmittable diseases and to prevent immunologic reactions. Rib or pinna cartilage is frequently used; however, donor site morbidity, developmental anomalies of the donor structure, early resorption of the graft, limited volume, and poor bonding characteristics of the cartilage available are main disadvantages [1–3]. These disadvantages could be partly overcome either by in vitro engineered cartilage or by the heterotopic induction and formation of new cartilage in vivo [4–6].

In various animal studies, perichondrium has been described as forming new cartilage [7–10]. However, if any cartilage was formed, the amount was variable and limited [11–13]. Previously, we described a technique to generate autologous cartilage in a high incidence [14]. In young rabbits, trabecular demineralized bovine bone matrix was wrapped in ear perichondrium and transformed into cartilage in a period of 3 weeks. This method is based on the chondrogenic potential in the combination of perichondrium and demineralized bone matrix. The matrix serves as inductor for the perichondrium to produce chondrogenic cells and as scaffold for the differentiating cartilage. In later animal studies, the viability of this newly formed cartilage was demonstrated by successful application in reconstructing laryngeal structures of young and adult rabbits [14,15]. In the young animals, the cartilage graft appeared to grow along with the reconstructed cricoid. In the adult rabbits, the perichondrium of the implant facing the airway was an excellent base for the regenerating ciliated epithelium [14,15]. A first report of the reconstruction of a nasal septum with heterotopically induced cartilage (at the dorsal side of the auricle) in a child has been published more recently [16]. Now, after a follow-up of 4 years, an excellent biocompatibility and commensurate growth of the nose are observed (Pirsig, personal communication).

Several authors have stated that for cartilage generation the perichondrial flap should be pedicled [6,10,17]. It is evident that for clinical use the dimensions of the auricle set restrictions to the size of the graft generated. Hence, in the present animal study the chondrogenic potential of a pedicled perichondrial flap is compared with the efficacy of a free perichondrial flap in combination with trabecular demineralized bovine bone matrix, implanted at sites with a variable degree of vascularization. An experiment with trabecular

demineralized bovine bone matrix implanted, without perichondrial cover, was included in this study, because cortical demineralized bovine bone matrix was reported to induce chondrogenesis [18].

Materials and methods

Experimental Procedure

Twenty-four young female New Zealand White rabbits, weighing 1200 to 1800 g, were included in this study. The animal protocol was approved by the Animal Ethics Committee, Erasmus University Medical Center Rotterdam (protocol no. 1269501). Anesthesia was effectuated by means of intramuscular injection of 2% xylazine-hydrochloride (Rompun, Bayer, Leverkusen, Germany) 0.5 ml/kg body weight and 10% ketamine hydrochloride (Ketalin, Apharma, Arnhem, The Netherlands) 0.5 ml/kg body weight.

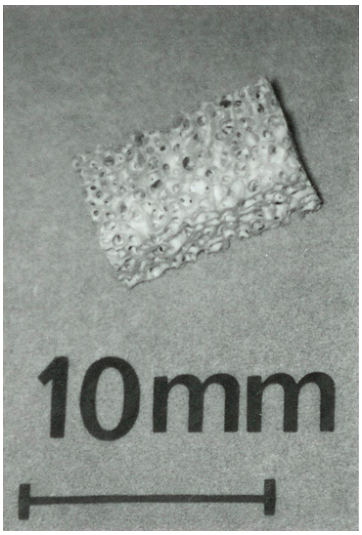

Fig. 1. Piece of trabecular demineralized bovine bone matrix, with noticeable porosity.

The operation site was shaved and disinfected with 70% ethanol. To gain access to the perichondrium an L-shaped incision was made at the concave side of the ear. The skin was elevated, and the perichondrium was dissected from the underlying cartilage. A rectangular piece of trabecular demineralized bovine bone matrix (Osteovit®, Braun Gmbh, Melsungen, Germany), measuring ±4x4x8 mm and weighing ±20 mg (Fig. 1), was wrapped in the elevated perichondrium in such a way that the perichondrium side dissected from the cartilage in the transitional layer faced the demineralized bovine bone matrix surface. Either a pedicled perichondrial flap or a free perichondrial flap was wrapped around trabecular demineralized bovine bone matrix. The composite graft of a pedicled perichondrial flap and demineralized bovine bone matrix was left in situ in the ear (series 1). The demineralized bovine bone matrix block wrapped in a free perichondrial flap was placed at three

Table 1. Experimental design of distribution of seven grafts (series 1, 2a–c, 3a–c) in 24 rabbits harvested after 3 and 6 weeks.

Number of rabbits	Procedure	Period of implantation (weeks)
6	series 1 (left pinna) series 2b (right pinna) series 3a (abdominal wall)	3
3	series 1 (Left and right pinna) series 3a (left and right side abdominal wall)	6
3	series 2b (left and right pinna)	6
6	series 2a (left and right side abdominal wall) series 3c (left and right quadriceps muscle)	3 and 6
6	series 2c (left and right quadriceps muscle) series 3b (left and right pinna)	3 and 6

Series 1: Pedicled perichondrial flap + demineralized bovine bone matrix. Series 2: Free perichondrial flap + demineralized bovine bone matrix; a. abdominal wall, b. subcutaneously in the pinna, c. quadriceps muscle. Series 3: demineralized bovine bone matrix; a. abdominal wall, b. subcutaneously in the pinna, c. quadriceps muscle

different locations with various degrees of vascularization (series 2). Furthermore, blocks without perichondrial cover were placed at similar locations (series 3).

The following conditions were studied:

- Series 1: demineralized bovine bone matrix wrapped in a perichondrial flap, pedicled at the proximal side of the pinna (n=12);
- Series 2a: demineralized bovine bone matrix wrapped in a free perichondrial flap, implanted subcutaneously in the abdominal wall (n=12);
- Series 2b: demineralized bovine bone matrix wrapped in a free perichondrial flap, implanted subcutaneously in the pinna (n=12);
- Series 2c: demineralized bovine bone matrix wrapped in a free perichondrial flap, implanted in the quadriceps muscle (n=12);
- Series 3a–c: Implantation of demineralized bovine bone matrix without perichondrial cover at sites indicated above (n=12).

In each rabbit, two flaps of perichondrium could be made (left and right pinna). Consequently, series 1 and 2a–c were assigned to 24 rabbits (Table 1). In 21 rabbits, next to combined grafts, blocks of trabecular demineralized bovine bone matrix without perichondrial cover (series 3a–c) were implanted. Grafts were harvested after 3 weeks (n=6) and 6 weeks (n=6).

Histologic analysis

All specimens were cut in two equal parts; one part was fixed in 4% phosphate buffered formalin, decalcified with 10% ethylenediaminetetra-acetic acid and embedded in paraffin. Serial sections were cut (7 μm) and stained with Alcian blue to study cartilage matrix formation or with resorcin-fuchsin (elastin van Giesson) to investigate the presence of elastic fibers. The other part of each graft was frozen in liquid nitrogen and stored at –80 °C until cryosections (6 μm) were cut. Immunohistochemistry was performed on these sections to characterize the newly generated matrix. After fixation in acetone, sections for collagen staining were treated with hyaluronidase (Sigma, St Louis, Mo.); sections for staining of the hyaluronic acid binding regions were reduced in dithiothreitol (Sigma), alkylated with iodoacetate (Sigma), and treated with chondroitinase ABC (Sigma). The sections were incubated overnight at 4 °C with primary antibodies, i.e., monoclonal antibodies against collagen type II (CIICI; 1:100; Developmental Studies Hybridoma Bank), procollagen type I (M38; 1:1000; Developmental Studies Hybridoma Bank) and hyaluronic acid binding regions (1C6; 1:100; Developmental Studies Hybridoma Bank), respectively. Sections were counterstained with Gill's hematoxylin and embedded in gelatinglycerin.

In the histologic sections from each graft, the incidence of cartilage and bone formation was scored. For quantitative evaluation, histomorphometry was performed on two representative sections that were located at least 140 μm apart. A VIDAS (Kontron Image Analysis Division, Zeiss) running on an 80386 personal computer was used. Images of histologic sections were recorded by a Sony CCD/RGB color video camera through which the images were displayed on a monitor. With the use of a computer mouse, a digitalization tablet, and on-line visualization on a monitor, certain areas in the image of the histologic section were marked for quantification by the image analysis system. The area of the graft, marked by the inner lining of the perichondrium, was measured. Then the areas of newly formed cartilage, bone, biomaterial residue, and other tissues were identified and measured. Hence, the percentage of each area as part of the graft area was calculated.

Statistical analysis

Two independent observers scored cartilage and bone formation. The incidence was calculated for each group. Because the number of specimens in

each group was small, Fisher's exact test was used as an alternative to chisquare association in 2x2 tables. Furthermore, mean and standard deviation of four different tissue areas, i.e., cartilage, bone, demineralized bovine bone matrix remnants, and other tissues, were calculated for each group. For both implantation intervals, Kruskal-Wallis one-way analysis of variance was used to evaluate the quantity of newly formed cartilage at different implantation sites ($p < 0.05$ was considered statistically significant). For each group, the confidence interval between two independent groups (Wilcoxon rank sum test) was calculated. No correction was made for multiple testing; a confidence limit of at least 95 percent (p value < 0.05) was defined as statistically significant.

Results

All animals gained weight and showed no signs of distress. Infection of the composite graft was observed in one animal after implantation in the quadriceps muscle. In one instance, 6 weeks after implantation in the ear, the graft was lost because of a surgical failure. Both samples were excluded from this study. All other composite grafts could be harvested easily from the implantation site. Macroscopically, these explants were covered with smooth fibrous tissue; elastic resistance was felt under manual pressure of the specimen.

In histologic sections, the composition of the grafts was classified as biomaterial residue, newly formed cartilage, bone, and fibrous or fatty tissue (Figs. 2 and 3). Fragments of demineralized bovine bone matrix could be traced in free flap specimens from less-vascularized locations such as ear (series 2a) and abdominal wall (series 2b). At well-vascularized sites (series 2c), all trabecular demineralized bovine bone matrix was resorbed within 3 weeks and for the most part replaced by cartilage.

The incidence of cartilage formation in the composite grafts was defined (Table 2). Trabecular demineralized bovine bone matrix wrapped in a pedicled perichondrial flap formed cartilage in five of six implants after 3 weeks and in all implants after 6 weeks (series 1). When demineralized bovine bone matrix was covered with a free perichondrial flap, the incidence of cartilage formation depended on the location and duration of implantation. Three weeks after implantation subcutaneously in the abdominal wall (series 2a) cartilage was only found once, whereas cartilage was significantly more frequently found in grafts harvested from the quadriceps muscle (series 2c). After 6 weeks, cartilage formation could be detected in all but two grafts. Once, 6 weeks after implantation of the composite graft in the quadriceps muscle, some bone was formed.

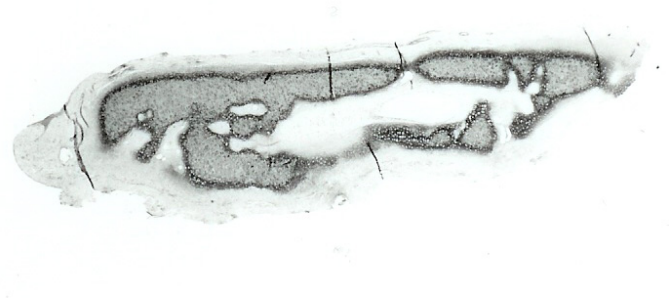

Fig. 2. Histologic section of trabecular demineralized bovine bone matrix wrapped in a pedicled perichondrial flap for 6 weeks. Dotted line indicates inner lining of the perichondrium (graft area). In this specimen, 65 percent of the graft is cartilaginized (Alcian blue; x12.5).

The amount of cartilage present in the grafts was assessed by histomorphometry (Fig. 4). After 3 weeks, significantly more cartilage was generated in the ear or muscle (series 1, 2b, 2c; (Fig. 4), above) than in the abdominal wall (series 2a). After 6 weeks, specimens harvested from the abdominal wall (series 2a) still formed significantly less cartilage compared with demineralized bovine bone matrix wrapped in a free perichondrial flap implanted in the quadriceps muscle (series 2c; (Fig. 4), below). In grafts with a pedicled or free perichondrial flap extirpated after 6 weeks from the ear, approximately half of the graft was cartilaginized. The largest quantity of cartilage was found, 6 weeks after implantation, in grafts at intramuscular locations. All grafts showed an increase in the amount of cartilage from 3 to 6 weeks (Fig. 4).

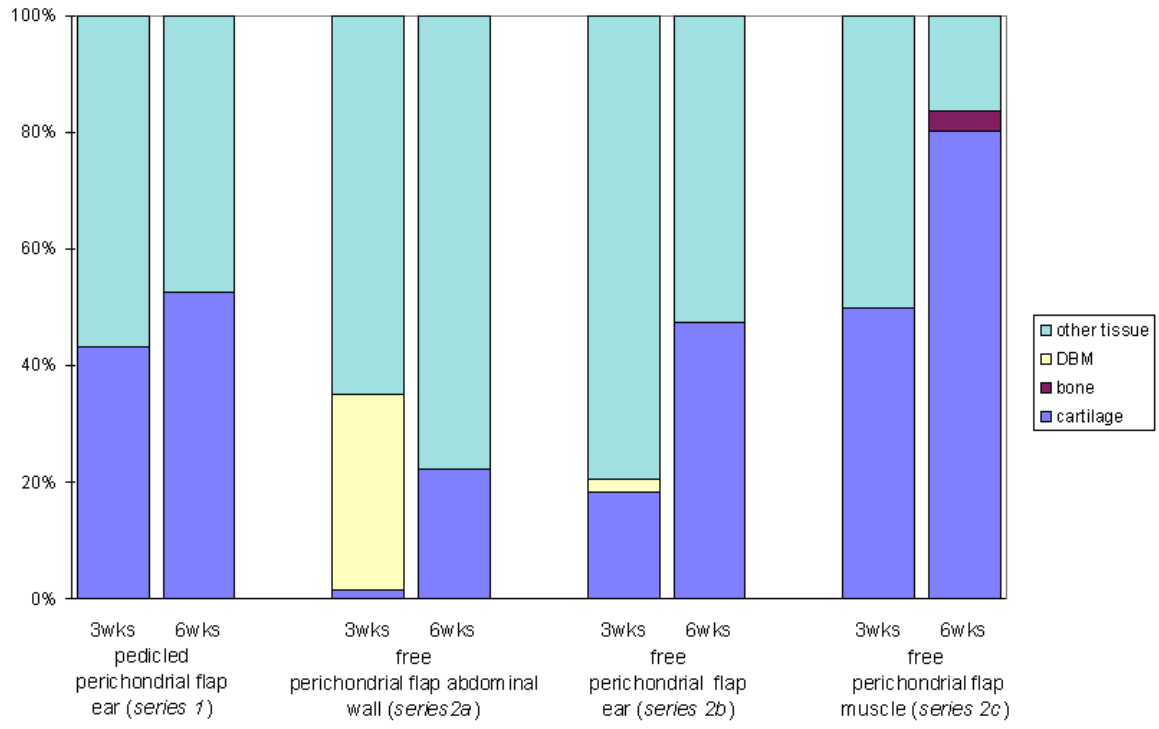

Fig. 3. Combined graft of trabecular demineralized bovine bone matrix (DBM) wrapped in perichondrium 3 and 6 weeks after implantation at various sites. Histomorphometric analysis of the proportion of cartilage, bone, demineralized bovine bone matrix residue, and fibrous or fatty tissue in the graft.

Table 2. Incidence of cartilage and bone formation in grafts harvested after 3 and 6 weeks from different implantation sites (n=6).

	3 weeks				6 weeks			
	Pedicled perichondrial flap	Free perichondrial flap			Pedicled perichondrial flap	Free perichondrial flap		
	Ear	Ear	Abdominal wall	Muscle	Ear	Ear	Abdominal wall	Muscle
Cartilage	5/6	3/6	1/6	5/6	6/6	5/5*	4/6	5/5#
Bone	0/6	0/6	0/6	0/6	0/6	0/5*	0/6	1/5#

* One implant was lost during the surgical procedure
# One implant was excluded from this study because of infection

Because cartilage formation was of main interest in this study, the tissue was further characterized for all series. In correspondence with the Alcian blue staining, the matrix was positive for hyaluronic acid binding region (using mAb 1C6) and collagen type II (mAb CIICI). Hyaluronic acid binding regions and collagen type II stained complementary with procollagen type I (mAb m38) (Fig. 5). A small overlap, however, was observed between the procollagen type I and collagen type II positive areas. The newly induced cartilage matrix also stained positive for resorcin-fuchsin, suggesting the presence of elastic fibers (Fig. 6).

In blocks of trabecular demineralized bovine bone matrix implanted without a perichondrium envelope, no cartilage or bone was formed. In this series, all blocks implanted subcutaneously in the abdominal wall (series 3a) could be retraced and extirpated after 3 or 6 weeks. In these implants, remnants of the trabecular demineralized bovine bone matrix were fragmented and encapsulated by fibrous tissue. Three of six implants placed subcutaneously at the dorsal side of the pinna (series 3b) were completely resorbed within 3 weeks. Hence, no traces of demineralized bovine bone matrix could be found after 6 weeks. In the quadriceps muscle, all trabecular demineralized bovine bone matrix was resorbed within 3 weeks (series 3c).

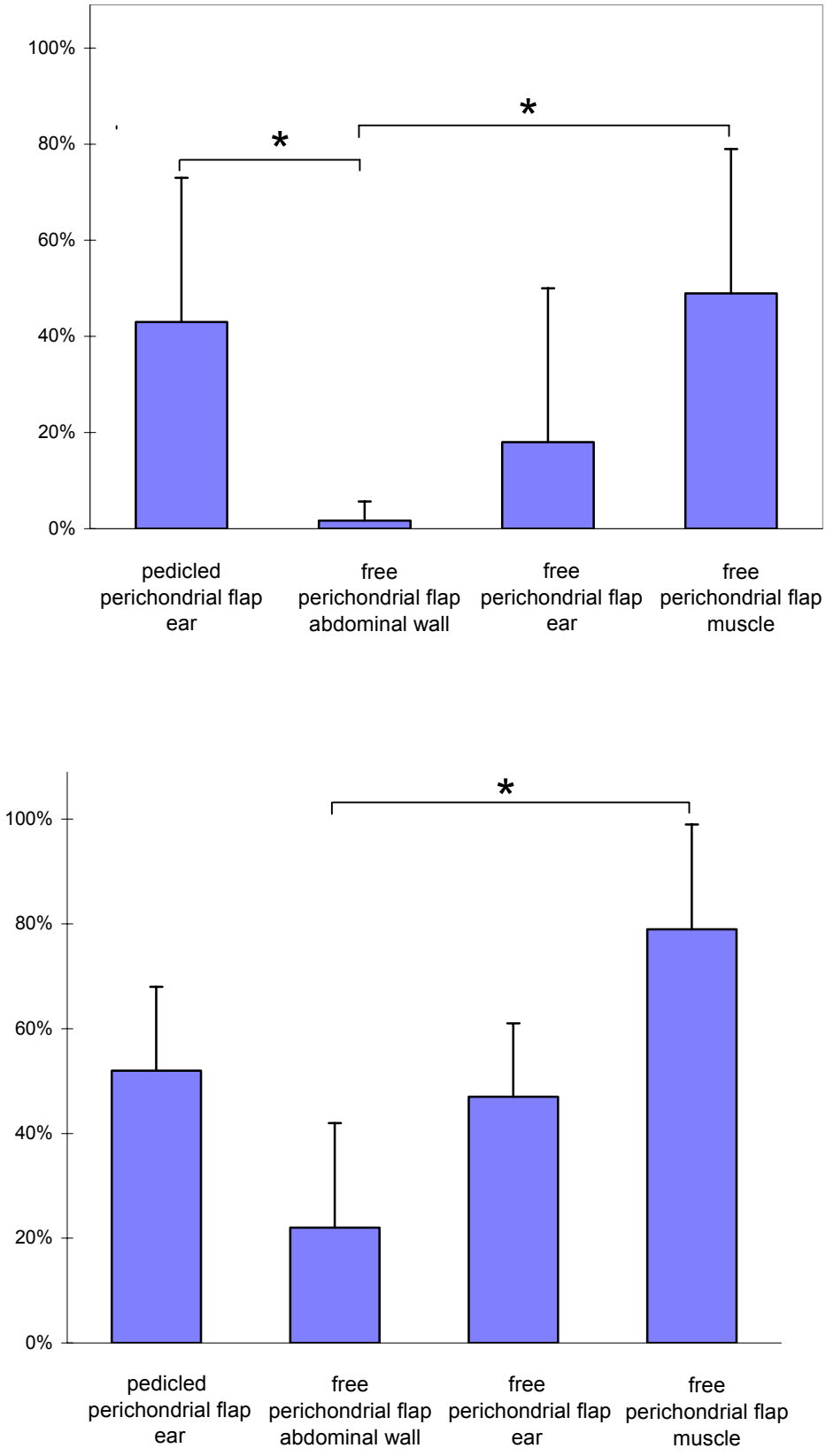

Fig. 4. The amount of newly generated cartilage, calculated as percentage of the graft area, harvested from different locations. (Above) 3 weeks after implantation. (Below) 6 weeks after implantation. Mean ±SD are presented; * indicate significant differences in quantity.

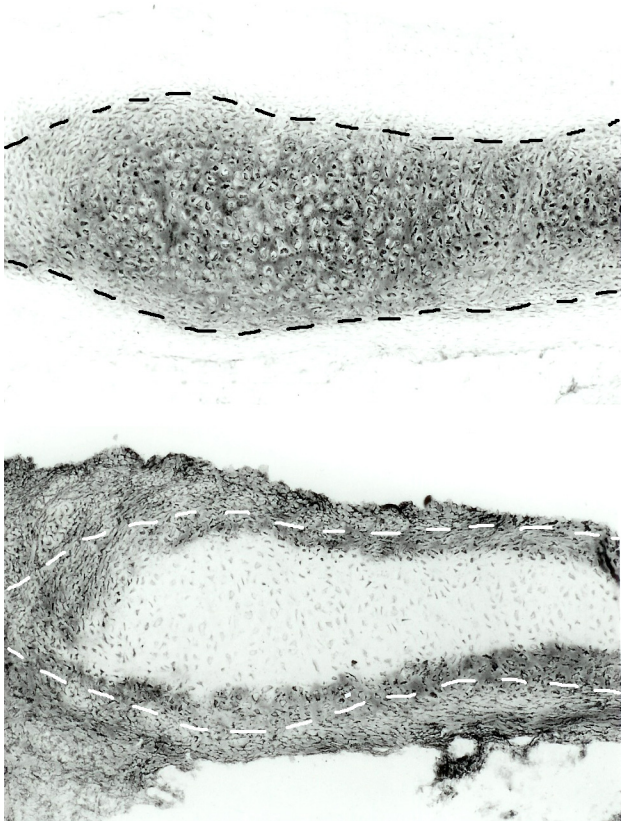

Fig. 5. Immunohistochemical staining of two serial sections of trabecular demineralized bovine bone matrix wrapped in a free perichondrial flap and harvested 6 weeks after intramuscular implantation. (Above) Area between dotted lines stains positively for collagen type II (100x, mAB CIICI). (Below) Complementary staining for procollagen type I (100x, mAb M38). Cartilage at the outer border of the graft, indicated by the dotted line, stains positively for both collagen type II and procollagen type I.

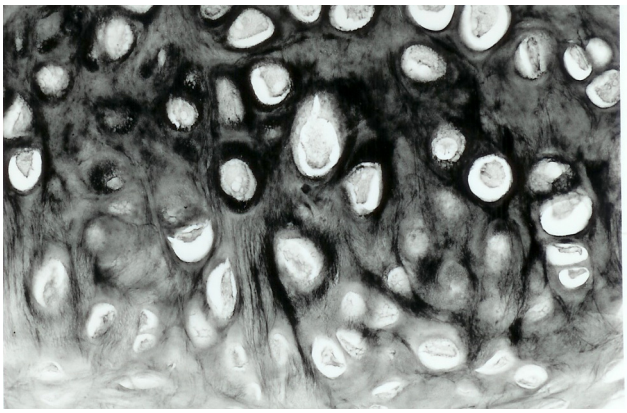

Fig. 6. Trabecular demineralized bovine bone matrix wrapped in pedicled ear perichondrium and harvested after 6 weeks. Under high-power magnification (resorcin-fuchsin; x600), elastic fibers are demonstrated.

Discussion

A composite graft of trabecular demineralized bovine bone matrix in an envelope of perichondrium is capable of heterotopic cartilage formation within 3 weeks [6]. Chondrogenic cells from the perichondrium infiltrate the trabecular demineralized bovine bone matrix before differentiating into a cartilage structure with form and dimensions of the implanted trabecular demineralized bovine bone matrix. Actually, there are two simultaneous processes: degradation of demineralized bovine bone matrix and neoformation of carti-

lage. This study was primarily designed to test the feasibility of a free perichondrial flap as an alternative for a pedicled perichondrial flap to induce cartilage in trabecular demineralized bovine bone matrix. Because the vascularization of the perichondrial flap was considered to be an important factor in cartilage generation, composite grafts of trabecular demineralized bovine bone matrix in an envelope of free perichondrium were implanted for 3 and 6 weeks at locations with rich or poor vascularization. The amount of cartilage generated after 6 weeks of implantation increased only slightly. Therefore, implantation no longer than 6 weeks seems appropriate.

As a control, trabecular demineralized bovine bone matrix was implanted without a perichondrial envelope (series 3). The present study showed complete resorption of the trabecular demineralized bovine bone matrix without cartilage or bone formation. The rate of resorption of the matrix seemed to depend on the vascularization of the implantation site. Whereas trabecular demineralized bovine bone matrix implanted at poorly vascularized sites such as the abdominal wall (series 3a) was still present after 6 weeks, trabecular demineralized bovine bone matrix implanted intramuscularly (series 3c) was completely resorbed within 3 weeks. This resorption could be explained by the important role of macrophages in the process of degradation of the matrix [19]. Because the availability of macrophages is related to the vascularity, early resorption is expected at richly vascularized implantation sites. Furthermore, the presence of perichondrium seemed to accelerate the degradation of trabecular demineralized bovine bone matrix. Fragments of trabecular demineralized bovine bone matrix implanted in the ear (series 3b) were still present 3 weeks after implantation, whereas no traces of trabecular demineralized bovine bone matrix were found when implanted as a composite graft with perichondrium (series 1 and 2b).

Urist et al. were the first to describe enchondral bone formation after subcutaneous implantation of cortical demineralized bovine bone matrix in the rat [18]. In contrast to cortical demineralized bovine bone matrix, trabecular matrix did not show any cartilage or bone formation at extraskeletal implantation sites. Factors of the recipient animal (vascularity of the implantation site, age, and species) and of the implant (weight and the three-dimensional structure) are reported to influence the chondrogenesis and osteo genesis [20–24]. The three-dimensional structure of the trabecular matrix and the possible absence of specific growth factors in the matrix might explain the difference in osteoinductive properties between cortical and trabecular demineralized bovine bone matrix.

In search of a possibility to generate larger grafts, trabecular demineralized bovine bone matrix was consequently wrapped in a free ear perichondrial flap at an extra-auricular site. No significant difference in cartilaginization of the graft could be observed between a pedicled perichondrial flap left in

situ in the ear and a free perichondrial flap placed intramuscularly. However, when demineralized bovine bone matrix wrapped in perichondrium was implanted subcutaneously in the abdominal wall, cartilage formation slowed. It is hypothesized that the obvious difference in degree of vascularization of these areas, as demonstrated during surgical exposure, could be the decisive factor. The cellular processes involved with cartilage f ormation, differentiation and mitosis of perichondrial cells, are related to the metabolic activity of the cells, which depends on the degree of vascularity. It seemed not necessary to leave the perichondrium pedicled to achieve demineralized bovine bone matrix implant, on the condition that the location of implantation is well vascularized. It has been suggested that the type of perichondrium is important in chondrogenesis. Engkvist et al. and Kon et al. noticed that rib perichondrium has a better chondrogenic potential than ear cartilaginization of the trabecular perichondrium [12,25]. Perichondrium dissected from hyaline rib cartilage includes the inner transitional layer, whereas in perichondrium stripped from elastic ear cartilage, the layer of natural separation does not include the innermost, transitional layer [12]. Takato et al. reported no differences between rib and ear perichondrium, but they emphasized the importance of including the transitional layer when dissecting the perichondrium of the underlying cartilage [26]. Consequently, when using ear perichondrium, as in our experiments, it is important to denude the underlying cartilage completely from its perichondrium, in this way including the transitional layer. The amount of cartilage generated by solitary perichondrium is limited, if any is formed at all [27,28]. Matsuda et al. [29] placed a double folded perichondrial free flap subcutaneously for 7 weeks; in their experiments, only half of the explants formed cartilage. Moreover, the amount of newly formed cartilage was small. We could confirm the observation of Matsuda et al. [29] that cartilage generated by a perichondrium flap, was minimal (data not shown).

Perichondrial grafts in combination with other biomaterials have been described in the literature [29,30]. Matsuda et al. [29] implanted a collagen sponge enwrapped in perichondrium subcutaneously in the back of rabbits. After 7 weeks, in 10 of 21 explants cartilage formed. The amount of newly generated cartilage in combined grafts was three times the amount of cartilage generated in grafts of perichondrium folded in two without collagen sponge. Ruuskanen et al. [30] implanted a combined graft of polyglycolic acid and perichondrium in a muscular pouch. In their experiments, cartilage formed in seven of eight explants. In general, in these studies the incidence of cartilage formation in the explants harvested from specific sites with different vascularity seemed to be comparable to our results (Table 1). This finding emphasizes the importance of vascularization of the implantation site, when a free perichondrial flap is used. The trabecular demineralized bovine bone ma-

trix we used demonstrated an early infiltration of the trabecular structure with perichondrial and mesenchymal cells and rapid formation of cartilage within the trabecular structure, resulting in total replacement of the trabecular demineralized bovine bone matrix by cartilage. In contrast, polyglycolic acid only molded the shape of the cartilage generated by the perichondrial cover. After 7 weeks, the polyglycolic acid fleece was fragmented, without any infiltration by chondrocytes [30]. Likewise, hydroxylapatite wrapped in perichondrium formed minimal cartilage along the biomaterial, no infiltration of chondrocytes in the pores of the hydroxylapatite and after 20 weeks no signs of resorption [31].

Pinna cartilage contains elastic fibers. Therefore, it could be expected that the newly generated cartilage would contain elastic fibers. The newly generated cartilage matrix stained positively for resorcin-fuchsin, suggesting the presence of elastic fibers. However, the amount was less and the distribution varied considerably within and between specimens. Moreover, the cartilage we generated contained collagen type II and hyaluronic acid binding regions, whereas collagen type I was absent. Because these cartilage matrix characteristics are specific for hyalin and elastic cartilage, this tissue is appropriate to be used in closing cartilage defects in nose, ear, larynx, and joints.

In the muscle, 6 weeks after implantation, next to the cartilage, small islets of bone were observed. Previous studies have shown that small islets of bone were frequently found 20 weeks after implantation of such a cartilage graft in the rabbit larynx [14]. Furthermore, in adult animals, bone formed more frequently [15]. Also in cartilage generated with perichondrium in combination with polyglycolic acid, bone formed [30]. Therefore, bone formation is probably not induced by the trabecular demineralized bovine bone matrix. Recent studies have shown that indomethacin reduces the calcification in free perichondrial grafts placed intra-articularly [32]. Whether indomethacin would reduce bone formation in the composite ear perichondrium demineralized bovine bone matrix graft is under current investigation.

Conclusions

1. A composite graft consisting of trabecular demineralized bovine bone matrix in an envelope of perichondrium is capable of heterotopic cartilage formation; this in-vivo engineered cartilage has been successfully applied to reconstruct the cartilaginous framework of nose and larynx.
2. Wrapped around trabecular demineralized bovine bone matrix, pedicled perichondrial flaps and free flaps in highly vascularized areas are equally productive in generating cartilage.

3. Trabecular demineralized bovine bone matrix is completely resorbed; the resorption rate depends on the vascularization of the implantation site.
4. The complete resorption of trabecular demineralized bovine bone matrix, the practicability of a free perichondrial flap, and the quality of the cartilage produced suggest further exploration of clinical use of this in vivo engineered cartilage.

Acknowledgments

The authors thank the Department of Pathology (Erasmus University Rotterdam) for the kind hospitality at their laboratory, Frank van der Panne for microscopy photography and the Animal Experimental Center (Erasmus University Rotterdam) for care of the rabbits. The antibodies II-II6B3 and M38 were obtained from the Developmental Studies Hybridoma Bank maintained by the Department of Pharmacology and Molecular Sciences, Johns Hopkins University School of Medicine, Baltimore, Md., and the Department of Biological Sciences, University of Iowa, Iowa City, Iowa, under contract N01-HD-6-2915 from the NICHD. The research of Dr. van Osch is supported by the Technology Foundation (STW), applied science division of the Dutch Foundation for Scientific Research (NWO) and the technology programme of the Ministry of Economic Affairs.

References

[1] Ohara, K., Nakamura, K., and Ohta, E. Chest wall deformities and thoracic scoliosis after costal cartilage graft harvesting. Plast. Reconstr. Surg. 99: 1030, 1997.

[2] Duncan, M. J., Thomson, H. G., and Mancer, J. F. K. Free cartilage grafts: The role of perichondrium. Plast. Reconstr. Surg. 73: 916, 1984.

[3] Eisemann, M. L. The growth potential of autograft cartilage: An experimental study. Arch. Otolaryngol. 109: 469, 1983.

[4] Cao, Y., Vacanti, J. P., Paige, K. T., Upton, J., and Vacanti, C. A. Transplantation of chondrocytes utilizing a polymer-cell construct to produce tissue-engineered cartilage in the shape of a human ear. Plast. Reconstr. Surg. 100: 297, 1997.

[5] Sims, C. D., Butler, P. E. M., Casanova, R., et al. Injectable cartilage using polyethylene oxide polymer substrates. Plast. Reconstr. Surg. 98: 843, 1996.

[6] Bean, J. K., Verwoerd-Verhoef, H. L., and Verwoerd, C. D. A. Chondroneogenesis in a Collagen Matrix. In A. Dixon and B. Sarnat (Eds.), Fundamentals of Bone Growth. Boca Raton, Fla.: CRC Press, 1991.

[7] Ohlsen, L. Cartilage regeneration from perichondrium: Experimental studies and clinical applications. Plast. Reconstr. Surg. 62: 507, 1978.

[8] Donski, P., and O'Brien, B. M. Perichondrial microvascular free transfer: An experimental study in rabbits. Br. J. Plast. Surg. 33: 46, 1980.

[9] Homminga, G. N., van der Linden, T. J., Terwindt-Rouwenhorst, E. A. W., and Drukker, J. Repair of articular defects by perichondrial grafts: Experiments in the rabbit. Acta Orthop. Scand. 60: 326, 1989.

[10] Hartig, G. K., Esclamado, R. M., and Telian, S. A. Chondrogenesis by free and vascularized rabbit auricular perichondrium. Ann. Otol. Rhinol. Laryngol. 103: 901, 1994.

[11] Rice, D. H., and Coulthard, S. W. The growth of cartilage from a free perichondrial graft in the larynx. Laryngoscope 88: 517, 1978.

[12] Engkvist, O., Skoog, V., Pastacaldi, P., Yormuk, E., and Juhlin, R. The cartilaginous potential of the perichondrium in rabbit ear and rib: A comparative study in vivo and in vitro. Scand. J. Plast. Reconstr. Surg. 13: 275, 1979.

[13] Upton, J., Sohn, S. A., and Glowacki, J. Neocartilage derived from transplanted perichondrium: What is it? Plast. Reconstr. Surg. 68: 166, 1981.

[14] Bean, J. K., Verwoerd-Verhoef, H. L., Meeuwis, J., and Verwoerd, C. D. A. Reconstruction of the growing cricoid with a composite graft of demineralized bovine bone and autogenous perichondrium: A comparative study in rabbits. Int. J. Pediatr. Otorhinolaryngol. 25: 163, 1993.

[15] Bean, J. K., Verwoerd-Verhoef, H. L., and Verwoerd, C. D. A. Reconstruction of the anterior laryngeal wall with a composite graft of demineralized bovine bone matrix and autogenous perichondrium: An experimental study in adult rabbits. ORL J. Otorhinolaryngol. Relat. Spec. 56: 224, 1994.

[16] Pirsig, W., Bean, J. K., Lenders, H., Verwoerd, C. D. A., and Verwoerd-Verhoef, H. L. Cartilage transformation in a composite graft of demineralized bovine bone matrix and ear perichondrium used in a child for the reconstruction of the nasal septum. Int. J. Pediatr. Otorhinolaryngol. 32: 171, 1995.

[17] Naficy, S., Esclamado, R. M., and Clevens, R. A. Reconstruction of the rabbit trachea with vascularized auricular perichondrium. Ann. Otol. Rhinol. Laryngol. 105: 356, 1996.

[18] Urist, M. Bone formation by auto induction. Science 150: 893, 1965.

[19] van Osch, G. J. V. M., ten Koppel, P. G. J., van der Veen, S. W., Poppe, P., and Verwoerd-Verhoef, H. L. The role of a trabecular demineralized bone matrix in combination with perichondrium in the generation of cartilage grafts. Biomaterials (in press).
[20] Inoue, T., Deporter, D. A., and Melcher, A. H. Induction of chondrogenesis in muscle, skin, bone marrow, and periodontal ligament by demineralized dentin and bone matrix in vivo and in vitro. J. Dent. Res. 65: 12, 1986.
[21] Sampath, T. K., and Reddi, A. H. Importance of geometry of the extracellular matrix in endochondral bone differentiation. J. Cell. Biol. 98: 2192, 1984.
[22] Jergesen, H. E., Chua, J., Kao, R. T., and Kaban, L. B. Age effects on bone induction by demineralized bone powder. Clin. Orthop. 268: 253, 1991.
[23] Douglas, J., and Clarke, A. Response to demineralized bone matrix implantation in foals and adult horses. Am. J. Vet. Res. 56: 649, 1995.
[24] Muthukumaran, N., Ma, S., and Reddi, A. H. Dose-dependence of and threshold for optimal bone induction by collagenous bone matrix and osteogeninenriched fraction. Coll. Relat. Res. 8: 433, 1988.
[25] Kon, M., and van den Hooff, A. Cartilage tube formation by perichondrium: A new concept for tracheal reconstruction. Plast. Reconstr. Surg. 72: 791, 1983.
[26] Takato, T., Harii, K., and Nakatsuka, T. The development of bone after perichondrial grafting: An experimental study using ear and rib perichondrium in rabbits. Br. J. Plast. Surg. 40: 636, 1987.
[27] Skoog, T., Ohlsen, L., and Sohn, S. A. Perichondrial potential for cartilaginous regeneration. Scand. J. Plast. Reconstr. Surg. 6: 123, 1972.
[28] Ohlsen, L., and Nordin, U. Tracheal reconstruction with perichondrial grafts. Scand. J. Plast. Reconstr. Surg. 10: 135, 1976.
[29] Matsuda, K., Nagasawa, N., Suzuki, S., Isshiki, N., and Ikada, Y. In vivo chondrogenesis in collagen sponge sandwiched by perichondrium. J. Biomater. Sci. Polym. Ed. 7: 221, 1995.
[30] Ruuskanen, M. M., Virtanen, M. K., Tuominen, H., Tormala, P., and Waris, T. Generation of cartilage from auricular and rib free perichondrial grafts around a self-reinforced polyglycolic acid mould in rabbits. Scand. J. Plast. Reconstr. Surg. Hand Surg. 28: 81, 1994.
[31] Verwoerd, C. D. A, Adriaansen, F. C., v d Heul, R. O., and Verwoerd-Verhoef, H. L. Porous hydroxylapatite-perichondrium graft in cricoid reconstruction. Acta Otolaryngol. 103: 496, 1987.
[32] Bouwmeester, S. J., Beckers, J. M. H., Kuijer, R., van der Linden, A. J., Bulstra, A. K. Longterm results of ribperichondrial graft for the repair of cartilage defects in the human knee. Int. Orthop. 21: 313, 1997.

3B

The role of trabecular demineralized bone in combination with perichondrium in the generation of cartilage grafts

Biomaterials 1999;20:233–240

The role of trabecular demineralized bone in combination with perichondrium in the generation of cartilage grafts

Gerjo J.V.M. van Osch, Paul G.J. ten Koppel, Simone W. van der Veen,
Pawel Poppe, Elisabeth H. Burger, Henriette L. Verwoerd-Verhoef

Abstract

The use of a composite graft of bovine trabecular demineralized bone matrix (DBM) and perichondrium has been found a reliable method for in vivo generation of cartilage. In the present study, the mechanism whereby this commercially available matrix increases cartilage formation was investigated.

First, the time course of cartilage formation in vivo, in the combined implant of perichondrium and DBM in the rabbit ear was studied, with special focus on tissue reactions to DBM. DBM was colonized by macrophages from day 3 post-operatively, reaching a maximum after 2 weeks. Only a minimal number of neutrophils was found. After 3 weeks the DBM appeared to be resorbed. In the first week the DBM was invaded with chondroblasts, and chondrogenesis occurred between the first and second week of implantation. After 3 weeks, the initially formed islets of cartilage had fused.

Next, the chondrogenic capacity of DBM itself was investigated by implantation of DBM without perichondrium. This never resulted in cartilage formation. Immunohistochemistry showed only a faint staining of the DBM for growth factors. This indicates a minimal chondrogenic effect of DBM alone and the requirement of perichondrium as cell provider.

In order to define the conditions which cause chondrogenesis in composites of perichondrium and DBM, a series of in vitro culture experiments was performed in which the in vivo situation was mimicked step by step. The basic condition was perichondrium cultured in medium with 10% FCS. In this condition, cartilage formation was variable. Because in the in vivo situation both DBM and macrophages can release growth factors, the effect of IGF1, TGFβ2 or OP1 added to the culture medium was tested. Neither the incidence nor the amount of cartilage formation was stimulated by addition of growth factors. Perichondrium wrapped around DBM in vitro gave cartilage formation in the perichondrium but the incidence and amount were not significantly stimulated compared to cultures of perichondrium without DBM. However, cartilage-like cells were found in the DBM suggesting an effect of DBM on perichondrium-derived cells.

Finally, macrophages and/or blood were added to the composite DBM-perichondrium to mimic the in vivo situation as close as possible. However, no effect of this treatment was found.

In conclusion, this study indicates that DBM itself has few chondrogenic qualities but functions merely as a spacer for cell ingrowth. The fast resorption of DBM by macrophages in vivo seems of importance for the cartilage forming process, but in vitro the presence of macrophages (in combination with blood) could not enhance chondrogenesis.

Introduction

Defects in the cartilage of nose, cricoid, ear or articular joints show limited tendency of spontaneous healing. For repair of these defects with transplants, the use of autologous tissue is preferred in order to avoid immunological reactions and the risk of transmittable diseases. The amount of autologous cartilage that can be harvested is limited and the consequent donor site morbidity is high. In contrast, isolation of autologous perichondrium is relatively easy for patient and surgeon and results in minimal donor site morbidity and a low complication rate. Therefore, perichondrium has been suggested as a producer of new cartilage [1–5]. The amount of cartilage generated from perichondrium in vivo, however, appeared to be variable and unpredictable [1–3]. In previous research, our group has demonstrated a new experimental method using rabbits: a composite graft of trabecular demineralized bone matrix (DBM) and perichondrium can provide much more consistent results [6,7]. Perichondrium wrapped around DBM leads to gradual replacement of the DBM by autologous cartilage tissue [6] even in the child [8]. Implanted subcutaneously in the ear or intramuscularly in the quadriceps of rabbits the grafts showed cartilage formation in 100% of the samples after 3-6 weeks [7].

In our studies a trabecular matrix (DBM, Osteovit®) was chosen because the porosity of the matrix was considered of importance for the ingrowth of cells. The role of DBM for chondrogenesis could be 'physical', by acting as a spacer for cell ingrowth or 'chemical', induced by growth factors which are suggested to be present in the matrix. The aim of this study was to investigate the role of the trabecular DBM in this process in more detail. We first studied the time course of the cartilage generating process in vivo with special focus on cellular responses to DBM. The chondrogenic capacities of the material itself were evaluated by implantation of the material without perichondrium. In the literature, cortical DBM is often described to induce chondro- and osteogenesis and

is demonstrated to contain growth factors [9,10]. We studied the presence of growth factors in our matrix using immunohistochemistry. Since TGFβ, BMP and IGF are recognized as factors present in DBM [9,10] and are described to induce chondrogenesis [11–15], they were added to perichondrium in culture to study the effects on chondrogenesis. In a further attempt to define the conditions that permit chondrogenesis in the composite of perichondrium and DBM, we mimicked the in vivo procedure in culture. Perichondrium was wrapped around DBM and cultured in vitro and the effects of addition of macrophages and blood was evaluated on histology.

Materials and methods

The various experimental conditions are outlined in Table 1.

In vivo studies

Twelve female New Zealand White rabbits were used (weighing 1200–1800 g, age 6–12 weeks). Anaesthesia was given with xylazine-hydrochloride (Rompun, Bayer, Leverkusen, Germany) 10 $mgkg^{-1}$ body weight and ketamine-hydrochloride (Ketalin, Apharma, Arnhem, Netherlands) 50 $mgkg^{-1}$ body weight via intramuscular injection.

The operation site was shaved and disinfected with 70% ethanol. After making a rectangular incision (approximately 2x6 cm^2) at the concave side of the ear, the skin was elevated and the perichondrium dissected from the underlying cartilage. A rectangular piece of trabecular DBM (Osteovit•, Braun Gmbh, Melsungen, Germany) measuring approximately 4x4x8 mm^3 was soaked in blood. This block was wrapped in perichondrium such that the perichondrial side dissected off the cartilage (the cambium layer) faced the DBM surface, and left in situ in the ear for 3 days, 1, 2 or 3 weeks. Furthermore, DBM was implanted subcutaneously without perichondrial envelope and left in the ear for 1, 3 or 6 weeks.

In vitro studies

Ear perichondrium was obtained from 15 young female New Zealand White rabbits (age 6–12 weeks) as described above. After washing with physiological saline containing gentamicin (0.5 μgml^{-1}) and fungizone (0.5 μgml^{-1}) to remove blood and contaminants, the perichondrium was cut into pieces of about 2 mm^2 using scalpels. Four explants were cultured per well of a 24-wells plate in DMEM/Ham's F12 (1:1) medium (Life Technologies, Breda, The Netherlands)

Table 1. Overview of all experimental conditions tested in vivo and in vitro with time of harvesting (time) and sample size (n)

Experimental conditions	Time	n
(a) In vivo experiments with DBM		
DBM with perichondrium	d3	6
	wk1	6
	wk2	6
	wk3	6
DBM without perichondrium	wk1	6
	wk2	6
	wk3	6
(b) In vitro experiments of perichondrium with growth factors		
Perichondrium + FCS	wk3	66
Perichondrium + FCS + TGFβ	wk3	17
Perichondrium + FCS + OP1	wk3	16
Perichondrium + FCS + IGF1	wk3	15
Perichondrium – FCS + IGF1+TGFβ2	wk3	15
(c) In vitro experiments of perichondrium with DBM, cultured in 10% FCS		
Perichondrium – DBM	wk3	66
Perichondrium + DBM	wk3	47
Perichondrium + DBM + macrophages	wk3	10
Perichondrium + DBM + blood	wk3	14
Perichondrium + DBM + macrophages + blood	wk3	10
Perichondrium + DBM colonized in vivo	wk3	5
DBM colonized in vivo	wk3	5

The operation site was shaved and disinfected with 70% ethanol. After making a rectangular incision (approximately 2x6 cm^2) at the concave side of the ear, the skin was elevated and the perichondrium dissected from the underlying cartilage. A rectangular piece of trabecular DBM (Osteovit®, Braun Gmbh, Melsungen, Germany) measuring approximately 4x4x8 mm^3 was soaked in blood. This block was wrapped in perichondrium such that the perichondrial side dissected off the cartilage (the cambium layer) faced the DBM surface, and left in situ in the ear for 3 days, 1, 2 or 3 weeks. Furthermore, DBM was implanted subcutaneously without perichondrial envelope and left in the ear for 1, 3 or 6 weeks.

containing 10% heat-inactivated FCS, 25 $\mu g ml^{-1}$ L-ascorbic acid (Sigma), 50 $\mu g ml^{-1}$ gentamicin and 0.5 $\mu g ml^{-1}$ fungizone. The explants were cultured for 3 weeks and medium was changed three times per week. Results were evaluated using histological analysis.

The in vitro studies attempted to mimic step by step the in vivo situation (Fig. 1). As possible chondrogenic factors, growth factors were added to cultures of perichondrium or perichondrium was combined with DBM. Addition of macrophages, important for resorption of the matrix in-vivo, was studied next. Finally, DBM was 'colonized' by cells in vivo before it was enwrapped with perichondrium and subsequently cultured in vitro.

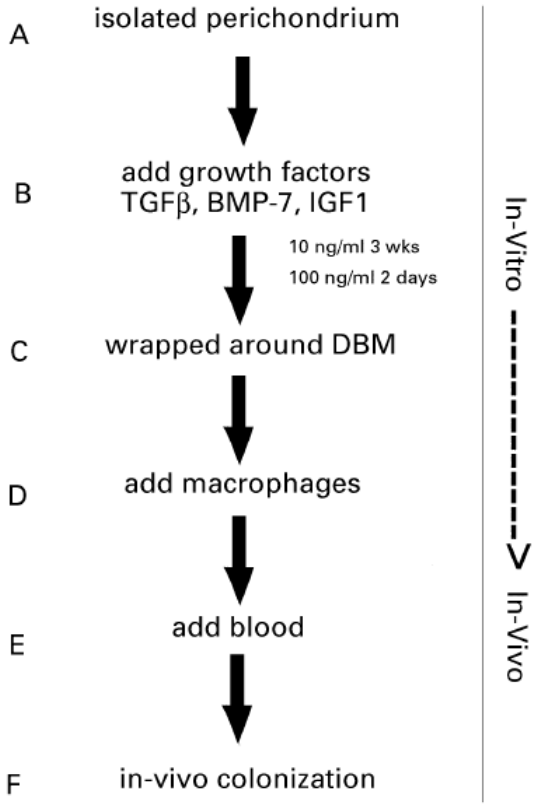

Fig. 1. Experimental design of in vitro conditions to mimic step by step the in vivo situation.

To test the effects of growth factors, rhTGFβ2 (Sandoz, Switzerland), rhOP1 (Creative Biomolecules, Hopkinton, Massachusetts) or rhIGF1 (Boehringer-Mannheim, Almere, The Netherlands) were added to ear perichondrium cultured in medium with 10% FCS. TGFβ2 and OP1 were added in a concentration of 10 $ngml^{-1}$ continuously or as a pulse treatment in a concentration of 100 $ngml^{-1}$ for the first 2 days only. IGF1 was added in a concentration of 10 $ngml^{-1}$ continuously. Furthermore, the effect of a combination of 10 $ngml^{-1}$ IGF1 and 10 $ngml^{-1}$ TGFβ2 added for 3 weeks was tested under serum-free conditions in DMEM/Ham's F12 medium with 0.1% BSA and 25 μgml^{-1} L-ascorbic acid. All concentrations were based on data from literature [11–17].

DBM was cut into pieces of 2–6 mm^3 and a combination of DBM and perichondrium were tested under the following conditions:

1. Perichondrium explants excised at a size of approximately 2x7 mm and wrapped around the DBM matrix, with the layer which faced the cartilage towards the DBM, and cultured for 3 weeks;
2. DBM seeded with macrophages before perichondrium was wrapped around it. Autologous macrophages were isolated together with the perichondrium by washing the peritoneal cavity of the rabbit with PBS immediately after killing the animal. The peritoneal cavity was opened with a small incision and 0.3–0.5 l PBS was introduced in the cavity. After closing the incision, the abdomen was gently massaged to allow solvation of peritoneal macrophages in PBS. Then, as much PBS (with cells) as possible was retained from the cavity through a disposable needle (1.1 mm x 40 mm). The cells were separated from the solution by centrifugation. Cytospins stained with mAb CD68 showed that >95% of the isolated cells were macrophages. After washing, the cells were seeded in DBM in a density of $5x10^7$ cells ml^{-1} to allow a large amount of macrophages to adhere to and degrade the DBM. After incubation for at least 30 min, the DBM-macrophage composite was enwrapped in perichondrium;
3. DBM (with or without macrophages) soaked in autologous blood and cultured in vitro;
4. DBM pre-incubated in vivo by implantation of 10x10x3 mm DBM subcutaneously in the ear for 6 days. After harvesting, the DBM was cultured with or without perichondrial envelope.

Histology

Presence of growth factors in DBM

Cryosections of pure DBM were prepared. Sections of human demineralized bone were used as control. To evaluate the effectiveness of the demineralization procedure, staining according to Goldner was used. Immunohistochemical staining for growth factors IGF1 (using a rabbit polyclonal, GroPep, Adelaide, Australia), TGFβ2 and 3 (using rabbit polyclonals 1:50, Santa Cruz Biotechnology, CA) was performed after formalin fixation in the absence and presence of saponin. A signal was made visible using 3-amino-9-ethylcarbazole (AEC) as substrate.

In vivo cartilage formation

To study the chondrogenic potential of DBM, implants without perichondrium were harvested after 1, 3 or 6 weeks. Implants with perichondrium were harvested after 3 days, 1, 2 and 3 weeks (n=6) for each time point) to assess chondrogenesis and cellular response to DBM. All specimens were cut into two equal parts; one part was fixed in 4% phosphate-buffered formalin, decalcified with 10% EDTA and embedded in paraffin. Serial sections were cut (7 μm) and stained with Alcian Blue 8GX (Sigma, St Louis, MO) to study cartilage matrix formation. The other part was frozen in liquid nitrogen and stored at –80 ℃ until cryosections (6 μm) were made. Immunohistochemistry was performed on these sections to characterize the matrix generated and to evaluate the cell-mediated resorption of DBM. Sections were fixed in acetone. For collagen staining the sections were treated with hyaluronidase (Sigma, St Louis, MO), for chondroitin sulfate staining the sections were treated with chondroitinase ABC (Sigma). The sections were incubated overnight at 4 ℃ with mAb against collagen type II (CIICI; 1:100; Developmental Studies Hybridoma Bank), pro-collagen type I (M38; 1:1000; Developmental Studies Hybridoma Bank) or chondroitin 6-sulfate (3B3; 1:1000; ICN Biomedicals, Costa Mesa, CA). To study host tissue reactions against DBM, sections were incubated for 2 h at room temperature with mAbs against macrophages using CD68 (1:50; Behring, Marburg, Germany) and neutrophils using α-lactoferrine (1:25; Pharmingen, San Diego, CA). After incubation with primary antibodies, sections were treated with goat-anti-mouse biotin, followed by streptavidin alkaline phosphatase (Supersensitive, Biogenics, Clinipath, Duiven, The Netherlands). Alkaline phosphatase activity was demonstrated using a New Fuchsin substrate (Chroma, Kongen, Germany). This resulted in a red coloured signal. Endogenous alkaline phosphatase activity was inhibited with levamisol (Sigma). Sections were counterstained with Gill's haematoxylin and embedded in gelatin-glycerin.

In vitro cartilage formation

After three weeks in vitro, the explants were harvested, fixed in 4% phosphate buffered formalin and embedded in paraffin. Sections of 6 μlm thickness were cut and four sections, spaced 60 μm apart, were mounted on one slide, stained with Alcian Blue 8GX and counterstained with Nuclear Fast Red.

The incidence of new cartilage formation in the explants was scored. A Fisher's exact test was used for statistical analysis. The percentage of the area stained with Alcian Blue was quantified using image analysis using Videoplan software (Kontron, Zeiss, The Netherlands) using two high quality sections at least 200 μm apart, for each sample. Since small pieces of cartilage could be in-

cluded when perichondrium was dissected (accounting for up to 10% of the tissue area), distinction was made between pre-existing and newly formed cartilage based on the intensity of Alcian Blue staining and the morphology of the cells. The amount of newly formed cartilage was expressed as a percentage of the total area corrected for pre-existing cartilage and calculated as follows:

Area newly formed cartilage / (Total area – Area pre-existing cartilage)

The median and range were calculated and Kruskall Wallis one-way ANOVA and rank sum test were used for statistical analysis. A p value < 0.05 was considered statistically significant.

Finally, immunohistochemical stainings for collagen type II was performed on the paraffin sections. Sections were pretreated with pronase type XIV (Sigma) to regain antigenicity which was lost due to formalin fixation, and with hyaluronidase (Sigma) to obtain better antibody penetration. Incubation with monoclonal antibody II-II6B3 (Developmental Studies Hybridoma Bank) was followed by incubation with a second antibody conjugated with alkaline phosphatase. Alkaline phosphatase activity was demonstrated with a New Fuchsin substrate, resulting in a red color.

Results

In vivo

DBM without perichondrium

Without perichondrial cover, no cartilage or bone was ever formed subcutaneously in the DBM. After three weeks, the DBM was completely resorbed in three out of six samples. After 6 weeks complete resorption of DBM had occurred in all samples.

DBM with perichondrium

Cartilage formation. Three and seven days after implantation, no cartilage formation was present in the DBM. The perichondrium stained positive for (pro)collagen type I and chondroitin sulfate. In addition, the inner layer of the perichondrium stained positive for collagen type II. After 7 days, cells and loose fibrous tissue was found between the trabeculae of the DBM. Many of the cells stained positive for chondroitin sulfate and occasionally for (pro)collagen type I. After 2 weeks, islets of cartilage were found in the pores of the DBM (Fig. 2).

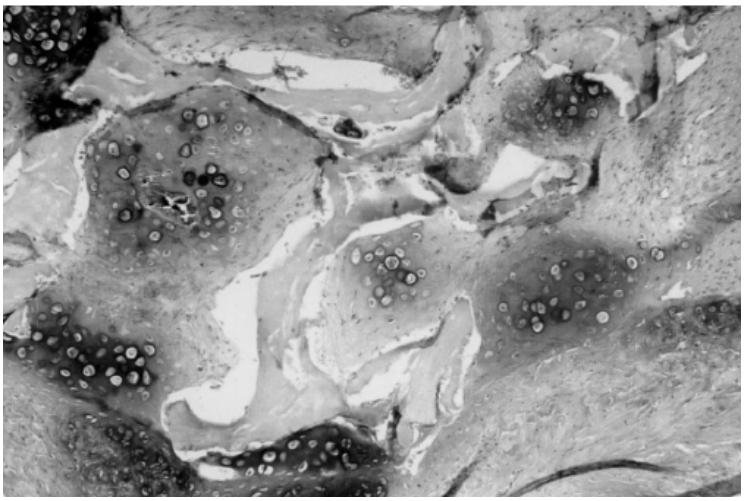

Fig. 2. Cartilage formation in vivo in a composite graft of demineralized bovine bone matrix and ear perichondrium after 2 weeks. Alcian Blue staining, original magnification 100x.

Fig. 3. Cartilage formation in a composite graft of demine-ralized bovine bone matrix and ear perichondrium, 3 weeks after implantation in vivo. Alcian Blue staining, original magnification 100x.

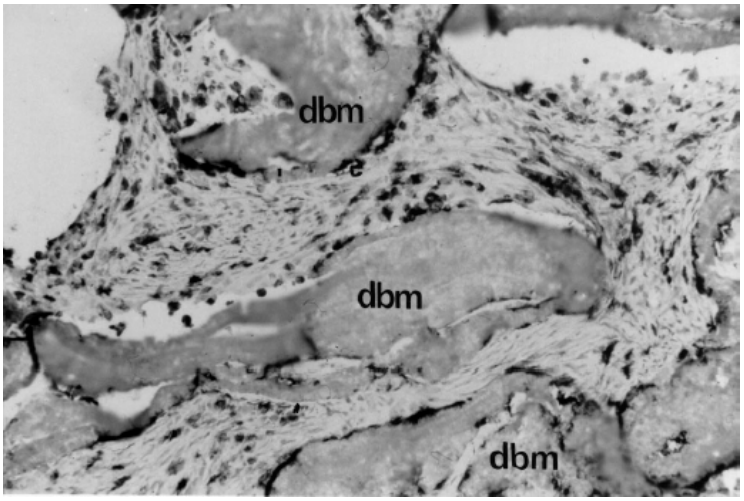

Fig. 4. Macrophages invading the DBM after 14 days implantation in the rabbit ear. Macrophages are stained immunohisto-chemically with mAb CD68, sections are counterstained with haema-toxylin. Note macrophages are located between the trabeculae of the DBM but also attached to the DBM. Original magnification 200x.

These islets showed positive staining for Alcian Blue, chondroitin sulfate and collagen type II. After 3 weeks the islets of cartilage had fused to a massive cartilaginous structure (Fig. 3). Occasionally, cysts and bloodvessels were found in the cartilage.

Resorption of DBM. After 3 days the perichondrium was markedly thickened. Macrophages were present in the perichondrium tissue and some had also invaded the graft and were attached to DBM. The first 2 weeks after implantation, the number of macrophages in perichondrium as well as DBM gradually increased (Fig. 4). After 2 weeks, the DBM was fragmented and after 3 weeks no signs of DBM were observed any more and the amount of macrophages was strongly reduced. Some macrophages were still present where islets of cartilage were not completely fused.

Only a few neutrophils could be detected during the whole period.

In vitro

Both the incidence and the amount of cartilage formed in cultures with 10% FCS (controls) of auricular perichondrium appeared to be variable. Cartilage formation varied between none or a few chondrocytes to a maximum of half of the explant area (Fig. 5). To investigate the role of DBM in chondrogenesis in vivo, the presence of growth factors in demineralized bovine trabecular bone matrix was tested. Immunohistochemistry demonstrated a faint staining for IGF1 and TGFβ2, 3. The absolute amounts could not be determined this way, but staining was generally much lower than in human trabecular bone which had been demineralized by acetic acid and was used as a positive control.

Addition of the recombinant growth factors IGF1, TGFβ2 or OP1 to perichondrium cultures in the presence of 10% FCS, did not improve incidence nor amount of cartilage formation (Table 2). Since we could not demonstrate a difference between continuous or pulsed addition of growth factors, these two conditions were combined in the results. Serum free cultures to which a combination of IGF1 and TGFβ2 was added for three weeks did not result in stimulation of chondrogenesis.

The use of DBM in perichondrium cultures did not change the incidence nor the amount of cartilage formation after 3 weeks (Table 2). Besides induction of cartilage in the explants, colonization of the DBM by cells was observed (Fig 6). These cells had a round shape and a halo of matrix that stained positively with Alcian Blue. Immunohistochemistry for collagen type II was not feasible on these sections because the DBM did not remain attached to the slide surface during the staining procedure. The variability in the results with DBM were thought to be partly due to variable adhesion of perichondrium tissue to DBM.

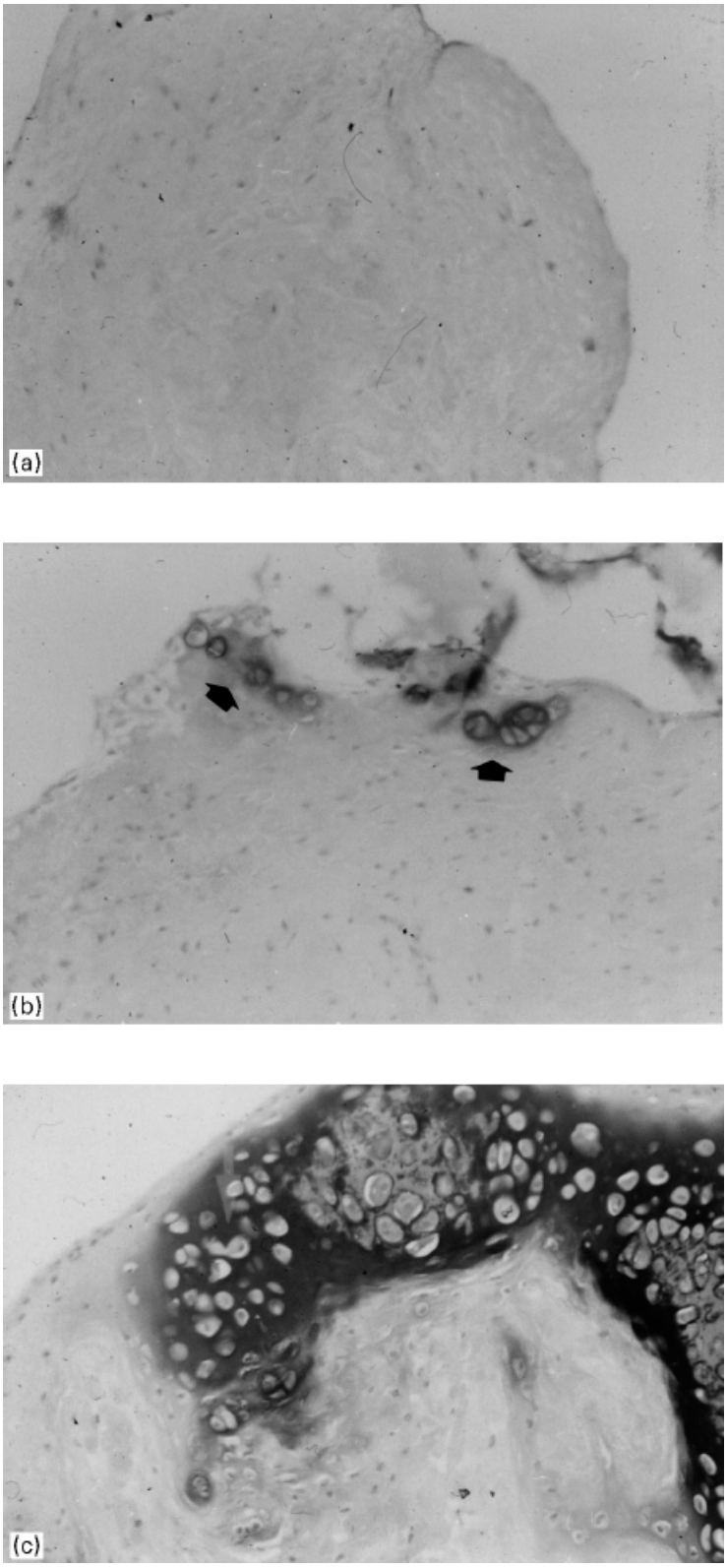

Fig. 5. Chondrogenesis in perichondrium in vitro after 3 weeks, showing the variation in results: (a) no chondrogenesis; (b) a few chondrogenic cells (indicated with arrows); (c) more extensive cartilage formation. Original magnification 200x.

Table 2. Incidence of chondrogenesis and amount of cartilage formation in vitro in perichondrium after 3 weeks of culture under various conditions. The amount of cartilage formation was quantified using image analysis in the samples where chondrogenesis was present and is presented as % of the total area of the explant. No statistically significant differences were found.

Experimental condition	Incidence	% Area cartilage	
		Median	Range
Control (10% FCS)	16/66	9	0–32
TGFβ2	4/17	23	6–53
OP1	2/16	6	0–11
IGF1	1/15	2	n.a.
Serum free with IGF1 and TGFβ2	0/15	n.a.	n.a.
DBM	13/47	6	1–40
DBM + macrophages	1/10	3	n.a.
DBM + blood	6/14	10	1–47
DBM+ macrophages + blood	2/10	39	15–62
DBM colonised in vivo	2/5	4	1–6
DBM(colonised in vivo) without perichondrium	1/5	n.a.	n.a.

n.a. not available

Attempts were made to advance the adhesion by soaking the DBM in autologous blood before it was wrapped in the perichondrium. This, however, did not influence incidence nor amount of cartilage formation.

In vivo studies have demonstrated that resorption of DBM is performed mainly by macrophages. In vitro macrophages seeded in DBM did not result in visible resorption of the DBM in 3 weeks. Also it did not increase cartilage formation. Combination of blood and macrophages could not mimic the in vivo situation. Since adhesion and activity of the macrophages was questionable, DBM was implanted subcutaneously in the ear for 6 days before culturing with or without perichondrium in vitro. As described in the in vivo experiments, after 6 days subcutaneous implantation, macrophages, mesenchymal cells and some fibrous tissue were present in the DBM but at this point cartilage formation was still absent. Then this DBM was cultured for 3 weeks with or without a perichondrial envelope, and cartilage formation could be observed in the DBM, however, it was independent of the presence or absence of a perichondrial envelope. Visible resorption of DBM after 6 days in vivo implantation was not observed after 3 weeks of culture.

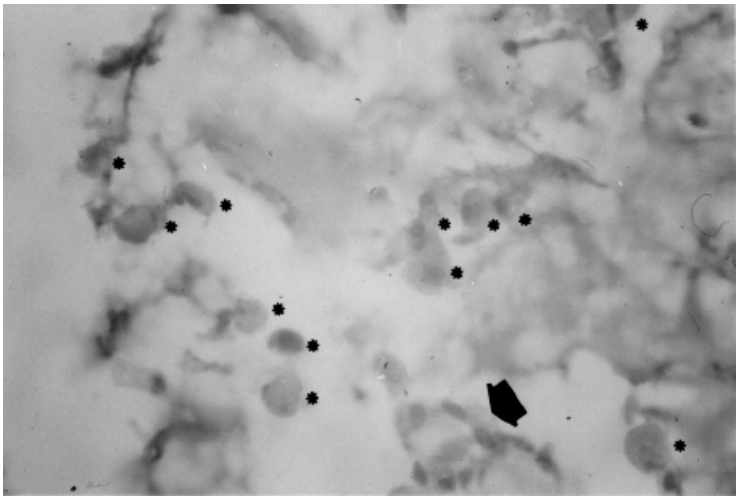

Fig. 6. Cells colonizing the DBM in vitro after 3 weeks. Note the round cell shape and the Alcian Blue staining pericellular matrix. The asterisks indicate the chondrogenic cells, the thick arrow indicate a group of fibroblast-like cells. Original magnification 400x.

Discussion

In the literature cortical DBM has been demonstrated to contain growth factors which are held responsible for the chondro- and osteogenic potential of this matrix [9,10]. The trabecular bovine DBM we used in this study, showed only a faint staining for growth factors. Although in earlier studies addition of growth factors in vitro was demonstrated to induce chondrogenesis in periost [11–16], we could not confirm this for perichondrium; the addition of IGF1, TGFβ2 or OP1 in vitro did not improve chondrogenesis. The difference between perichondrium and periost or the variability in composition of the serum, might explain this discrepancy in results. Yaeger et al. [17] showed that addition of IGF1and TGFβ2, to cultures in serum-free medium could induce redifferentiation of human articular chondrocytes which had lost their phenotype by culturing in monolayer. Even this combination of IGF1 and TGFβ2 however, did not stimulate cartilage formation from rabbit ear perichondrium.

So this study does not provide evidence for a role of growth factors from the DBM for chondrogenesis. The physical properties of trabecular DBM may be of more importance. Although the present study showed that neither the incidence nor the amount of cartilage generated in vitro was stimulated by the use of DBM, colonization of the DBM by cells could be observed. These cells survived in culture and even had a round shape and produced an Alcian Blue positive matrix, indicating viable cartilage-like cells. This suggests that DBM acts more as a scavenger for chondrogenic cells.

In vivo, resorption of DBM seems to be performed mainly by macrophages. Peritoneal macrophages have been demonstrated to manifest bone re-

sorption [18]. Murine peritoneal macrophages in culture could absorb 40-50% of small bone particles in two days. In the present study, peritoneal macrophages were isolated, seeded in DBM and cultured together with perichondrium in vitro. Resorption of DBM was not seen macroscopically and contrary to the in vivo situation, DBM was still present after 3 weeks culture. Holtrop et al. [19] suggested that interaction of two cell types is needed for the resorption of bone fragments: one cell type inducing pre-digestion of the matrix with enzymes, and subsequently the macrophages will be able to phagocytize the debris. So probably, macrophages alone are not able to digest such large parts of DBM and addition of enzymes in vitro might be needed to optimize the action of macrophages. Landesman and Reddi [20] reported that the chondro-osteogenic potential of DBM is initially enhanced after implantation in vivo and at its highest point the first 5–7 days in vivo. Therefore, we implanted DBM in vivo for 6 days to obtain colonization with cells and a possible pre-digestion of the DBM, before culturing with perichondrium in vitro for 3 weeks. This combined in vivo/in vitro procedure, however, did not result in visible better resorption of the DBM nor did it increase chondrogenesis.

As another important factor in the in vivo process, the presence of clotted blood in contact with perichondrium is described to be necessary for cartilage formation [21]. Clotted blood consists of many platelets which contain growth factors like PDGF and TGFβ. Cells of the perichondrium are described to grow in the blood clot and form cartilage [22]. However, neither addition of autologous blood nor addition of blood in combination with peritoneal macrophages to our cultures resulted in any stimulation of chondrogenesis.

DBM by itself (without perichondrium) demonstrated no cartilage formation after 3-6 weeks of subcutaneous implantation in vivo. However, culturing in vitro after 6 days of subcutaneous implantation in vivo, chondrogenesis was found in one out of five samples. This indicates that cartilage generation in DBM without perichondrium in principle is possible. Chondrogenic cells were scavenged by the DBM and these cells could originate from the skin [23,24]. Subcutaneous implantation of DBM without perichondrium for longer periods (3–6 weeks) never generated cartilage. The reason might be the early resorption of the matrix before cartilage is formed. It could be concluded that because of the fast resorption, pure trabecular bovine DBM is insufficient for cartilage production. Perichondrium is a prerequisite for fast delivery of large amounts of chondrogenic cells. Other matrices have been described in combination with perichondrium [25–27]. When a matrix of collagen, hydroxyapatite or polyglycolic acid was used, increased cartilage formation could be found, however, cartilage did not or minimally invade the biomaterial pores, but mainly lined the biomate-

rial [25–27]. This again suggests that fast resorption of DBM compared to these other materials might be an important factor in the process of cartilage graft formation.

In vivo, the use of a composite graft of perichondrium and DBM has shown to be a reliable method to generate new cartilage [6,7]. Such cartilage formation could not be mimicked in vitro by addition of IGF1, TGFβ2. OP1, DBM, macrophages or blood. It is suggested that this trabecular DBM has few chondrogenesis inducing qualities but functions mostly as a spacer for cell ingrowth. The generation of new cartilage by the proper cells migrating into the 'spacer' together with an optimal period for resorption of the biomaterial makes DBM an excellent matrix for chondrogenesis in vivo.

Acknowledgements

The authors would like to thank the Department of Pathology of the Erasmus University Rotterdam for the kind hospitality at the laboratory. Pieter Derkx is especially acknowledged for performing the immunohistochemical stainings on DBM. Wim van Vianen of the Department of Clinical Microbiology is acknowledged for his help with the isolation of peritoneal macrophages and the Central Animal Laboratory for taking care of the rabbits.

OP1 was a kind gift of Creative Biomolecules (Dr. K. Sampath). The monoclonal antibody II-II6B3 was obtained from the Developmental Studies Hybridoma Bank maintained by the Department of Pharmacology and Molecular Sciences, John Hopkins University School of Medicine, Baltimore, MD, and the Department of Biological Sciences, University of Iowa, Iowa City, IA, under contract N01-HD-6-2915 from the NICHD.

This study was supported by the Sophia Foundation and by the Technology Foundation (STW), applied science division of NWO and the technology programme of the Ministry of Economic Affairs.

References

[1] Skoog T, Ohlsen L, Sohn SA. Perichondrial potential for cartilage regeneration. Scand J Plast Reconstr Surg 1972;6:123-5.

[2] Engkvist O, Wilander E. Formation of cartilage from rib perichondrium grafted to an articular defect in the femur condyle of the rabbit. Scand J Plast Reconstr Surg 1979;13:371-6.

[3] Engkvist O, Skoog V, Pastacaldi P, Yormuk E, Juhlin R. The cartilaginous potential of the perichondrium in rabbit ear and rib. A comparative study in vivo and in vitro. Scand J Plast Reconstr Surg 1979;13:269-74.

[4] Homminga GN, Van der Linden TJ, Terwindt-Rouwenhorst EAW, Drukker J. Repair of articular defects by perichondrial grafts. Experiments in the rabbit. Acta Orthop Scand 1989;60:326-9.

[5] Homminga GN, Bulstra SK, Bouwmeester PS, Van der Linden AJ. Perichondral grafting for cartilage lesions of the knee. J Bone Jt Surg 1990;72B:1003-7.

[6] Bean JK, Verwoerd-Verhoef HL, Verwoerd CDA, van der Heul RO. Chondrogenesis in a collagen matrix. In: Dixon A, Sarnat B, editors. Fundamentals of bone growth. Boca Raton, USA: CRC Press, 1991:113-20.

[7] en Koppel PGJ, van Osch GJVM, Verwoerd-Verhoef HL. A method to generate a cartilage graft; perichondrium combined with spongeous demineralized bovine bone matrix. Trans ORS 1997;22:538.

[8] Pirsig W, Bean JK, Lenders H, Verwoerd CDA, Verwoerd-Verhoef HL. Cartilage transformation in a composite graft of demineralized bovine bone matrix and ear perichondrium used in a child for the reconstruction of the nasal septum. Int J Ped ORL 1995;32:171-81.

[9] Urist MR, Mikulski A, Lietze A. Solubilized and insolubilized bone morphogenetic protein. Proc Natl Acad Sci USA 1979;75:1828-32.

[10] Sampath TK, Nathanson MA, Reddi AH. In vitro transformation of mesenchymal cells derived from embryonic muscle into cartilage in response to extracellular matrix components of bone. Proc Natl Acad Sci USA 1984;81:3419-23.

[11] Dieudonne« SC, Semeins CM, Goei SW, Vukicevic S, Klein Nulend J, Sampath TK, Helder M, Burger EH. Opposite effects of osteogenic protein and tranforming growth factor β on chondrogenesis in cultured long bone rudiments. J Bone Miner Res 1994;9:771-80.

[12] Iwasaki M, Nakata K, Nakahara H, Nakase T, Kimura T, Kimata K, Caplan AI, Ono K. Transforming growth factor- β1 stimulates chondrogenesis and inhibits osteogenesis in high density culture of periosteum-derived cells. Endocrinology 1993; 132:1603-8.

[13] Izumi T, Scully SP, Heydemann A, Bolander ME. Transforming growth factor β1 stimulates type II collagen experession in cultured periosteum-derived cells. J Bone Miner Res 1992; 7:115-21.

[14] Moar G, Hochberg Z, Silbermann M. Insulin-like growth factor I accelerates proliferation and differentiation of cartilage progenitor cells in cultures of neonatal mandibular condyles. Acta Endocrinol 1993;128:56-64.

[15] Miura Y, Fitzsimmons JS, Commisso CN, Gallay SH, O'Driscoll SW. Enhancement of periosteal chondrogenesis in vitro. Doseresponse for transforming growth factor-β1. Clin Orthop Relat Res 1994;301:271-80.
[16] O'Driscoll SW, Recklies AD, Poole AR. Chondrogenesis in periosteal explants. An organ culture model for in vitro studies. J Bone Jt Surg 1994;76a:1042-51.
[17] Yaeger P, Kaluzhny J, Masi TL, Tubo R, McPherson J, Binette F. Synergistic action of TGF- β and IGF-1 is sufficient for redifferentiation of adult human articular chondrocytes in defined medium. Trans Orthop Res Soc 1997;22:515.
[18] Teitelbaum SL, Stewart CC, Kahn AJ. Rodent peritoneal macrophages as bone resorbing cells. Calcif Tissue Int 1979;27:255-61.
[19] Holtrop M, Cox KA, Glowacki J. Cells of the mononuclear phagocytic system resorb implanted bone matrix: a histologic and ultrastructural study. Calcif Tissue Int 1982;34:488-94.
[20] Landesman R, Reddi AH. In vivo analysis of the half-life of the osteoinductive potential of demineralized bone matrix using diffusion chambers. Calcif Tissue Int 1989;45:348-53.
[21] Donski P, O'Brien BMcC. Perichondrial microvascular free transfer: an experimental study in rabbits. Br J Plast Surg 1980;33:46-53.
[22] Ohlsen L. Cartilage regeneration from perichondrium. Experimental studies and clinical applications. Plast Reconstr Surg 1978;62:507-13.
[23] Inoue T, Deporter DA, Melcher AH. Induction of chondrogenesis in muscle, skin, bone marrow and periodontal ligament by demineralized dentin and bone matrix in vivo and in vitro. J Dent Res 1986;65:12-22.
[24] Glowacki J. Cellular reactions to bone-derived material. Clin Orthop Relat Res 1996;324:47-54.
[25] Verwoerd CD, Adriaansen FC, van der Heul RO, Verwoerd- Verhoef HL. Porous hydroxylapatite-perichondrium graft in cricoid reconstruction. Acta Oto-Laryngol 1987;103:496-502.
[26] Ruuskanen MM, Virtanen MK, Tuominen H, Tormala P, Waris T. Generation of cartilage from auricular and rib free perichondrial grafts around a self-reinforced polyglycolic acid mould in rabbits. Scand J Plast Reconstr Surg Hand Surg 1994;28:81-6.
[27] Matsuda K, Nagasawa N, Suzuki S, Isshiki N, Ikada Y. In vivo chondrogenesis in collagen sponge sandwiched by perichondrium. J Biomater Sci Polym Ed 1995;7:221-9.

3C

A new in vivo model for testing cartilage grafts and biomaterials: the 'rabbit pinna punch-hole' model

Biomaterials 2001;22:1407-14

A new in vivo model for testing cartilage grafts and biomaterials: the 'rabbit pinna punch-hole' model

Paul G.J. ten Koppel, Gerjo J.V.M. van Osch,
Carel D.A. Verwoerd, Henriette L. Verwoerd-Verhoef

Abstract

In this study an animal model was developed for evaluation of the feasibility of cartilage grafts. In the cartilage of the external ear of the rabbit multiple holes, 6mm in diameter, were punched, leaving the adherent skin intact. Different experimental groups were evaluated. First, the punch-hole model was validated under various conditions to study spontaneous or perichondrial initiated regeneration of the cartilage defect. When both cartilage and perichondrium was excised no spontaneous repair of the cartilage defect was observed. When perichondrium is present, variable patch-like closure of the punch hole was found. As 'golden standard' a punched out piece of cartilage was reimplanted directly. This condition showed adequate closure of the punch hole, however, no perfect integration of graft and surrounding cartilage was observed. Secondly, to evaluate the 'punch-hole model' a biomaterial, trabecular demineralized bovine bone matrix (DBM), was implanted and tested as a scaffold for tissue engineering techniques in vivo and in vitro. Direct implantation of DBM did not lead to any cartilage formation to close the defect. In vivo engineered cartilage, generated by enveloping DBM in perichondrium for 3 weeks, could adequately close the punch hole. When DBM was seeded with isolated chondrocytes in vitro before implantation in the defect, a highly fragmented graft, with some islets of viable cells was seen. To promote an effcient and reliable evaluation of cartilage grafts a semi-quantitative grading system was developed. Items such as quality, quantity and integrity of the cartilage graft were included in a histomorphological grading system to provide information about the properties of a specific cartilage graft. To validate the grading system, all conditions were scored by two independent observers. An excellent reliability (R=0.96) was seen between the observers. In summary, the rabbit pinna punch-hole model is a reliable and efficient method for first evaluation of cartilage grafts. The results can be easily analyzed using a semi-quantitative grading system.

Introduction

Repair of lost or damaged cartilage has been a challenging field of research in the last decade. Latest research is focussed on techniques of tissue engineering and the integration of tissue engineered grafts, next to the use of bank cartilage or autologous cartilage harvested at a donor site. Considerable efforts have been put in the improvement of the efficacy of various cartilage grafts in the field of otorhinolaryngology, plastic- and reconstructive surgery and orthopedic surgery. The potency of newly engineered cartilage grafts in vivo has been evaluated mainly at subcutaneous implantation sites [1–5]. Implantation under the skin is easy and many grafts can efficiently be studied in one animal. However, cartilage grafts should be designed to close a cartilage defect. Assessment of the properties of a cartilage graft placed subcutaneously is not always sufficient. Bonding of the graft to the host cartilage in situ is of paramount importance. In the ideal situation cartilage grafts should be implanted at clinically relevant sites when tested in animal models. However, graft implantation in the nasal septum, larynx or knee is technically difficult, a burden to the animal and only one cartilage graft can be tested in each animal.

In search for an animal model to test both graft and bonding characteristics, we developed the 'rabbit pinna punch-hole' model. In contrast to cartilage at other locations, pinna (auricle) cartilage is easy to reach, making the procedure fast and causing minimal distress to the animals. In each pinna up to four punch holes were made; in this way as many as eight grafts can be tested in one animal. The punch-hole model was validated using various conditions to study spontaneous closure and the influence of perichondrium on cartilaginous filling of the defect. As 'golden standard' a punched out piece of cartilage was reimplanted directly. Repair of cartilage defects with trabecular demineralized bovine bone matrix (DBM) was studied earlier [6,7]. To validate the model, trabecular DBM was treated in different ways. It was implanted directly in the defect to study whether colonization of cells from the surrounding tissue in the biomaterial initiate regeneration of the defect. In addition, two different tissue engineering techniques were used to create a cartilage graft using DBM, firstly by allowing perichondrial cells to colonize the trabecular DBM in vivo and secondly by seeding freshly isolated chondrocytes in the matrix in vitro, prior to implantation.

To evaluate the feasibility of various cartilage grafts, a semi-quantitative grading system was developed inspired by O'Driscoll et al. [8]. Items such as quantity and quality of the cartilage graft, and the bonding with the surrounding cartilage were included in the grading system. Summarizing, the purpose of this study was to develop a model for adequate and rapid evaluation of a variety of cartilage grafts, thus giving insight in the capacity of such

a graft for implantation at a more relevant site. Hence, we validated and evaluated the punch-hole model and grading system with various grafts.

Materials and methods

All animal experimental procedures in this study were approved by the Animal Ethics Committee (protocol no. 1269501) and carried out in accordance with the guidelines of the Erasmus University Rotterdam (the Netherlands).

Punch-hole procedure

Twelve young (1500–2000 g; 8–10 weeks) and five adult (3500–4500 g; > 30 weeks) New Zealand White rabbits were used. Anaesthesia was effectuated with 2% xylazine-hydrochloride (Rompun, Bayer, Leverkusen, Germany) 0.5 ml/kg body weight and 10% ketaminehydrochloride (Ketalin, Apharma, Arnhem, the Netherlands) 0.5ml/kg body weight via intramuscular injection.

Fig. 1. Per-operative view of punch-hole procedure, the overlying skin is elevated ▽. Punched-out piece of cartilage covered with perichondrium **O**. Device to protect contra-lateral skin, biopsy punch device ▲. Scale indicates millimeters; the diameter of the punch hole is 6 mm.

The operation sites were shaved and disinfected with 70% alcohol. The skin at the concave side was incised and bluntly elevated. An oblique incision, approximately 1 cm, in the cartilage and perichondrium was made taking care not to damage the skin at the contralateral, convex side. Through this cartilage-slit the contralateral skin could be tunneled. A plastic device was temporarily brought in this tunnel to protect the contralateral skin when a punch hole was made (Fig. 1). Four punch holes (biopsy punch device; Stiefel, im-

ported by Bipharma, the Netherlands), 6mm in diameter, could be made in each pinna in a way they were sufficiently separated from each other. The skin was closed and wounds were dressed with gauzes (Bethadine, Asta Medica, the Netherlands) which were removed one day after surgery. After 6 weeks the cartilage grafts were excised with adjacent cartilage and processed for histology.

The punch-hole model was validated using three different conditions (series 1).

Series 1a. Punch hole through cartilage and perichondrium (n=10).
Series 1b. Punch hole through cartilage alone, the perichondrial cover on both sides of the cartilage defect was left intact (n=10).
Series 1c. Punch hole grafted with the punched out ear cartilage and perichondrium that was 180° rotated (n=10).

In series 1a–c five young and five adult animals were included.

Subsequently a biomaterial, trabecular demineralized bovine bone matrix (DBM; Osteovit, Braun GmBH, Melsungen, Germany) was used to evaluate the feasibility of the model (series 2).

Series 2a. Punch hole grafted with trabecular DBM (n=10).
Series 2b. Punch hole grafted with newly formed autologous cartilage, in vivo generated by combining DBM and perichondrium (n=10).
Series 2c. Punch hole grafted with autologous chondrocytes seeded in DBM in vitro (n=7).

In series 2a and b five young and five adult animals were included. Series 2c contained seven (only) young animals to obtain the best possible graft using these tissue engineering methods.

For series 2a, discs of trabecular DBM with a diameter of 6mm and a thickness of 2–3mm were punched out and directly placed into the defect. In series 2b, a new piece of cartilage was generated in vivo with the use of trabecular DBM and perichondrium, according to a previously described method [9]. In short, a piece of DBM measuring 8x8x2 mm was wrapped in a pedicled flap of ear perichondrium. After 3 weeks the matrix was cartilaginized and the graft harvested [6]. Then, this piece of newly generated cartilage was adjusted to the dimensions of the punch hole using a biopsy punch, and implanted in defects created in the other ear. To secure the graft to the surrounding host cartilage, the perichondrium of the graft was sutured with Vicryl 8.0 atraumatic absorbable sutures (Ethicon GmbH & Co.KG, Norderstedt, Germany) to the perichondrium covering the host cartilage. In series 2c, chondrocytes were isolated from a large piece of aseptically har-

vested cartilage from the right ear. This, piece, measuring about 20x40x2 mm, was rinsed twice in saline with gentamicin (50 µg/ml) and fungizone (0.5 µg/ml); and then sliced into small pieces none greater than 2x2x2 mm. Slices were incubated for 2 h at 37 °C with protease (2 mg/ml; Sigma, St.Louis, MO) in saline followed by overnight incubation at 37 °C with collagenase B (2 mg/ml; Boehringer, Mannheim, Germany) in medium with 10% FCS. The suspension was filtered using a filter with a pore size of 100 µm, to remove undigested parts. These isolated chondrocytes were washed with saline. Cell viability was tested using the trypan blue exclusion test. To obtain an equal distribution of chondrocytes in the biomaterial and to achieve the highest possible seeding density, all isolated cells were suspended in 1.2% low-viscosity alginate gel (Keltone LV, Kelco, Chicago, IL) in saline, resulting in a density of $1\text{-}3x10^7$ cells/ml of gel. The gel then was absorbed by a punched out piece of trabecular DBM, 6mm in diameter and 2–3mm in thickness, so that all pores of the DBM matrix were filled with cells suspended in gel. The alginate in the graft was allowed to polymerize for a period of 10 min in a 102 mM $CaCl_2$ solution, and thereafter washed with saline. Finally, the graft was implanted in a punch-hole defect created in the left ear.

Histomorphological analysis

In all series the cartilage grafts were excised after 6 weeks. The adjacent cartilage was included in the resection area in order to study the interface characteristics of graft and surrounding host cartilage. The specimens were transversely cut in two equal parts. One part was stored at –80 °C for future analysis, the other part was fixed in 4% phosphate buffered formalin, decalcified with 10% EDTA and embedded in paraffin. Serial sections (5 µm) were cut, stained with Alcian Blue and counterstained with Nuclear Fast Red.

Of each cartilage graft two histological sections, at least 150 µm apart, were examined using a histomorphological grading system inspired by O'Driscoll et al. [8]. This grading system consists of two parts: (1) quality and quantity of the cartilage graft, (2) structural characteristics of the cartilage graft (Table 1). In the first part the cellular morphology of the cartilage-like tissue in the defect was graded. Normal mature cartilage cells are round shaped and located in the lacunae of the cartilage matrix. Immature cartilage cells are smaller and often triangular. Morphological characteristics and by the absence of Alcian Blue staining make distinction possible between fibrous tissue, bone and cartilage. Secondly, the staining of the cartilage matrix was classified. Blue staining of the matrix suggests a high glycosaminoglycan content indicating the presence of cartilage. The amount of cartilaginous tissue filling the defect was estimated ranging from complete closure (1) to no cartilage present in the defect (0). This number was used as a multiplier for both items scored on the first part of the grading (quality and quantity of cartilage

graft). In this way, next to cell and matrix morphology of the cartilage graft, the amount of cartilage filling the defect was scored.

In the second part of the grading system the integrity of the graft and the bonding with the surrounding cartilage was scored. The structural integrity was included because one or multiple interruptions will have an adverse effect on the solidity of the cartilage graft. Slight disruption of the graft was defined as the presence of cysts or blood vessels in an otherwise continuous cartilage graft. When the graft showed gross continuity but at least one interruption this was scored accordingly. Finally, severe disintegration of the grafts or bone formation was graded zero points. The cartilage graft with the surrounding host cartilage was dissected as one block, making it possible to grade the bonding between graft and host cartilage. Integrating of the graft with the present cartilage was scored ranging from cartilage bonding on both

Table 1. Histomorphological grading of cartilage grafts

1. Quality and quantity (max.6 points)	
Nature of cartilage like tissue[a]	
Cellular morphology	
Differentiated cartilage	4
Young incompletely differentiated	2
No cartilage	0
Alcian Blue staining of the matrix	
Normal or near normal	2
Moderate/slight	1
None	0
2. Structural characteristics (max.6 points)	
Structural integrity of the graft	
Normal	3
Slight disruptions, cysts or blood vessels	2
One or multiple interruptions	1
Bone formation or severe disintegration	0
Bonding to existing cartilage	
Both sides with cartilage	3
One side with cartilage	2
Bonded with fibrous tissue	1
Not bonded at all	0
Total score: item 1+2 (max.12 points)	

[a] Percentage of cartilage like tissue filling the defect 100% (complete) – 0% (none) multiplication factor 1.0...0.0 for points scored on item 1.

sides, fibrous bonding and no bonding at all. The total score for a graft was calculated by summarizing the score the first and second section of the grading table.

Statistical analysis

Two independent observers examined the microscopic sections. For each graft the mean score of two representative sections was calculated. The inter-observer correlation was calculated by 2-tailed Spearman rank correlation test. The correlation coefficient was calculated for the total score (R_t) and for the two separate parts of the grading table, quality and quantity of the cartilage graft (R_q) and structural characteristics (R_s), respectively. In this study the correlation coefficients were used as measure for reproducibility of the grading system. Values equal to or greater than 0.75 were interpreted as excellent reliability, values between 0.4 and 0.75 represented fair reliability, while values below 0.4 represented poor reliability. Confidence resemblance between two independent observers was calculated by Wilcoxon paired-rank test.

Kruskal-Wallis one-way ANOVA was used to evaluate differences between the experimental groups, $p < 0.05$ was considered statistically significant. Differences between the various groups, were calculated using Wilcoxon paired-rank test, $p < 0.05$ was defined statistically significant.

Results

All animals gained weight and showed no sign of distress. No infection or perforation of the skin covering the implant was observed. Within experimental groups no differences were found between young and adult animals; therefore they were considered as one group.

Validation of the punch-hole model

In an ungrafted defect (series 1a), no spontaneous regeneration was observed (Table 2). At the cut edges the cartilage seemed vital and was sometimes overgrown by perichondrium (Fig. 2a). In six out of 10 specimens the cut edge was thickened by cartilage apposition most probably generated by the perichondrium. In the second group (series 1b; Fig. 2b) the punch hole was covered on both sides with perichondrium. The amount of cartilage generated from the perichondrium varied considerably between the specimens. Filling of the defect varied from cartilage to completely fibrous tissue (Table 2). Using an autologous cartilage graft (series 1c), five out of 10 specimens demonstrated complete closure of the defect (Fig. 2c). In three specimens the graft was attached to the surrounding host cartilage only on

Table 2. Grading scores of grafts[a]

	Parameters (see Table 1)	Median	Inter quartile range	Total range
Ungrafted defect (series 1a)	1	0.0	0.0–0.2	0.0–0.9
	2	0.0	0.0–0.2	0.0–0.0
	Total score	0.0	0.0–0.2	0.0–0.9
Ungrafted defect, perichondrium intact (series 1b)	1	4.8	4.5–5.5	3.0–5.7
	2	3.8	3.5–4.5	1.0–4.8
	Total score	8.6	6.5–9.7	5.5–10.5
Autologous cartilage (series 1c)	1	6.0	6.0–6.0	6.0–6.0
	2	5.5	5.5–6.0	4.0–6.0
	Total score	11.5	11.5–12.0	10.0–12.0
Demineralized bone matrix (DBM) (series 2a)	1	0.0	0.0–0.0	0.0–0.5
	2	0.0	0.0–0.0	0.0–0.0
	Total score	0.0	0.0–0.0	0.0–0.5
Cartilage generated in vivo (series 2b)	1	5.9	5.7–6.0	1.2–6.0
	2	3.5	3.0–4.0	2.0–6.0
	Total score	9.4	8.8–10.0	4.2–12.0
Chondrocytes seeded in DBM in vitro (series 2c)	1	3.8	3.8–3.8	1.0–4.0
	2	1.0	1.0–2.0	1.0–2.0
	Total score	4.8	4.5–5.5	2.5–6.0

[a]n=10 for series 1a–c, 2a and b; n=7 for series 2c mean of two observers are presented.

one side, in two specimens no cartilaginous bonding could be detected (Table 2). Although cartilaginous bonding was seen in most specimens, no real integration of the cartilage matrices of the graft and the surrounding host cartilage was observed; the connection was mostly side to side initiated by neo-cartilage generated by the perichondrium (Fig. 2c and d). Consequently, the level of the cartilage graft was never completely in line with the surrounding cartilage. In fact, angulation with oblique interposition of the graft was found in three specimens.

Using a Kruskal-Wallis one-way ANOVA, a significant difference was found between conditions used for validation of the punch-hole mode ($p < 0.001$). A defect with perichondrial cover (series 1b) scored significantly better than a punch hole through both cartilage and perichondrium (series 1a). Closing the punch-hole with an autologous cartilage graft (series 1c) scored significantly best.

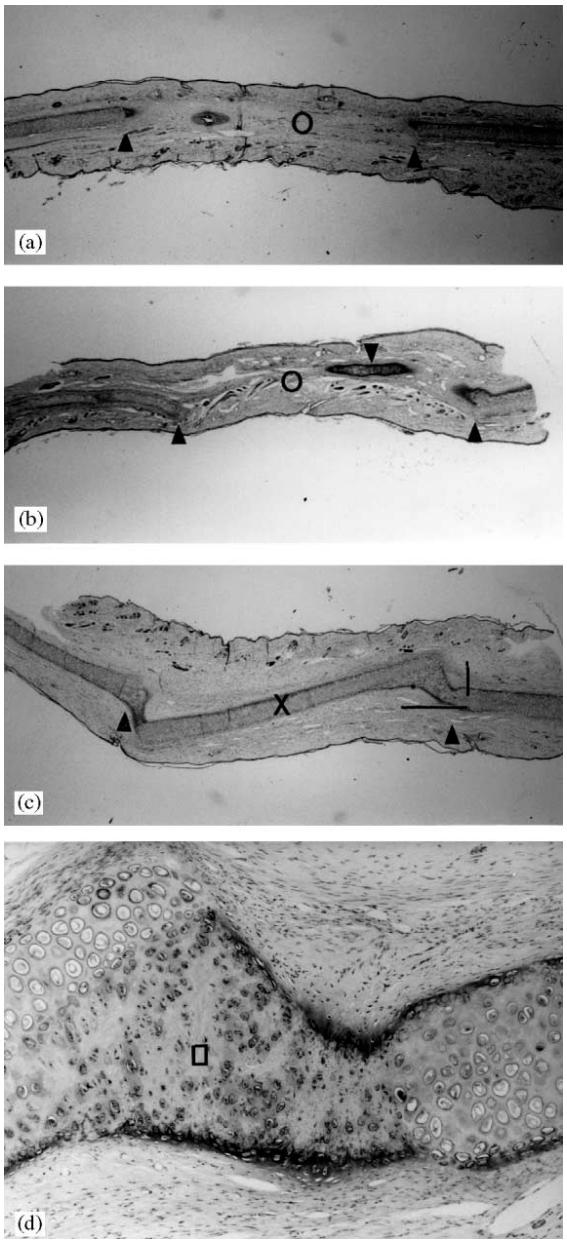

Fig. 2. Histologic sections of various conditions to validate the punchhole model (Alcian Blue, 12.4x,) cutting edge ▲, punch hole **O**: (a) punch hole (series 1a); (b) cartilage punched out but perichondrial cover left intact (series 1b); note islet of newly generated cartilage ▼; (c) autologous cartilage graft (series 1c); (d) High power magnifcation of the area indicated in (c). Note the newly formed cartilage generated by perichondrium □. The union between graft and cutting edge is angulated (Alcian Blue, 40x).

Evaluation of a biomaterial (trabecular DBM) in the punch-hole model

When trabecular demineralized bovine bone matrix (DBM) was directly implanted in the defect (series 2a), no traces of biomaterial or cartilage generation were observed after 6 weeks (Table 2). Only fibrous tissue was present in the punch hole. This condition was not significantly different from an ungrafted punch hole. When in vivo engineered cartilage was implanted in the punch hole (series 2b), a complete cartilaginous filling of the defect was found in five out of 10 specimens (Fig. 3a; Table 2). In one specimen the graft became partially necrotic leading to a filling of less than 50% of the defect diameter with cartilage, leading to a very poor score (4.2) of this particular specimen. In vivo engineered cartilage scored higher compared to

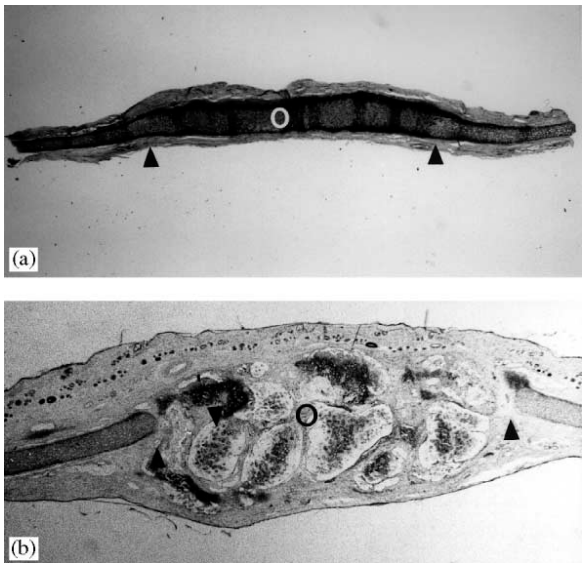

Fig. 3. Evaluation of a biomaterial, trabecular demineralized bovine bone matrix (DBM), in the punch-hole model; cutting edge ▲, graft **O** (Alcian Blue, 12.4): (a) in vivo engineered cartilage (series 2b); (b) chondrocytes seeded in trabecular DBM (series 2c). Islets of newly generated cartilage are present ▼.

cartilage generated by perichondrial cover only, however, this difference was not significant.

Trabecular DBM in vitro seeded with chondrocytes and implanted for 6 weeks, demonstrated islets of vital chondrocytes surrounded by newly generated cartilage matrix (Fig. 3b). In this condition the cartilage graft was highly fragmented, there was no cartilaginous continuity as was found in the in vivo engineered DBM graft. Graft of chondrocytes seeded in DBM in vitro (series 2c) scored significantly lower than the graft engineered in vivo (series 2b), scores of 4.8 and 9.4, respectively.

Grading system

The interobserver correlation of the total score (R_t) calculated for the validation (series 1) was 0.97, the correlation of the conditions tested in the evaluation group (series 2) was 0.98, both indicating excellent reliability (Table 3). All series but series 1c, were scored with excellent reliability. In this condition (defect grafted with autologous cartilage) the range of scores between different grafts was minimal (Table 2), therefore a small variation between observers leads to relatively low correlation. This could erroneously be misinterpreted as poor quality of grading. In addition to the inter-observer correlation of the total score, the correlations for both separate items of the grading system, quality and quantity and structural characteristics, were calculated. In the validation group the correlation coefficients were 0.89 and 0.97, respectively. Even higher correlations were found in the second group (series 2), 0.96 and 0.98, respectively.

Table 3. Inter-observer correlation of grading system

	Total score	
	Correlation	p
Validation group (series 1a,b,c)	0.97	<0.01
Ungrafted defect (series 1a)	0.92	<0.01
Ungrafted defect, perichondrium intact (series 1b)	0.86	<0.01
Autologous cartilage (series 1c)	0.70	0.24
Evaluation group (series 2a,b,c)	0.98	<0.01
Demineralized bone matrix (DBM) (series 2a)	1.00	<0.01
Cartilage generated in vivo (series 2b)	0.78	<0.01
Chondrocytes seeded in DBM in vitro (series 2c)	0.88	<0.01

Discussion

New biomaterials and tissue engineering techniques are more frequently used for the development of cartilage grafts [2–5,10–13]. After in vitro testing on cell viability and cytotoxicity, rapid in vivo evaluation would facilitate the evaluation of feasibility of a cartilage graft. Subsequently more extensive testing, such as long-term studies and studies at the target location, are to be performed. In this study we present a new model for in vivo evaluation of biomaterials and cartilage grafts. In this model, next to the structural characteristics of a potential cartilage graft, the junction between graft and surrounding host cartilage can be studied. Previously, rabbit ear cartilage has been used to study tissue repair processes of skin, perichondrium and cartilage [14,15]. The rabbit's ear is large and its cartilage is easily accessible. Hence, multiple punch-hole defects can be made in one ear. Implantation of cartilage grafts is technically not difficult and the whole procedure causes minimal morbidity to the rabbit.

In the punch-hole model no spontaneous cartilaginous closure of the defect was found. Grafting the defect with the punched-out piece of cartilage, inclusive of the perichondrial cover, showed good cartilaginous closure of the defect. The graft was viable and cartilaginous bonding to the surrounding host cartilage was found in most specimens. This is consistent with earlier results of Duncan et al. [16] and Eisemann [17], who found good repair of cartilage defects with autologous cartilage covered by perichondrium. When the properties of a cartilage graft are to be evaluated in a model, excluding the effects of perichondrium on the graft, the punched-out piece of cartilage should include the perichondrial cover. When perichondrium was left intact while the cartilage was removed, some cartilage neoformation was found,

however, the quantity was highly variable. This finding supports earlier observations in the rabbit where perichondrium was demonstrated to induce some new cartilage [18–20]. Likewise, after resection, submucoperichondrial, of part of the nasal cartilage, complete bridging of the defect by newly generated cartilage was never found [21]. Sometimes, however, the influence of remaining perichondrium can be of interest. Various biomaterials have been tested for augmentation of cartilage after submucoperichondrial resection in nasal surgery [22–25]. To evaluate the feasibility of cartilage grafts to be used for such purposes, the graft could be placed in the cartilage defect between perichondrial sheets completely covering the graft. Hence, in our model it is possible to punch out cartilage, leaving the perichondrium intact. Interposition of biomaterials between a perichondrial sandwich mimics the situation of submucoperichondrial insertion of a graft as in nasal surgery.

A histomorphological grading system based on a system of O'Driscol et al. [8] was developed to provide efficient evaluation of cartilage grafts. In this way the quality, quantity and integrity of the grafts could be graded. Since surrounding host cartilage was taken out along with the graft, the interface (bonding characteristics) could also be evaluated and is added as a special feature to the grading table. The correlation between two independent observers was excellent. Earlier, Ostergaard et al. [26] found a poor inter-observer reproducibility evaluating the semi-quantitative histologic/histochemical grading system for osteoarthritis developed by Mankin and coworkers [27]. In their study the reproducibility of three subcategories were evaluated; the category 'structure' scored relatively low because assessment variables in this group were not clearly defined and grading was performed according to eight different features. Therefore, consensus was rare. In the grading system we designed, four subcategories were scored; in each subcategory a maximum of only four items were graded. Examining the histologic sections, gross features were scored and consensus between observers was frequent. This way the inter-observer correlation is high and the semi-quantitative grading system is suitable for the evaluation of different cartilage grafts.

Earlier, Urist has shown cortical DBM to have a chondrogenic potential when implanted in vivo [28]. Later, we have demonstrated cartilage formation in trabecular DBM when brought into close contact with perichondrium [6,7,29]. In the present study, no cartilage formation was found 6 weeks after implantation of 'bare' trabecular DBM in a punch-hole defect. Filling the punch hole with a cartilaginized composite graft of trabecular DBM and perichondrium, provided good cartilaginous restoration of the defect and bonding to the surrounding host cartilage. The mean score in this group was slightly less compared to implantation of autologous cartilage because the integrity of the newly generated cartilage was not always perfect; the graft

sometimes showed some interruptions. Finally, trabecular DBM was tested as a scaffold to seed freshly isolated young chondrocytes in vitro. Madsen et al. [30] demonstrated that the synthesis of cartilage matrix molecules such as proteoglycans, collagen and elastin declines in the adult specimen. Therefore, only young autologous cartilage cells were seeded in order to obtain the best possible graft. Although the chondrocytes were vital producing cartilage matrix after implantation in vivo, the integrity of the generated cartilage graft after 6 weeks was poor. Also, Nehrer et al. [31] found adverse effects on the morphology of cartilage cells seeded into a collagen type I matrix with a large pore size. Before seeding in the biomaterial, this trabecular DBM basically is a collagen type I scaffold with a large pore size. Although the cells were suspended in alginate before seeding in DBM, facilitating seeding of cells uniform in the matrix, we concluded that DBM is not suitable as a scaffold for tissue engineering.

Finally, in the punch-hole model, other items like tissue adhesives can be studied. Recently, the use of different tissue adhesives have been advocated for cartilage grafts [32–35]. In the punch-hole model the interface between graft and surrounding host cartilage can be easily studied, also after application of adhesives.

In summary, the rabbit pinna punch-hole model is an efficient method for first evaluation of cartilage grafts or biomaterials. The results can be quickly analyzed using a semi-quantitative grading system with an excellent inter-observer correlation. In this way multiple grafts can be tested neatly in each rabbit, with minimal animal distress. Hence, grading the cartilage graft by focusing on different items included in our grading table will give the researcher more insight in the specific properties of different grafts.

Acknowledgements

The authors like to thank the animal center, Erasmus University Rotterdam, for taking care of the rabbits. Frank van de Panne is acknowledged for his excellent photographical assistance and Koen Bos for critical reading of the manuscript. The research of GvO is supported by the Technology Foundation (STW), applied science division of NWO and the technology program of the Ministry of Economic Affairs.

References

[1] Vacanti CA, Paige KT, Kim WS, Sakata J, Upton J, Vacanti JP. Experimental tracheal replacement using tissue-engineered cartilage. J Pediatr Surg 1994;29:201–4.

[2] Puelacher WC, Mooney D, Langer R, Upton J, Vacanti JP, Vacanti CA. Design of nasoseptal cartilage replacements synthesized from biodegradable polymers and chondrocytes. Biomaterials 1994;15:774–8.

[3] Matsuda K, Nagasawa N, Suzuki S, Isshiki N, Ikada Y. In vivo chondrogenesis in collagen sponge sandwiched by perichondrium. J Biomater Sci Polym Ed 1995;7:221–9.

[4] Aigner J, Tegler J, Hutzler P, Campaccia D, Pavesia A, Hammer C, Kastenbauer E, Naumann A. Cartilage tissue engineering with novel nonwoven structured biomaterial based on hyaluronic acid benzyl ester. J Biomed Mater Res 1998;42:172–81.

[5] Marijnissen WJCM, van Osch GJVM, Aigner J, Verwoerd-Verhoef HL, Verhaar JAN. Tissue engineered cartilage using serially passaged mature articular chondrocytes. Biomaterials 2000; 21:571–80.

[6] Bean JK, Verwoerd-Verhoef HL, Meeuwis J, Verwoerd CD. Reconstruction of the growing cricoid with a composite graft of demineralized bovine bone and autogenous perichondrium: a comparative study in rabbits. Int J Pediatr Otorhinolaryngol 1993;25:163–72.

[7] Ten Koppel PGJ, van Osch GJVM, Verwoerd CDA, Verwoerd- Verhoef HL.E Efficacy of perichondrium and a trabecular demineralized bone matrix for generating cartilage. Plast Reconstr Surg 1998;102:2012–20.

[8] O'Driscoll SW, Keeley FW, Salter RB. The chondrogenic potential of free autogenous periosteal grafts for biological resurfacing of major full-thickness defects in joint surfaces under the influence of continuous passive motion. An experimental investigation in the rabbit. J Bone Jt Surg Am 1986;68:1017–35.

[9] Bean JK, Verwoerd-Verhoef HL, Verwoerd CDA. Chondrogenesis in a Collagen Matrix. Fundamentals of bone growth. 1991. p. 113–20 [Chapter 8].

[10] Bujia J, Sittinger M, Hammer C, Burmester G. Culture of human cartilage tissue using a perfusion chamber. Laryngorhinootologie 1994;73:577–80 (in German).

[11] Haisch A, Schultz O, Perka C, Jahnke V, Burmester GR, Sittinger M. Tissue Engineering of human cartilage tissue for reconstructive surgery using biocompatible resorbable fibrin gel and polymer carriers. Hno 1996;44:624–9 (in German).

[12] Cao Y, Vacanti JP, Paige KT, Upton J, Vacanti CA. Transplantation of chondrocytes utilizing a polymer-cell construct to produce tissue-engineered cartilage in the shape of a human ear. Plast Reconstr Surg 1997;100:297–302.

[13] Rotter N, Aigner J, Naumann A, Planck H, Hammer C, Burmester G, Sittinger M. Cartilage reconstruction in head and neck surgery: comparison of resorbable polymer scaffolds for tissue engineering of human septal cartilage. J Biomed Mater Res 1998;42:347–56.

[14] Joseph J, Dyson M. Tissue replacement in the rabbit's ear. Br J Surg 1966;53:372–80.

[15] Urist MR, Raskin K, Goltz D, Merickel K. Endogenous bone morphogenetic protein: immunohistochemical localisation in repair of a punch hole in the rabbit's ear. Plast Reconstr Surg 1997;99:1382–9.

[16] Duncan MJ, Thomson HG, Mancer JF. Free cartilage grafts: the role of perichondrium. Plast Reconstr Surg 1984;73:916–23.
[17] Eisemann ML. The growth potential of autograft cartilage. An experimental study. Arch Otolaryngol 1983;109:469–72.
[18] Skoog T, Ohlsen L, Sohn SA. Perichondrial potential for cartilagenous regeneration. Scand J Plast Reconstr Surg 1972;6:123–5.
[19] Engkvist O, Skoog V, Pastacaldi P, Yormuk E, Juhlin R. The cartilaginous potential of the perichondrium in rabbit ear and rib. A comparative study in vivo and in vitro. Scand J Plast Reconstr Surg 1979;13:275–80.
[20] Homminga GN, van der Linden TJ, Terwindt-Rouwenhorst EA, Drukker J. Repair of articular defects by perichondrial grafts. Experiments in the rabbit. Acta Orthop Scand 1989;60:326–9.
[21] Meeuwis J, Verwoerd-Verhoef HL, Verwoerd CDA. Normal and abnormal nasal growth after partial submucous resection of the cartilaginous septum. Acta Otolaryngol 1993;113:379–82.
[22] Je!ries DJ, Rhys Evans PH. Cartilage regeneration following septal surgery in young rabbits. J Laryngol Otol 1984;98:577–83.
[23] Petruson B. Reconstruction of the anterior nasal septum by transplantation. Rhinology 1986;24:147–50.
[24] Sta!el G, Shockley W. Nasal implants [Review] [78 refs]. Otolaryngol Clin North Am 1995;28:295–308.
[25] Lopez Aguado D, Monserrat JR, Perez Pinero B, Campos Banales ME, Gutierrez R, Diaz Flores L. Neochondrogenesis in the septal area after submucous cartilaginous resection. Acta Otolaryngol 1992;112:539–44.
[26] Ostergaard K, Petersen J, Andersen CB, Bendtzen K, Salter DM. Histologic/histochemical grading system for osteoarthritic cartilage: reproducibility and validity. Arthritis Rheum 1997;40: 1766–71.
[27] Mankin HJ, Dorfman H, Lippiello L, Zarins A. Biochemical and metabolic abnormalities in articular cartilage from osteo-arthritic human hips. J Bone Jt Surg 1997;53A:523–37.
[28] Urist MR. Bone: formation by autoinduction. Science 1965;150: 893–9.
[29] Van Osch GJVM, ten Koppel PGJ, van der Veen SW, Poppe P, Burger EH, Verwoerd-Verhoef HL. The role of trabecular demineralized bone in combination with perichondrium in the generation of cartilage graft. Biomaterials 1999;20:233–40.
[30] Madsen K, Moskalewski S, von der Mark K, Friberg U. Synthesis of proteoglycans, collagen, and elastin by cultures of rabbit auricular chondrocytes –– relation to age of the donor. Dev Biol 1983;96(1):63–73.
[31] Nehrer S, Breinan HA, Ramappa A, Young G, Shortkro! S, Louie LK, Sledge CB, Yannas IV, Spector M. Matrix collagen type and pore size influence behaviour of seeded canine chondrocytes. Biomaterials 1997;18:797–876.
[32] Harper MC.Stabilization of osteochondral fragments using limited placement of cyanoacrylate in rabbits. Clin Orthop 1988;231:272–6.
[33] Quatella VC, Futron ND, Frisina RD.E !ects of cyanoacrylate tissue adhesive on cartilage graft viability. Laryngoscope 1993;103:798–803.
[34] Brown PN, McGu! HS, Noorily AD. Comparison of N-octylcyanoacrylate vs suture in the stabilization of cartilage grafts. Arch Otolaryngol Head Neck Surg 1996;122:873–7.

[35] Jurgensen K, Aeschlimann D, Cavin V, Genge M, Hunziker EB. A new biological glue for cartilage–cartilage interfaces: tissue transglutaminase. J Bone Jt Surg Am 1997;79:185–93.

Chapter 4

Summary and conclusions

Injury and distortion of cartilage

Introduction

Distortion of a cartilage structure is defined as an acute change of form in reaction to a local injury. Wound healing is restricted to the site of the lesion (Chapter 2A). Distortion may extend to non-injured parts or even to the total structure. Injury-induced distortions have previously been reported for rib cartilage [1,2] and nasal septum cartilage [3–6]. Distortion is considered to depend on cartilage specific biophysical properties. The resilient and elastic quality of cartilage has been ascribed to the high content (80%) of water bound by hydrophilic proteins embedded in a 3-dimensional network of collagen fibres. The fibrous component determines the specific form of the structure. Interruption of the fibrous network will alter the balance between the network and the protein-bound water, and cause an immediate change of form –distortion– of the cartilage by a 'release of interlocked stresses' [5].This hypothetical mechanism has been first exploited in surgery of the nasal septum. Straightening of a curved part of septum cartilage can be accomplished by 'controlled distortion', effectuated by a few parallel incisions (scoring) on the concave side [3].

Cricoid pathology, as observed in a few post-mortem specimens from neonates or very young children, also points to injury-induced distortion [7]. The results from previous animal studies, focusing on the long-term effects of various types of endolaryngeal trauma, further supported the hypothesis of injury-induced distortion [8–11]. Finally, in surgical practice it is common knowledge that an anterior split of the cricoid –as a first step in larynx surgery– invariably leads to an immediate gap between the cut ends due to retraction (distortion) of the cartilage on both sides.

The Chapters 2B, 2C and 2D focus on injury-induced distortion and deal with the following questions:

1. Is the gap, following an anterior cricoid split, the result of an intrinsic distortion of the cartilage and/or the effect of extrinsic forces from outside the cartilage, originating in soft tissues with an insertion on the cricoid?
2. Does the distortion of a split cricoid show any changes during a long-term follow-up?
3. Is the immediate and long-term distortion of a cricoid cartilage related to age?

Injury-induced distortion of cartilage, intrinsic factors

To answer the first question distortion was initially studied 'ex vivo' in cricoid rings of rabbits immediately after dissection (Chapter 2B). In these

isolated cricoids the prompt result of an anterior split was a gap measuring 1.7 mm (total range: 0.9–2.1 mm). This observation proved that splitting of the cricoid suffices to produce an anterior gap without any interference of inserting soft tissues. Apparently, distortion is governed by factors intrinsic to cartilage.

The combination of an anterior split with bilateral scoring of the *outer* contour of the cricoid cartilage leads to increased bending of the cartilage on both sides of the split and in this, way, to a narrowing of the gap and even an overlap of the cut edges. Scoring of the *inner* contour of the cartilage, however, caused a widening of the gap, the split cricoid adapting a U-form (Chapter 2B). The inward or outward bending of the scored cricoid parts seem similar to the distortional effects on septum cartilage after unilateral scoring. Both are being considered to be due to a release of interlocked stresses in the cartilage [3].

It might also be concluded that when selected injuries are subsequently inflicted the result is a combination of cartilage distortions, which can be expected to occur after each of these injuries.

Injury-induced distortion of cartilage, in relation to the depth of incision

In the above-mentioned experiments the degree of distortion (bending) induced by scoring either on the interior or exterior contour of the split cricoid, showed small but obvious differences between individual animals within each of both experimental series. A possible explanation might be a variation in the depth of the incisions, made during the scoring procedure.

Such a relation between degree of distortion and depth of incision was studied ex vivo in isolated rabbit septum cartilage, in collaboration with the '*Netherlands Structural Optimisation and Computational Mechanics Group, Faculty of Design, Engineering and Production, Delft University of Technology'* (Chapter 2C). The septa were immersed in a physiologic solution of constant temperature and measured under weightless conditions. Optimal measuring instruments were available as well as the technical conditions and expertise for an adequate control of the depth of the incisions from 0.05 to 0.50 mm; the mean thickness of the septum at the site of the incisions equalled 0.68 mm (total range: 0.56–0.81 mm). The depth of the incision (D) was calculated as a ratio (D_r) to the septum thickness. When incisions were made with a depth ranging from 15% to 50% of the cartilage thickness, a linear correlation was found between the depth of incision and the measured angle of the bend cartilage (Bα) according to the formula:

$$B\alpha = (30.9)\ (D_r) \pm 0.05$$

Incisions involving more than 50% of the cartilage thickness demonstrated substantial variation in the degree of bending. In all specimens measurable bending was only observed after incising the cartilage of at least 15% of the thickness.

The experiments confirm the hypothesis of release of interlocked stresses as cause of progressive distortion. Effects on strength were not studied.

Injury-induced distortion of cartilage, intrinsic and extrinsic factors

Whether and to what extent extrinsic factors might influence or even induce cartilage distortion was studied in live animals (Chapter 2D). The first observations in young rabbits, 8 weeks of age, demonstrated that the dimensions of the gap after making an anterior split of the cricoid without interfering with other anatomical structures of the larynx, were smaller (median: 0.3 mm; total range: 0.1–0.6 mm) than previously found in ex-vivo isolated cricoids (median: 1.7 mm; total range: 0.9–2.1 mm). The difference suggests that extrinsic forces are restricting the dimensions of the gap. In further experiments a progressive increase of the distance between the cut ends of the split cricoid was demonstrated after subsequent transection of the cricothyroid ligament, transection of the cricotracheal ligament and elevation of the cricovocal membrane respectively (Table 3, Chapter 2D). The final dimensions of the anterior gap following this stepwise in-vivo procedure appeared to measure in the same range (median: 1.8 mm; total range: 1.4–2.3 mm) as was previously observed in ex-vivo isolated cricoids (median: 1.7 mm; total range: 0.9–2.1 mm). The (unexpected) restriction of the distortion by the cricovocal membrane may be due to a 'centripetal' force exerted by the circular tunica elastica, which is part of the subglottic mucosa and connected to the internal surface of the cricoid ring. Based on these observations it was concluded that distortion of a split cricoid reflects the resultant of changing intrinsic forces, inherent to the cartilage, and extrinsic forces from ligaments and membranes. In these experiments the influence of muscles was not yet investigated.

Injury-induced distortion of cartilage, progression during growth

The evolution of distortion during growth was studied by comparing the cricoid immediately after surgery at the age of 8 weeks, as discussed above, and 20 weeks later, when the animals have reached the adult stage (Chapter 2D). During this period the width of the anterior gap in the various experiments appeared to increase both in absolute dimensions as in proportion to the total circumference of the cricoid. Obviously growth did not mitigate the distortion. Relative differences between the effects of a single cricoid split and a cricoid split in combination with separation of inserting soft tis-

sues, remained manifest or appeared even more prominent in the adult stage. An altered balance between intrinsic and extrinsic forces seems not only responsible for immediate distortion but exert also a definite influence on the pattern of later growth of the injured cricoid.

Injury-induced distortion of cartilage, the cricothyroid muscle as extrinsic factor

As was previously discussed, separation of the cricothyroid and cricotracheal ligaments with elevation of the cricovocal membrane gave the option of additional scoring of the inner contour of a split cricoid on both lateral sides (Chapter 2D). Dramatic changes were observed from the time of surgery up to the adult stage. During further growth the U-formed cricoid demonstrated an extreme outward bending of both cut ends. Obviously this progressive malformation seemed a further expression of the initial distortion induced by scoring. In these experiments also a marked influence of the cricothyroid muscles could be demonstrated, causing an upward-outward rotation of the extreme ends of the split cricoid. A rotation of the cut ends was not found in the earlier discussed experiments. Apparently weakening of the cricoid structure by scoring made the cut ends react stronger to action of the cricothyroid muscles.

Injury-induced distortion of cartilage, in relation to age

In adult animals the extent of direct distortional changes induced by various surgical interventions was similar to those in young animals (Chapter 2D). In both age groups distortion of the split cricoid cartilage seems to be governed by the same intrinsic and extrinsic forces.

In follow-up studies the progression of the distortion appeared to be less prominent after surgery in adult than in young animals. This suggests that growth enhances distortion in the long run. However, the limited progression of distortion in adult animals, during a 20-week period, indicates a gradual adaptation of even mature cartilage to an altered balance between intrinsic and extrinsic forces. Although, in this macroscopic study the immediate injury-induced distortion appeared to be similar in adult (28 weeks of age) and young rabbits (8 weeks of age), earlier histological studies focusing on wound-healing of the cricoid cartilage showed marked differences in relation to age [8,12–14]. Contrary to young animals, adult animals demonstrated no or extremely poor healing of cartilage defects. The dissociation between injury-induced distortion and wound healing of cartilage should further be investigated.

Distortion of human specimens

In clinical reports cricoid cartilage distortion have been described as a consequence of endolaryngeal trauma [7].

In 1992 Monnier [15] introduced a new surgical method, partial cricotracheal resection with re-anastomosis of larynx and trachea, as therapy for subglottic stenosis grade 3 and 4 according to Cotton [16]. Previous to referral to the ENT department of the University of Lausanne, most patients had been treated with more conservative methods like anterior cricoid split, dilation of the narrowed lumen or endoscopic laser resection of the stenotic ring.

The resection specimens, collected by Prof. Monnier, included the ventral and lateral parts of the cricoid as well as the compact scar tissue surrounding the stenosic lumen. In most specimens the resected part of the cricoid ring appeared to be incomplete; remaining parts showed signs of damage, repair with fibrosis and distortion. In some cases the cricoid arch was complete and irregular but demonstrated no obvious distortion [17].

The post-mortem data of neonates and infants are still too fragmentary to allow further conclusions on the frequency of cricoid distortion. More information may be expected when the partial cricotracheal resection has become a more widely spread way of treatment.

In this study, we demonstrated a mechanical balance between the intrinsic 'stability' of injured cartilage and extrinsic forces such as induced by membranes, ligaments, muscles and tunica elastica. The postnatal development of the split cricoid may be thoroughly influenced, and thus manipulated by various surgical interventions. Surgical methods might be designed to redirect a distorted cricoid into a functional cricoid ring.

Wound healing and cartilage engineering

Introduction

Injury of cartilage results in local damage of the tissue and distortion of the structure. Processes underlying distortion were discussed above. Damage of tissue often leads to necrosis and ultimately to a cartilage defect. The wound healing capacity of cartilage is generally considered to be poor. Previously, wound healing and regeneration of cartilage were studied in rabbits of different age groups [13,14]. In the adult animals the dominant reaction to injury appeared to be necrosis. For at least twenty weeks after trauma necrotic material remained present, and no formation of new cartilage could be observed. On the contrary, when a similar injury was inflicted on young animals, no necrotic material but even signs of new cartilage was found, after a similar follow-up period. The capacity of wound healing seems to decrease with increasing age.

In 1991 Bean et al. [18] published a method to generate new –young– cartilage in vivo. Demineralized bone matrix (DBM) sculpted as an anterior cricoid arch, was wrapped in a pedicled perichondrial flap [19]. Cells originating from the perichondrium invaded the DBM, redifferentiated and formed cartilage. In a few weeks time the a-vital matrix was resorbed. In this way, a new cartilaginous cricoid arch was produced and successfully used as a graft to reconstruct an anterior cricoid defect. These grafts of 'young' cartilage demonstrated excellent re-integration with the edges of the original mature cricoid cartilage.

In the Chapters 3A, 3B and 3C a first attempt is made to answer the following questions:

1. Is a pedicled perichondrial flap as 'partner' in a DBM-perichondrium construct necessary to produce cartilage cells or is a free flap equally efficient?
2. Is it possible to generate cartilage from the DBM-perichondrium combination in an ex-vivo condition?
3. Is the rabbit ear punch model a useful tool to study re-integration of cartilage grafts?

Engineering cartilage in vivo

Like previously demonstrated for pedicled perichondrial flaps, a free perichondrial flap wrapped around DBM appeared to be capable of producing cartilage cells, provided the construct was implanted in richly vascularized host tissue, like muscles. The newly formed cartilage appeared to be of the hyaline type with collagen type II and elastic fibres. This result suggests that a pedicled muscular flap carrying a perichondrium-DBM construct could be

used for in situ reconstruction of a defective cartilage structure in a one-stage procedure. It might be added that in vivo engineering of cartilage has already been clinically and successfully used in a two-stage procedure [20]. The first step included new formation of cartilage from perichondrium and DBM on the posterior side of the external ear, followed by transfer of the newly formed cartilage to fill a nasal septum defect in a child [18,19].

Engineering cartilage ex-vivo

There are many reports in literature about successful ex-vivo engineering of cartilage. In some of the experiments autologous cartilage is harvested, the matrix enzymatic dissolved and the remaining chondrocytes subsequently seeded in a biodegradable scaffold [21-25]. The scaffold with chondrocytes is implanted in the experimental animal and the generation of cartilage is awaited for. In Chapter 3C we demonstrated that it is possible to generate cartilage implants by these ex-vivo/in-vivo techniques. However, because a large volume of cartilage should be harvested to generate a small piece of new cartilage, there are no clinical implications for this technique. Therefore, to enhance the practicability of cartilage engineering techniques it would be beneficial to generate autologous cartilage from only a few chondrocytes. This implies the multiplication of chondrocytes in ex-vivo cultures before implantation. By multiplication of cartilage cells only, a small biopsy of autologous cartilage would be theoretical sufficient to generate a large amount of cartilage. Though promising the drawback of multiplication of cartilage cells is that the cells change their phenotype in this process and thereby the generated cartilage is of lesser quality [26]. Although recent research demonstrated progress in cell multiplication by the use of growth factors [27,28], the donor site morbidity created by harvesting cartilage remains a disadvantage. This makes people looking for alternative cell sources to tissue engineer cartilage. Recently, successful reports of using bone marrow cells as chondrocyte precursor cells for autologous cartilage generation were published in literature [29,30] but perichondrium is also a well-known source of cartilage precursor cells [31]. Based on the positive results of earlier studies from our group, we explored the feasibility of perichondrium as a cell source for chondrocytes to generate cartilage ex-vivo. In these experiments (Chapter 3B) the incidence of cartilage formation in vitro in a perichondrium-DBBM construct was around 30%. Moreover the amount of cartilage formed was not only small but also highly variable. It was questioned why the in-vivo construct of perichondrium and DBM was more successful than the ex-vivo procedure and how to mimic the in-vivo conditions. Therefore, growth factors like rhTGF-β and IGF-1 were added to the culture medium in different concentrations, in a continuous and pulse regime. Furthermore, macrophages were added to facilitate DBM resorption, and DBM was

soaked in blood to improve the attachment of perichondrium. None of these refinements, however, could increase the incidence of cartilage formation nor the amount of cartilage.

In conclusion, although some cartilage could be generated ex-vivo, we were unable to adequately copy the in-vivo environment to produce the large amounts of cartilage observed in the in-vivo experiments.

Integration of cartilage grafts

Successful reconstructive surgery of cartilage defects and the prevention of (progressive) cartilage deformities depend on wound healing between a cartilage graft and the cartilage present around the defect. Potential (engineered) grafts should not only be evaluated by the quality and quantity of the tissue, but also by their wound healing and integration characteristics.

To promote an efficient and reliable evaluation of cartilage grafts in the experimental situation, a semi-quantative grading model was designed. Items such as quality, integrity and bonding characteristics were included in a histomorphological grading system to provide information about a specific graft (Chapter 3C).

To validate our screening model different conditions were studied in a punch-out model in cartilage. A defect, which was left ungrafted, showed no spontaneous restoration. On the other hand, reimplantation of a punched-out piece of cartilage demonstrated complete closure of the defect, although malalignement (dislocation) of the graft was observed in all specimens. When the cartilage defect was covered with perichondrium, fragments of new cartilage were found.

Newly generated cartilage from perichondrium and DBM in-vivo, used as a graft, demonstrated excellent alignment with the surrounding cartilage and adequate closure of the defect. Implantation of DBM without perichondrium in the punched out hole was completely resorbed within 3 weeks. Engineered cartilage grafts generated from autologous chondrocytes seeded in a DBM scaffold showed multiple disruptions and poor integration characteristics with the surrounding cartilage 3 weeks after implantation in the defect.

In conclusion, the rabbit pinna punch hole model is an efficient model for first evaluation of cartilage grafts or biomaterials; the results can be quickly analysed using a semi-quantative grading system. Again the important role of perichondrium in cartilage has been emphasized.

Clinical perspectives

Making wounds is part of daily surgical practise. Adequate wound healing is necessary for successful surgical interventions. The regenerative capacity of cartilage is minimal, at least in the adult stage. Injury of cartilage in the Head and Neck (ear, nose, larynx and trachea) due to trauma or

surgery may result in a local tissue defect and at the same time initiate a distortion of the structure involved.

Both phenomena are observed after an anterior cricoid split of the cartilaginous cricoid ring. Cut edges show a process of wound healing, whereas distortion of the split cricoid ring is responsible for a widening of the gap between the cut ends. The cartilage of the cricoid can also be damaged by endotracheal intubation for general anaesthesia or prolonged support of ventilation. At the subglottic level intubation injury involving the soft tissue lining of the airway as well as the cartilage of the cricoid ring, will initiate a process of wound healing with abundant scar formation, resulting in a subglottic stenosis [17]. Most severe cases have recently treated by resection of scar tissue and the ventral and lateral parts of the cricoid ring followed by laryngotracheal approximation [31]. Laryngotracheoplasty, augmentation of the subglottic wall, is the treatment of choice for moderate subglottic stenosis [32,33]. When the stenotic lumen is reached by a ventro-medial incision, the lumen is widened by grafting of rib cartilage between the anterior ends of the cricoid, in some cases combined with a second graft in the posterior wall. The formation of different types of subglottic stenosis in relation to specific endolaryngeal injuries has been investigated in a series of animal studies. The results appeared to be most useful for the interpretation of the histopathology of human specimen in the literature [7,34,35].

With the experiments reported in this thesis we made an attempt to contribute to the biology of surgical interventions on cartilage, in particular the cricoid. Various aspects of surgery-induced distortion and wound healing were studied, including their short- and long-term evolution, age-related differences, effects on growth and the role of attached soft tissues. These experiments were all performed in a previously normal larynx. However, the patient's problem is the post-traumatic stenotic larynx. A similar study on an already stenotic larynx has not yet been published, but would be most interesting for developing new surgical strategies.

The conclusion that the morphology of the split cricoid cartilage is governed by a balance between intrinsic and extrinsic forces is new. Previously, only intrinsic factors were considered to explain the distortion resulting in the anterior gap observed in patients immediately after a mid-ventral split of the cricoid ring. Our experiments demonstrated that the observed diameter of the anterior gap is to a large extent determined by extrinsic factors like laryngeal ligaments, membranes and muscles. It seems an interesting project to investigate whether a similar balance is present in the human body.

Intrinsic- and extrinsic forces are not only responsible for an immediate distortion after injury, but also for an increase of distortion during growth. At this point no clinical data are available. Further studies are necessary to

explore the application of controlled surgically induced distortion to correct the malformed cricoid.

The restricted wound-healing capacity of mature cartilage is well known and makes reconstruction of a fragmented cartilage structure nearly impossible. Our experiments demonstrated that even in adult animals it is possible to generate new-young-cartilage. Moreover this in vivo-engineered young cartilage showed an unexpected capacity of wound healing and reintegration when in contact with a cut edge of mature cartilage. The properties of this engineered cartilage should be studied in more detail before speculating about its potential use in cartilage surgery.

References

[1] Gibson, T., R.C. Curran, and W.B. Davis, The survival of living homograft cartilage in man. Transplant Bull, 1957;4(3):105-6.

[2] Gibson, T. and B.W. Davis, The distortion of the autogenous cartilage grafts: its cause and prevention. Br. J. Plast. Surg., 1958;10:257-274.

[3] Fry, H.J.H., Interlocked stresses in human nasal septal cartilage. Br J Plast Surg, 1966;19(3):276-8.

[4] Fry, H.J.H., Nasal skeletal trauma and the interlocked stresses of the nasal septal cartilage. Br J Plast Surg, 1967;20(2):146-58.

[5] Fry, H.J.H., Cartilage and cartilage grafts: the basic properties of the tissue and the components responsible for them. Plast Reconstr Surg, 1967;40(5):426-39.

[6] Fry, H.J.H. and W.V. Robertson, Interlocked stresses in cartilage. Nature, 1967;215(96):53-4.

[7] Chen, J.C. and L.D. Holinger, Acquired laryngeal lesions. Pathologic study using serial macrosections. Arch Otolaryngol Head Neck Surg, 1995;121(5):537-43.

[8] Adriaansen, F.C., et al., A morphometric study of the growth of the subglottis after endolaryngeal trauma. Int J Pediatr Otorhinolaryngol, 1986;12(2):217-26.

[9] Adriaansen, F.C., et al., Differential effects of endolaryngeal trauma upon the growth of the subglottis. Int J Pediatr Otorhinolaryngol, 1988;15(2):163-71.

[10]. Adriaansen, F.C., et al., Morphometric study of the growth of the subglottis after interruption of the circular structure of the cricoid. Orl J Otorhinolaryngol Relat Spec, 1988;50(1):54-66.

[11] Verwoerd, C.D., H.L. Verwoerd-Verhoef, and C.A. Meeuwis, Stress and woundhealing of the cartilaginous nasal septum. Acta Otolaryngol, 1989;107(5-6):441-5.

[12] Verwoerd, C.D., et al., Wound healing of the nasal septal perichondrium in young rabbits. Orl J Otorhinolaryngol Relat Spec, 1990;52(3):180-6.

[13] Bean, J.K., et al., The influence of ageing on wound healing of the cricoid. Acta Otolaryngol, 1992;112(2):362-5.

[14] Bean, J.K., H.L. Verwoerd-Verhoef, and C.D. Verwoerd, Injury- and age-linked differences in wound healing and stenosis formation in the subglottis. Acta Otolaryngol, 1995;115(2):317-21.

[15] Monnier, P., M. Savary, and G. Chapuis, Partial cricoid resection with primary tracheal anastomosis for subglottic stenosis in infants and children. Laryngoscope, 1993;103(11 Pt 1):1273-83.

[16] Cotton, R.T. and J.N. Evans, Laryngotracheal reconstruction in children. Five-year follow-up. Ann Otol Rhinol Laryngol, 1981;90(5 Pt 1):516-20.

[17] Duynstee, M.L., et al., Subglottic stenosis after endolaryngeal intubation in infants and children: result of wound healing processes. Int J Pediatr Otorhinolaryngol, 2002;62(1):1-9.

[18] Bean, J.K., H.L. Verwoerd-Verhoef, and C.D.A. Verwoerd, Chondroneogenesis in a Collagen Matrix. Fundamentals of bone growth, 1991;chapter 8:113-120.

[19] Bean, J.K., et al., Reconstruction of the growing cricoid with a composite graft of demineralized bovine bone and autogenous perichondrium; a comparative study in rabbits. Int J Pediatr Otorhinolaryngol, 1993;25(1-3):163-72.

[20] Pirsig, W., et al., Cartilage transformation in a composite graft of demineralized bovine bone matrix and ear perichondrium used in a child for the reconstruction of the nasal septum. Int J Pediatr Otorhinolaryngol, 1995;32(2):171-81.

[21] Vacanti, C.A. and J.P. Vacanti, Bone and cartilage reconstruction with tissue engineering approaches. [Review]. Otolaryngol Clin North Am, 1994;27(1):263-76.
[22] Park, S.S., et al., Biomechanical properties of tissue-engineered cartilage from human and rabbit chondrocytes. Otolaryngol Head Neck Surg, 2002;126(1):52-7.
[23] Haisch, A., et al., A tissue-engineering model for the manufacture of auricular-shaped cartilage implants. Eur Arch Otorhinolaryngol, 2002;259(6):316-21.
[24] Shieh, S.J., S. Terada, and J.P. Vacanti, Tissue engineering auricular reconstruction: in vitro and in vivo studies. Biomaterials, 2004;25(9):1545-57.
[25] Kamil, S.H., et al., Tissue engineering of a human sized and shaped auricle using a mold. Laryngoscope, 2004;114(5):867-70.
[26] von der Mark, K., et al., Relationship between cell shape and type of collagen synthesised as chondrocytes lose their cartilage phenotype in culture. nature, 1977. **267**(Jun 9): 531-2.
[27] van Osch, G.J., et al., The potency of culture-expanded nasal septum chondrocytes for tissue engineering of cartilage. Am J Rhinol, 2001;15(3):187-92.
[28] Mandl, E.W., et al., Multiplication of human chondrocytes with low seeding densities accelerates cell yield without losing redifferentiation capacity. Tissue Eng, 2004;10(1-2):109-18.
[29] Fuchs, J.R., et al., Fetal tracheal augmentation with cartilage engineered from bone marrow-derived mesenchymal progenitor cells. J Pediatr Surg, 2003;38(6):984-7.
[30] Kojima, K., et al., Tissue-engineered trachea from sheep marrow stromal cells with transforming growth factor beta2 released from biodegradable microspheres in a nude rat recipient. J Thorac Cardiovasc Surg, 2004;128(1):147-53.
[31] Hosokawa, K., et al., *Cartilage formation from perichondrium in a diffusion chamber.* Ann Plast Surg., 1988. 21(2): 140-2.
[32] Monnier, P., F. Lang, and M. Savary, Cricotracheal resection for pediatric subglottic stenosis. Int J Pediatr Otorhinolaryngol, 1999;49 Suppl 1:S283-6.
[33] Zalzal, G.H., Treatment of laryngotracheal stenosis with anterior and posterior cartilage grafts. A report of 41 children. Arch Otolaryngol Head Neck Surg, 1993;119(1):82-6.
[34] Cotton, R.T., et al., Pediatric laryngotracheal reconstruction with cartilage grafts and endotracheal tube stenting: the single-stage approach. Laryngoscope, 1995;105(8 Pt 1):818-21.
[35] Gould, S.J. and J. Graham, Long term pathological sequelae of neonatal endotracheal intubation. J Laryngol Otol, 1989;103(6):622-5.
[36] Holinger, L.D., Histopathology of congenital subglottic stenosis. Ann Otol Rhinol Laryngol, 1999;108(2):101-11.